Fall 2021

Geochemical Investigation of Monogenetic Volcanoes from the Pribilof Islands, Bering Sea, Alaska

Clayton L. Reinier
Missouri State University, Clayton098@live.missouristate.edu

GEOCHEMICAL INVESTIGATION OF MONOGENETIC VOLCANOES FROM THE PRIBILOF ISLANDS, BERING SEA, ALASKA

A Master's Thesis

Presented to

The Graduate College of

Missouri State University

In Partial Fulfillment

Of the Requirements for the Degree

Master of Science, Geography and Geology

By

Clayton Lane Reinier

December 2021

GEOCHEMICAL INVESTIGATION OF MONOGENETIC VOLCANOES FROM THE PRIBILOF ISLANDS, BERING SEA, ALASKA

Geology, Geography, and Planning

Missouri State University, December 2021

Master of Science

Clayton Lane Reinier

ABSTRACT

Small-volume basaltic magmas found at continental intraplate environments have not been as extensively studied compared to their polygenetic counterparts. Specifically, regions such as the Bering Sea basalt province, described as a diffuse igneous province, have commonly been overlooked. Assumptions that these systems are invoked by simple, single batches of magma has subsequently left a gap in understanding the processes responsible for primary magma generation away from plate boundaries with little tectonic influence. The following studies that constitute this thesis focus on an in-depth geochemical investigation at the crystal and sub-crystal scale to evaluate lithospheric mantle heterogeneities, processes that govern primary magma generation, and time scale estimations to constrain subsurface processes at monogenetic volcanic centers. The Pribilof Islands are one of approximately fifteen late Cenozoic (<6 Ma) monogenetic volcanic fields that are regionally dispersed in the Bering Sea. St. George and St. Paul, two of the principal Pribilof Islands, constitute the youngest volcanic remnants in the Bering Sea basalt province. Here, major and trace element contents of olivine phenocrysts from St. Paul lavas have been investigated to constrain pre-eruptive magmatic conditions and estimate time scales using Fe–Mg interdiffusion. Additionally, lherzolite xenoliths is host alkali basalts from St. George were investigated to constrain melt extraction and metasomatism of the lithospheric mantle underlying the Pribilof Islands. Trace and rare earth element contents were used to decipher and estimate the degree of partial melting and metasomatism prior to xenolith entrainment and transportation to the surface. These data suggest the source of magmatism for the Pribilof Islands, and likely the Bering Sea basalt province as a whole, is not sourced from mantle xenoliths. Instead, these data suggest magma is sourced from melt-extraction of a primitive mantle source likely initiated by lithospheric extension which triggered decompression melting of a metasomatized upper mantle.

KEYWORDS: Alaska, basalt, Bering Sea basalt province, geochemistry, xenolith, monogenetic volcanoes

GEOCHEMICAL INVESTIGATION OF MONOGENETIC VOLCANOES

FROM THE PRIBILOF ISLANDS, BERING SEA, ALASKA

By

Clayton Lane Reinier

A Master's Thesis
Submitted to the Graduate College
Of Missouri State University
In Partial Fulfillment of the Requirements
For the Degree of Master of Science, Geography and Geology

December 2021

Approved:

Gary Michelfelder, Ph.D., Thesis Committee Chair

Toby Dogwiler, Ph.D., Committee Member

Matthew McKay, Ph.D., Committee Member

Julie Masterson, Ph.D., Dean of the Graduate College

ACKNOWLEDGEMENTS

I would like to express my thanks to all the faculty and staff of the Department of Geography, Geology, and Planning for their support and contributions, not only to my success within the program, but to this project as well. I would like to especially thank Dr. Gary Michelfelder for developing this project and for his continued assistance every step of the way. I would like to thank Dr. Toby Dogwiler and Dr. Matt McKay for their assistance and thoughtful remarks regarding this project. Additionally, I would like to thank Kenny Horkley, from the University of Iowa, and Dr. Frank Ramos, from New Mexico State University, for their assistance collecting data in the lab. I would like to extend my thanks to the Missouri State University Volcanology, Petrology, and Geochemistry Research Group for their valuable contributions and assistance with this project. This project was financially supported by the NASA-Missouri Space Grant Consortium, the Geological Society of America – Bruce L. "Biff" Reed Specialized Award, and the Missouri State University Graduate College.

In addition to the people that have directly helped me on this project, I would like to thank everyone that supported me. To my family and friends, thank you. Thank you for the unconditional support, love, and motivation to keep pushing. Alyssa, thank you for keeping me sane and always being there when I needed it most. Lastly, and most important of all is my pup, Gus. You were by my side this entire journey, laying at my feet for countless hours as I studied and typed away. We got through the lows together and celebrated the highs. You deserve unlimited treats, belly rubs, and toys, my boy. I couldn't be more thankful for you.

TABLE OF CONTENTS

LIST OF TABLES

LIST OF FIGURES

Manuscript 1

Manuscript 2

OVERVIEW

Small-scale basaltic magmatic systems, despite being the smallest in terms of volume (magma reservoir <2 km^2), are the most abundant form of volcanism on Earth; and are commonly expressed at Earth's surface as monogenetic volcanic fields (Cañón-Tapia and Walker, 2004; McGee and Smith, 2016). Individual cones within a volcanic field are generally the result of a time-constrained series of eruptions that represent a distinct batch of magma (Németh and Kereszturi, 2015). They can occur at all major tectonic settings including intraplate, extensional, and subduction-related environments. Consequently, due to their small nature, they have commonly been overlooked and minimally studied relative to their polygenetic counterparts (Cañón-Tapia, 2016; McGee and Smith, 2016). The chemical composition of erupted cone building material provides insight into the processes of magma generation and differentiation in the magma plumbing system prior to eruption. This thesis and subsequent manuscripts focus solely on monogenetic volcanic centers from a continental intraplate environment. Magmatic systems in these environments represent snapshots of the processes responsible for mantle melting away from plate boundaries unbiased by tectonic-related processes (McGee and Smith, 2016). Although truly primitive basalts, which are magmas completely unmodified from the onset of melting to eruption, are extremely rare, igneous rocks from these environments represent some of the closest material to their primitive mantle source (McGee and Smith, 2016).

As interest in small-batch basaltic magmatic systems grows, general questions regarding source to conduit mechanics tend to increase. Basic questions guiding this work and regarding large-scale intraplate-related volcanism include: 1) what mechanisms trigger mantle melting within the interior of tectonic plates, 2) what are time scales of small-batch basaltic magmas, and

3) what influence does melting of individual mineral phases have on magma chamber development and evolution over time? This thesis aims to investigate the processes governing primary magma generation in time and space and the magmas generated at individual volcanic centers in diffuse igneous intraplate environments. Although this thesis cannot provide detailed answers to all these questions, it will contribute to the broader understanding of these systems, and hopefully, better guide future studies.

Here, I use lavas and monogenetic volcanic centers located in the Bering Sea basalt province (BSBP) to investigate these systems. Volcanoes here define a *diffuse* igneous province given the regionally dispersed intraplate-related volcanism in the Bering Sea region (Wirth et al., 2002). The primary area of focus for both studies is the Pribilof Islands, Alaska, which is one of approximately fifteen late Cenozoic (<6 Ma) volcanic fields associated with the BSBP (Moll-Stalcup, 1994). St. Paul and St. George islands, the two principal islands of the Pribilof's, contain some of the youngest volcanic remnants within the BSBP, thus providing an exceptional opportunity to investigate small-batch basaltic magmatism (Moll-Stalcup, 1994). Well-preserved volcanic sequences from monogenetic eruptive centers provide snapshots in time of the mantle source composition, and the melting and ascent processes that would otherwise be overwhelmed and homogenized in larger polygenetic volcanic systems. It is imperative to understand the evolution of single eruptive centers prior to addressing the large-scale questions on the behavior of monogenetic systems. The following chapters of this thesis outline two manuscripts that discuss a comprehensive and detailed petrological, geochemical, and isotopic study of individual mineral phases and mantle xenoliths hosted in alkalic basaltic lavas from monogenetic volcanic centers from the Pribilof Islands, Alaska. In conjunction with previously reported petrological and geochemical data from the Pribilof Islands (Chang et al., 2009; Winer et al., 2004; Feeley

and Winer, 1999), these studies constitute the most comprehensive data set for a single volcanic field in the BSBP to date.

In the first manuscript, *Resolving the Magmatic Plumbing System of Monogenetic Volcanoes from St. Paul Island, Alaska: Insights from Diffusion Chronometry*, I present olivine major and minor element mineral chemistry to understand pre-eruptive conditions for monogenetic volcanic centers on St. Paul Island. In this study, three populations of olivine exist within the analyzed lavas, which aid in deciphering the volcanic plumbing system and processes responsible for eruption. In addition to major and minor element compositions, Fe–Mg interdiffusion was used to constrain the timing of processes that led to an eruption. This study shows how small-batch basaltic magmas have more complex lithospheric magmatic histories than previously believed. Coupling detailed geochemical mineral data from manuscript one with a geochemical and isotopic study of mantle xenoliths from St. George Island allows for a better understanding of the sources of magmatism, the mechanisms responsible for melting, and the relationship between mantle xenoliths and their host basaltic lavas for the Pribilof Islands.

Manuscript two, *Lithospheric Melting and Metasomatism Beneath the Pribilof Islands: Insights from Spinel Peridotite Xenoliths from St. George Island, Alaska*, presents a comprehensive petrological, geochemical, and radiogenic isotope analysis of spinel-facies lherzolite mantle xenoliths hosted in alkali basalts from St. George Island. This study aims to use these data to document and investigate episodes of partial melting and metasomatism of the mantle lithosphere. In this study, two populations of mantle xenoliths are evident within St. George lavas. Whole-rock and clinopyroxene rare earth element (REE) systematics suggest that most St. George lherzolite xenoliths experience variable degrees of partial melting and

metasomatism. The analyzed xenoliths in this study reveal that the source of magmatism in the Pribilof Islands is not the melting of a mantle composition similar to the analyzed xenoliths.

MANUSCRIPT 1: RESOLVING THE MAGMATIC PLUMBING SYSTEM OF MONOGENETIC VOLCANOES FROM ST. PAUL ISLAND, ALASKA: INSIGHTS FROM DIFFUSION CHRONOMETRY

Abstract

Igneous rocks from small-volume basaltic magmatic systems provide insight into the mechanisms responsible for magma generation and the evolution of primitive basaltic magmas from the mantle, which would otherwise be overwhelmed and homogenized in larger magmatic systems. Lavas from small-volume volcanic systems at continental intraplate environments reveal chemical variability in both single eruptive sequences and across eruptive centers in a contiguous volcanic field. These variations are the likely result of different degrees of partial melting, crystallization, and magma storage. Chemical records retained within erupted crystals constrain the volcanic plumbing system immediately prior to an eruption. The Pribilof Islands, Alaska, contain intraplate late Cenozoic volcanic fields associated with the Bering Sea Basalt Province (BSBP). St. Paul Island (540–3.4 ka) is the youngest and most well-preserved volcanic field in the BSBP. Here, this study uses olivine major and trace element mineral chemistry from monogenetic volcanic centers on St. Paul Island. Olivine reveals two primary populations, type 1 and 2, and two sub-populations, type 1A and type 1B, based on unique textures and distinct chemical compositions. Modeling Fe–Mg inter-diffusion in olivine phenocrysts constrains the timing of mixing events in the crustal plumbing system. These data reveal that olivine accumulated in a primitive mantle-derived source and a separate more evolved magma source. Transects reveal the two batches of magma mixed ~20 days prior to eruption. Results of this study show small-batch basaltic magmas at continental intraplate environments have more complex lithospheric magmatic histories than previously believed.

Introduction

Small-volume monogenetic volcanism in diffuse igneous provinces has not been as meticulously studied as other intraplate related volcanic systems (e.g., ocean islands, continental rifts, mantle plumes, etc.) despite being the most coming types of volcanic centers on Earth (McGee and Smith, 2016). Basalts from such environments provide valuable insight into the processes responsible for magma generation and the evolution of primitive mantle magmas, which would otherwise be overwhelmed and homogenized in larger magmatic systems (McGee and Smith, 2016). Unfortunately, how fast mantle-derived magmas migrate from crust to surface

is poorly understood (Gordeychik et al., 2018). Chemical zoning patterns retained within igneous derived minerals have the potential to decipher subvolcanic processes leading to an eruption and aid in understanding timescales and processes operating during ascent (de Maisonneuve et al., 2016). *In situ* analysis across zoned grains links temporal information to specific magmatic processes, such as magma residence, mixing events, or melt migration (Costa and Dungan, 2005; Costa et al., 2008; Shea et al., 2015). Diffusion speedometry is an indispensable tool for exploring residence time scales of zoned crystals following mixing or recharge events.

To investigate mantle melting and residence time scales of small basaltic magmatic systems at continental intraplate environments, I combine geochemical data with textural features of olivine phenocrysts from St. Paul Island, Alaska, to constrain the timing and duration of magma generation and melt migration. The Pribilof Islands (Fig. 1A), situated ~400–450 km north of the Aleutian arc front, are a suite of four volcanic islands associated with the broader, late Cenozoic (<6 Ma) *diffuse* igneous Bering Sea basalt province (BSBP; Moll-Stalcup, 1994; Davis et al., 1994). St. Paul Island (~104 km^2; Fig. 1B), the primary focus of this study, is one of the youngest (540–3.2 ka) and most well-preserved volcanic centers in the BSBP providing an opportunity to investigate timescales at a potentially active volcanic center (Winer et al., 2004; Feeley and Winer, 2009; Chang et al., 2009). St. Paul Island has an east-west trending highland (>60 m) containing several monogenetic scoria cones (≤360 ka; 30–140 m high) and small polygenetic vents with low-viscosity basaltic lavas encompassing the highland (Fig. 1B; Winer et al., 2004; Chang et al., 2009). In general, basalts from St. Paul include basanites, alkali basalts, and trachybasalts. Lee-Wong et al. (1979), Feeley and Winer (1999), and Winer et al. (2004) present detailed petrographic description of St. Paul rocks, and therefore will not be discussed here. This study aims to constrain the timing of magma mixing leading to an eruption on St. Paul

Island using Fe–Mg zonation in olivine phenocrysts and diffusion speedometry. The resulting time scales were used to explore magma storage and transport to better constrain our understanding of mantle-derived, small-batch basaltic magmas at continental intraplate environments.

Methods

Four whole rock samples from St. Paul Island monogenetic lavas were characterized using standard polished thin sections. Mineral abundances, crystal sizes, crystal shape, and igneous textures and structures were determined using a standard binocular polarizing microscope. High-resolution backscatter electron (BSE) images were used to identify crystal zoning patterns and select olivine phenocrysts for geochemical analysis. Approximately fifteen olivine phenocrysts were selected from each lava sample for core-to-rim transect analysis with a minimum of five spots per transect. Detailed transects with a 5-micron step-size were collected on approximately five crystals per lava for a more detailed chemical analysis and diffusion modeling. Quantitative spot analyses were conducted on the samples using a JEOL JXA-8230 Superprobe electron-probe microanalyzer (EPMA) at the University of Iowa equipped with five wavelength-dispersive spectrometers and large-format diffracting crystals using the method and parameters described in Michelfelder et al. (2021). The EPMA was calibrated for Mg and Ni using San Carlos olivine (NMNH 111312-44) and Si, Fe, Ca, Ti, Mn, Cr, and Al using the Astimex Cr pyrope reference material.

Results

Olivine chemistry. Olivine occurs as euhedral to subhedral phenocrysts or euhedral to subhedral phenocrysts with skeletal crystal morphologies. Olivine phenocrysts from St. Paul Island lavas range in forsterite contents (Fo#) from 45 to 87 and averages 83, and Mg# from 31 to 78 and averages 73. Ca, Ti, and Mn decrease with increasing Fo#, while Ni and Cr tend to increase with increasing Fo#. Aluminum content is confined in lower Fo# olivine but exhibit greater variability in higher Fo# olivine.

Based on texture and core-to-rim major and minor element trends, two distinct olivine populations have been identified. Type 1 olivine are euhedral to subhedral crystals that have been further divided into two sub-populations, 1A and 1B. Type 1A display normal zoning profiles from core-to-rim, with core compositions that range in $Fo_{83–86}$ and have Ca and Ni contents that range from 3030–3706 ppm and 1830–2120 ppm, respectively. Type 1A rims (<50 μm) are lower in Fo_{69-82} and Ni (976–1792 ppm), and higher in Ca (3843–5022 ppm). Type 1B display normal zoning profiles on the outermost region of the crystal with a reverse zoning profile immediately outside the homogenous core and inside of the normal zoned portion near the thin Fe-rich rim (Fig. 2C). Core compositions range in Fo_{77-78} and have Ca and Ni contents that range from 2318–2830 ppm and 926–1094 ppm, respectively. Type 1B rims (<20 μm) are lower in Fo_{71-77} and Ni (739–1155 ppm), and higher in Ca (2318–2830 ppm). Compared to type 1B, type 1A olivine display a greater degree of diffusivity in core-to-rim transect profiles and higher Fo# content. Type 2 olivine are euhedral to subhedral phenocrysts with skeletal crystal morphologies. This population displays an overall normal zoning profile with most crystals recording high frequency Fe–Mg oscillations in the last ~50 μm towards the rim. Core compositions range in $Fo_{78–81}$ and have Ca and Ni contents that range from 1960–3500 ppm and 770–1910 ppm, respectively. Type 2 rims (<20 μm) are lower in $Fo_{62–72}$ and Ni (60–760 ppm),

and higher in Ca (3800–5760 ppm). Refer to appendix for a comprehensive table of major element contents for olivine.

Diffusion modeling. A crystal in equilibrium with a melt will attempt to re-equilibrate with the system if the host magma experiences any change in temperature, pressure, or composition. If the crystal remains under desirable conditions for diffusion of a particular element to occur over a period, the resulting compositional profile across a grain's boundaries will be smooth based on the element and the relaxation time (Costa and Morgan, 2011; Rae et al., 2016). In principle, it is possible to calculate the timescales of processes within a magmatic system (e.g., temperature, pressure, or composition) based on the geometry of the diffusion profile and pre-determined diffusion coefficients (Costa and Morgan, 2011). I selected sixty crystals across four lavas representing the three crystal types for one-dimensional diffusion modeling. Of these segments, eight traverses from three lava flow samples were suitable. I calculated timescales by modeling the partial relaxation of Fo content across distinct zoning segments via Fe–Mg interdiffusion. To model diffusion, I used DIPRA, or diffusion process analysis, for diffusion modeling of Fe–Mg across the selected olivine phenocrysts (Girona and Costa, 2013). Initial and boundary conditions were selected manually. Initial conditions were assumed to be the maximum concentration measured in the olivine crystal, and boundary conditions were set to reflect the concentration measured at the crystal rim, which is suggested to be in equilibrium with the host melt where the crystal resided (Costa et al., 2008; Girona and Costa, 2013). I used T = 1125°C with an uncertainty of ±10°C, P = 101,325 Pa, $fO_2 = 3.4\times10^{-4}$ Pa and Δx (step size) = 5 μm, which reflects the main thermodynamic parameters that control diffusion (Girona and Costa, 2013). Modeled crystals were well fitted by a simple one–dimensional diffusion profile. Timescales averaged ~19 days, with a maximum calculated time

of 38 days and a minimum of 16 days (Fig. 2B). Our results also imply that time scales of magma ascent were short and relatively consistent over ~100 k.y. of monogenetic volcanism.

Discussion

Although situated at a continental intraplate environment and a near-ridge feature, the Pribilof Islands and the BSBP as a whole have been difficult to explain by models such as the plume hypothesis (Wilson, 1963; Morgan 1971) or the large igneous province model (Coffin and Eldholm, 1994) due in part to the lack of evidence for time-transgressive volcanism, and low rates of melt production and eruptive activity (Mukasa et al., 2007; Chang et al., 2009). Based on the distribution of olivine core and rim compositions, crystal textures, and timescales, I suggest a more complex volcanic plumbing system for St. Paul Island than what has been previously described for the BSBP involving just a single, distinct batch of magma rapidly ascending to the surface with minimal time in crustal magma chambers (Davis et al., 1994; Moll-Stalcup, 1994). Feeley and Winer (1999) provide evidence for fractional crystallization, which indicates the melt responsible for the Pribilof Islands would have temporarily stalled in the crust prior to eruption. Our findings support short-term fractional crystallization, but this alone is not enough to explain compositional diversification and the reverse zoning trends observed in some of the detailed transects. Analyzed olivine profiles agree with the model proposed by Chang et al. (2009), suggesting primitive St. Paul rocks result from a mixing event between two compositionally distinct batches of magma late in the evolution of the Pribilof Islands magmatic system.

To further contribute to this model, I interpret the two pre-existing magma bodies containing a crystal load in equilibrium with the melt (Fig. 3). Prior to mixing the two magmas, one batch of magma hosted our type 1A crystal core population ($Fo_{83–86}$), which would have

nucleated in a primitive mantle-derived melt (Fo# ~86) and remained under conditions desirable to produce the observed homogenous cores. A separate batch of magma, more evolved (meaning less Mg, more Fe-rich) than the melt hosting type 1A cores, would have nucleated type 1B cores ($Fo_{77–78}$). Olivine profiles suggest these two distinct batches of magma mixed, forcing the system to re-equilibrate towards a hybridized 'midpoint' between a primitive magma composition and an evolved magma composition (Fo#=83). Zonation in the crystal cargo indicates one of two things: a change in the local environment (pressure, temperature, composition) or that the crystal has migrated out of the environment it originally nucleated in (Pankhurst et al., 2018). I suggest the primitive mantle-derived melt (type 1A cores) migrated into a shallower magma chamber where the evolved melt (type 1B cores) resided and eventually triggered an eruption. Normal zoning in our type 1A olivine population can be explained by progressive growth as the melt evolves through time to a higher Fe and lower Mg composition. This mixing event can explain reverse zoning in the evolved type 1B cores as Fo content would have slightly increased, which is evident in the detailed transects (Fig. 2C).

Immediately following the reverse zonation segments observed in the type 1B olivine population, all type 1 olivine crystals exhibit normal zoning prior to the steep compositional profiles caused by the thin, Fe-rich quenched rims (Fig. 2C; 2D). Diffusion models suggest that the crystal cargo resided within the liquid after the mixing event, housed in crustal magma chambers for ~20 days prior to eruption (Fig. 2A). Modeled crystals were well fitted by a simple one–dimensional diffusion profile. On average, timescales were calculated to be ~19 days, with a maximum calculated time of 38 days and a minimum of 16 days. Our results also imply that time scales of magma ascent were short and relatively consistent over ~100 k.y. of monogenetic volcanism. This is supported by positive correlations between MgO and compatible trace

element contents, positive correlations between compatible trace elements and modal olivine abundances, and variation in phenocryst size and composition (Feeley and Winer, 1999).

The type 2 subhedral olivine population is compositionally similar ($Fo_{78–81}$) to the type 1B olivine crystal population but display skeletal crystal morphologies, making them texturally distinct from the other observed olivine populations. I interpret this to be a late-stage phenomenon resulting in the magma rapidly ascending to the surface. This implication is further supported by the high-frequency Fe–Mg oscillations observed closer to the rim. Oscillatory zones of this nature likely formed within the final hours before quenching to be preserved and not diffusively re-equilibrate with the homogenous core (Pankhurst et al., 2018).

Conclusion

Variability in olivine phenocryst textures and chemical composition from St. Paul Island monogenetic lavas suggest a more vertically extensive plumbing system than previously reported (Davis et al., 1994; Moll-Stalcup, 1994). I suggest that a mantle-derived melt (~Fo_{86}) hosting chemically homogenous olivine type 1A crystal cores was injected into a shallower level, more evolved melt (~Fo_{77}) hosting type 1B olivine crystal cores. Type 1A phenocrysts are normally zoned in core-to-rim compositional profiles, suggesting fractionation and crystallization of the core occurred following magma mixing. Type 1B core-to-rim compositional profiles reveal reverse zoning profiles, recording a magma mixing event. Magma mixing occurred ~20 days prior to an eruption. As the magma rapidly ascended and degassed, type 2 olivine phenocrysts developed, recording insights into eruption dynamics. Based on these observations, I suggest the volcanic system is a multi-stage process that does not reflect a single, compositionally distinct batch of magma rapidly ascending to the surface with little to no residence time in crustal

reservoirs. My results reveal small-volume basaltic magmatic systems at continental intraplate environments have complex lithospheric magmatic histories that reflect open-system behavior.

Acknowledgements

This project was supported by Graduate Student Research grants from the Missouri State University Graduate College and the Bruce L. "Biff" Reed Scholarship Award, Geological Society of America awarded to CLR, and a Missouri Space Grant Affiliate Award to GSM. The authors would like to thank Frank Ramos, Toby Dogwiler, and Matthew McKay for their technical expertise and logistical support during this project and Todd C. Feeley for providing samples from NSF project EAR-0439676: "Evolution of Intraplate Volcanism in a Diffuse Igneous Province: A Case Study of the Pribilof Islands, Alaska."

References

Chang, J.M., Feeley, T.C., and Deraps, M.R., 2009, Petrogenesis of Basaltic Volcanic Rocks from the Pribilof Islands, Alaska, by Melting of Metasomatically Enriched Depleted Lithosphere, Crystallization Differentiation, and Magma Mixing: Journal of Petrology, v. 50, no. 12, p. 2249-2286, doi:10.1093/petrology/egp075.

Coffin, M.F., and Eldholm, O., 1994, Large igneous provinces: crustal structure, dimensions, and external consequences: Reviews of Geophysics, v. 32, p. 1-36.

Costa, F., and Dungan, M., 2005, Short time scales of magmatic assimilation from diffusion modeling of multiple elements in olivine: Geology, v. 33, no. 10, p. 837-840, doi:10.1130/G21675.1.

Costa, F., Dohmen, R., and Chakraborty, S., 2008, Time scales of magmatic processes from modeling the zoning patterns of crystals: Reviews in Minerology and Geochemistry, v. 69, no. 1, p. 545-594, https://doi.org/10.2138/rmg.2008.69.14.

Costa, F., and Morgan, D.J., 2011, Time constraints from chemical equilibration in magmatic crystals, *in* Dosseto, A., et al., eds., Time scales of magmatic processes: Chichester, UK, John Wiley & Sons, p. 125-159.

Davis, A.S., Marlow, M.S., and Wong, F.L., 1994, Petrology of Quaternary basalt from the Bering Sea continental margin, *in* Simakov, K.V., and Thurston, D.K., eds., Proc. Int. Arc. Mar., p. 124-137.

de Maisonneuve, C.B., Costa, F., Huber, C., Vonlanthen, P., Bachmann, O., and Dungan, M.A., 2016, How do olivines record magmatic events? Insights from major and trace element zoning: Contributions to Minerology and Petrology, v. 171, no. 6, doi: 10.1007/s00410-016-1264-6.

Feeley, T.C., and Winer, G.S., 1999, Evidence for fractionation of Quaternary basalts on St. Paul Island, Alaska, with implications for the development of shallow magma chambers beneath Bering Sea volcanoes: Lithos, v. 46, p. 661-676, https://doi.org/10.1016/S0024-4937(98)00070-X.

Feeley, T.C., and Winer, G.S., 2009, Volcano hazards and potential risks on St. Paul Island, Pribilof Islands, Bering Sea, Alaska: Journal of Volcanology and Geothermal Research, v. 182, p. 57-66, http://dx.doi.org/10.1016/j.jvolgeores.2009.02.005.

Gordeychik, B., Churikova, T., Kronz, A., Sundermeyer, C., Simakin, A., and Worner, G., 2018, Growth of, and diffusion in, olivine in ultra-fast ascending basalt magmas from Shiveluch volcano: Scientific Reports, v. 8, p. 1-15, doi:10.1038/s41598-018-30133-1.

Girona, T., and Costa, F., 2013, DIPRA: A user-friendly program to model multi-element diffusion in olivine with applications to timescales of magmatic processes: Geochemistry, Geophysics, and Geosystems, v. 14, no. 2, p. 422-431, doi:10.1029/2012GC004427.

Lee-Wong, F., Vallier, T.L., Hopkins, D.M., and Silberman, M.L., 1979, Preliminary report on the petrography and geochemistry of basalt from the Pribilof Islands and vicinity, southern Bering Sea: U.S. Geological Survey Open-File Report 79-1556, 51 p.

McGee, L.E., and Smith, I.E.M., 2016, Interpreting chemical compositions of small-scale basaltic systems: A review: Journal of Volcanology and Geothermal Research, v. 325, p. 45-60, https://doi.org/10.1016/j.jvolgeores.2016.06.007.

Michelfelder, G.S., Horkley, L.K., Reinier, C., and Hudson, S., 2021, A Preliminary Assessment of Olivine Phenocrysts from the Monogenetic Basalt of the McCartys Flow, Zuni Bandera Volcanic Field, New Mexico, *in* Frey, B.A., et al., eds., New Mexico Geological Society 72nd Annual Fall Field Conference Guidebook, p. 141-152.

Moll-Stalcup, E., Plafker, G., and Berg, H., 1994, Latest Cretaceous and Cenozoic magmatism in mainland Alaska, *in* Plafker, G., and Berg, H.C., eds., The geology of Alaska: Geological Society of America, The Geology of North America, p. 589-619.

Morgan, W.J., 1971, Convection plumes in the lower mantle: Nature, v. 230, p. 42-43.

Mukasa, S.B., Andronikov, A.V., and Hall, C.M., 2007, The $^{40}Ar/^{39}Ar$ chronology and eruption rates of Cenozoic volcanism in the eastern Bering Sea Volcanic Province, Alaska: Journal of Geophysical Research, v. 112, p. 1-18, doi:10.1029/2006JB004452.

Pankhurst, M.J., Morgan, D.J., Thordarson, T., and Loughlin, S.C., 2018, Magmatic crystal records in time, space, and process, causatively linked with volcanic unrest: Earth and Planetary Science Letters, v. 493, p. 231-241, https://doi.org/10.1016/j.epsl.2018.04.025.

Rae, A.S.P., Edmonds, M., Maclennan, J., Morgan, D., Houghton, B., Hartley, M.E., and Sides, I., 2016, Time scales of magma transport and mixing at Kilauea Volcano, Hawai'i: Geology, v. 44, p. 463-466, https://doi.org/10.1130/G37800.1.

Shea, T., Lynn, K.J., Garcia, M.O., 2015, Cracking to olivine zoning code: Distinguishing between crystal growth and diffusion: Geology, v. 43, no. 10, p. 935-938, doi:10.1130/G37082.1.

Wilson, J.T., 1963, A possible origin of the Hawaiian Islands: Canadian Journal of Physics, v. 41, p. 73-81.

Winer, G.S., Feeley, T.C., and Cosca, M.A., 2004, Basaltic volcanism in the Bering Sea: geochronology and volcanic evolution of St. Paul Island, Pribilof Islands, Alaska: Journal of Volcanology and Geothermal Research, v. 134, p. 277-301, doi:10.1016/j.jvolgeores.2004.02.003.

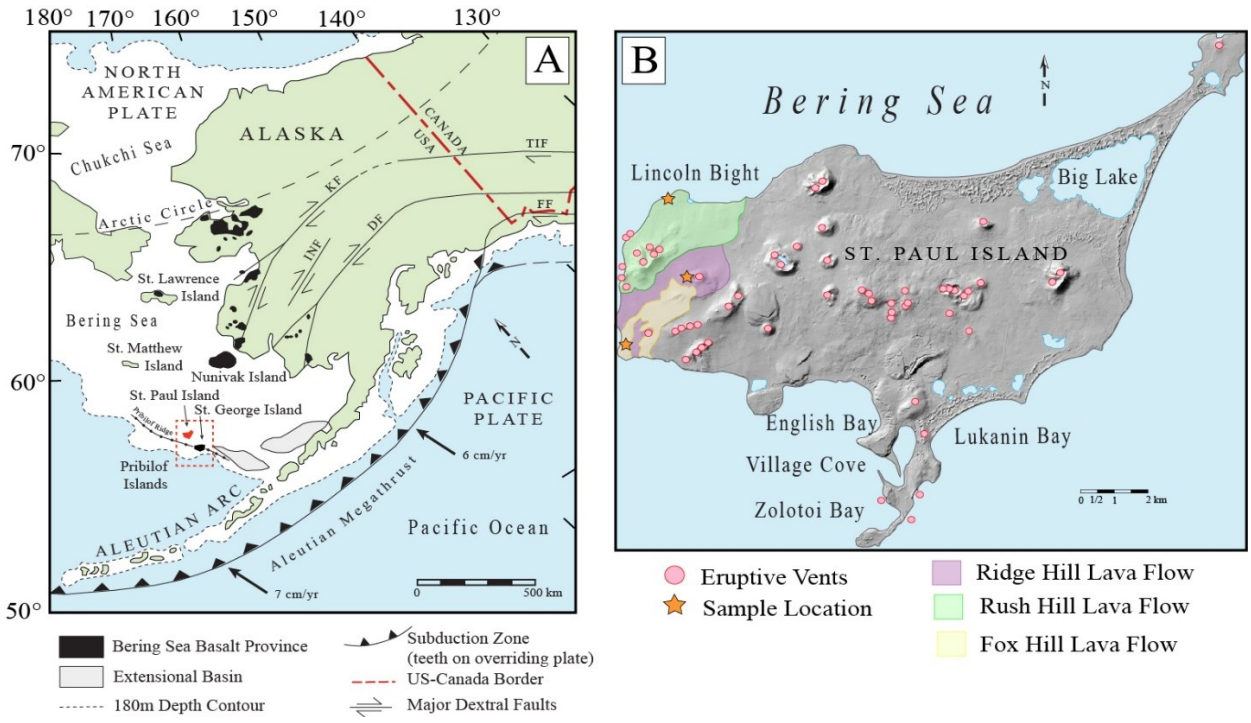

Figure 1. (A) Location diagram and generalized tectonic setting of the Pribilof Islands, Alaska located on the edge of the Bering Sea shelf (red dashed box) modified from Change et al. (2009). (B) Digital Earth Model of St. Paul Island showing topography and highlighting the lava flows and sample locations used in this study.

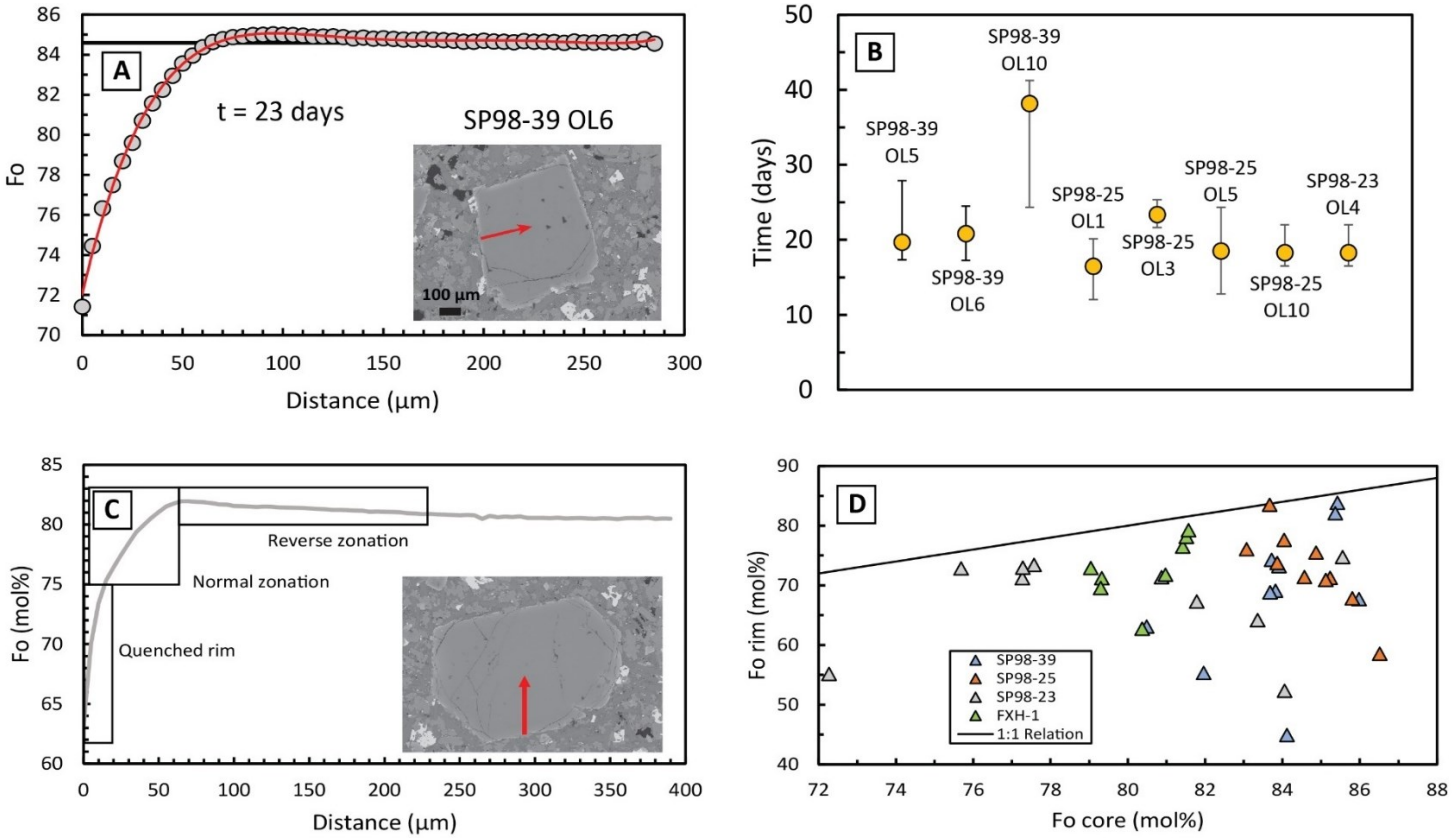

Figure 2. (A) Backscatter electron image (BSE) and compositional transect of forsterite (Fo) across an olivine phenocryst with a best-fit one-dimensional diffusion model (red line) fit to the natural data (grey circles). Dashed black line represents initial composition or core composition. (B) Comprehensive graph displaying calculated time scales with associated error bars for all the phenocrysts I found suitable for diffusion modeling (n=8). (C) Type 1B olivine phenocryst showing reverse zonation, normal zonation, and quenched outer rim. (D) Core vs. rim compositions of olivine phenocrysts from all studied St. Paul lava flows. FXH-1, SP98-39, and SP98-25 show less variability in core compositions than rim compositions. SP98-23 shows a larger variability in both core composition and rim composition. All phenocrysts plot below the black 1:1 line, meaning they have an overall normal zonation.

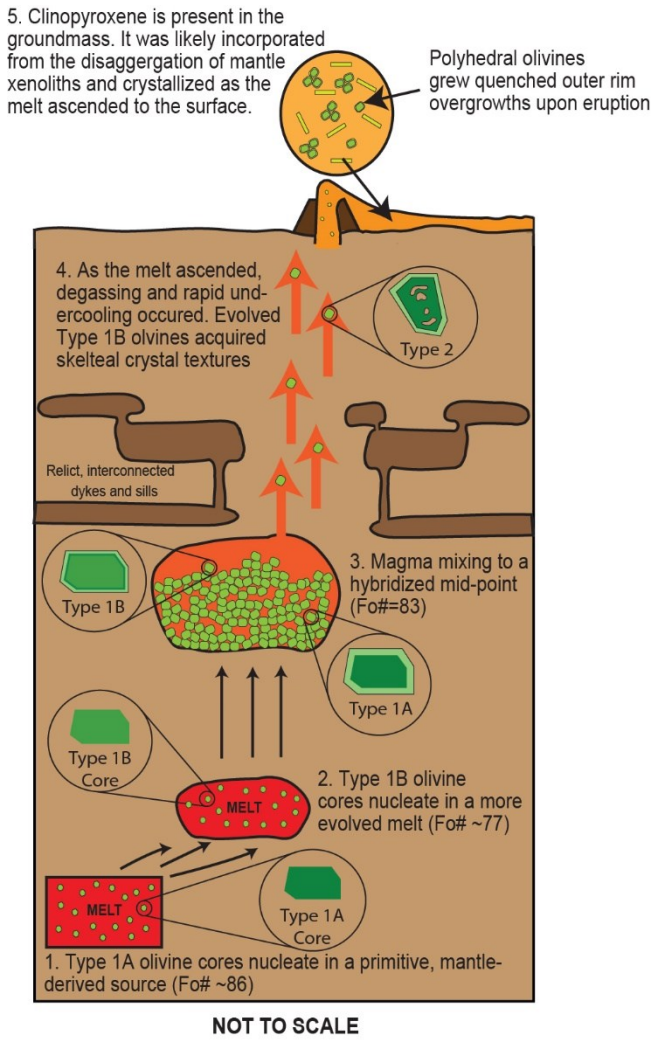

Figure 3. Schematic diagram modeling the volcanic plumbing system underlying St. Paul Island. At step 1, type 1A olivine cores nucleate in a primitive mantle melt (Fo_{86}). At step 2, type 1B olivine cores begin nucleating in a more evolved melt (Fo_{77}). The two magmas mix at step 3 in a melt that re-equilibrates to a mid-point between the two compositions (Fo_{83}). Type 1B cores are saturated in a higher Fo content magma, causing reverse zoning. Type 1A olivine cores are saturated in a slightly lower Fo melt, resulting in normal zoning. After ~20 days, the system exploits pre-existing fractures and rises to the surface. At step 4, the melt degasses causing rapid undercooling and evolved type 1B phenocrysts morph to skeletal crystal textures prior to their expulsion onto the surface. At the surface, olivine phenocrysts grow quenched, thin outer rim overgrowths. Modified from Couperthwaite et al. (2020).

MANUSCRIPT 2: LITHOSPHERIC MELTING AND METASOMATISM BENEATH THE PRIBILOF ISLANDS: INSIGHTS FROM SPINEL PERIDOTITE XENOLITHS FROM ST. GEORGE ISLAND, ALASKA

Abstract

Small volume basaltic magmas erupted at continental intraplate environments provide essential constraints on mantle melting and mantle heterogeneities. St. George Island, located approximately 400 km north of the Aleutian Island arc front, is of 15 regionally dispersed late Cenozoic (<6 Ma) volcanic fields making up the larger Bering Sea Basaltic Province. Alkali basalts host a suite of protogranular spinel-facies lherzolite xenoliths erupted from small volume monogenetic and shield volcanoes (2.8–1.4 Ma). Here, I present modal percentages and high precision major and trace element contents of clinopyroxene, olivine, and spinel from the xenoliths to investigate partial melting and metasomatism processes generating basaltic magma compositions. Lherzolite xenolith compositions range from fertile (15–19% modal diopside) to depleted (10–8% modal diopside) with variable degrees of melt extraction (7–18%) from a primitive mantle source. All the analyzed xenoliths show melt-reaction textures characterized by glass-bearing, sieved textured clinopyroxene and spinel rims. Several sieved-textured clinopyroxene crystals are associated with melt pockets of coinciding silicic glass and quench-textured olivine, spinel, and feldspar. In general, whole-rock and clinopyroxene primitive mantle-normalized REE trends are similar, suggesting that whole-rock compositions reliably recorded REE patterns of the xenoliths before transportation to the surface. Whole-rock and clinopyroxene REE patterns range from LREE-enriched to LREE-depleted, with several samples generally exhibiting flat MREE patterns. Melt-reaction textures indicate melt was present in the xenoliths at the time of eruption. However, xenoliths with the most significant melt infiltration lack a metasomatic signature in their REE and trace element contents. These data show that simple mixing relationships between host rock and xenoliths only permit small volumes of melt to infiltrate from the surrounding host basalt that entrains and transports the xenolith to the surface.

Introduction

Convection within the mantle and plate-tectonic related processes have long been recognized as mechanisms that generate heterogeneity within the mantle. Mantle xenoliths, fragments of Earth's upper mantle entrained in mafic magmas and transported to the surface, provide feedback on the geochemical processes occurring within the mantle. Extensive research has been conducted on the processes responsible for lithospheric mantle heterogeneities and how

the interaction between melt/fluid and xenoliths affects lithospheric fragments during their ascent to the surface (Batanova and Savelieva, 2009; Bodinier et al., 1990, 2004; Bodinier et al., 1987). However, it has only been within the past decade that *in situ* analytical techniques, such as microprobe analyses and laser ablation inductively coupled mass spectrometry (LA-ICP-MS), have been used to better understand rare earth element (REE) and trace element distributions of coexisting mineral phases within mantle xenoliths. This relatively new view on lithospheric mantle heterogeneities has been applied to spinel facies lherzolite xenoliths from the Pribilof Islands, Bering Sea, Alaska.

The Bering Sea basalt province (BSBP) is a minimally studied location of extensive regional intraplate volcanism behind the modern-day Aleutian arc front (Moll-Stalcup, 1994). Approximately 15 late Cenozoic (<6 Ma) volcanic fields constitute the BSBP, defining a *diffuse* igneous province (Wirth et al., 2002). Compared to other igneous-related environments, basaltic volcanism in diffuse igneous provinces has not been as aggressively studied. Most studies of the BSBP have only been regional, with little focus on the stratigraphy, evolution, and eruptive behavior of individual volcanic centers. Eruptive centers within the BSBP retain crucial information on the structural and magmatic setting of the Bering Sea region. Recent studies by Winer et al. (2004) and Chang et al. (2009) focused on individual eruptive centers to investigate magmatic evolution, mantle source compositions, potential mantle temperatures, and model petrogenetic processes. The results of these studies suggest basaltic rocks in the BSBP likely reflect the melting of a metasomatically enriched depleted lithosphere. However, the processes responsible for subcontinental lithospheric transformation are still not well constrained.

This paper describes the bulk compositions, petrography, and mineral chemistry of spinel facies lherzolite xenoliths from St. George Island, Pribilof Islands, Alaska, to better constrain

modification of the lithospheric mantle. The intent of this study is to use these data to differentiate between melting and metasomatic processes that affected the xenoliths while they resided in the mantle versus secondary processes imposed during or just prior to magmatic transport. This is important because bulk compositions of mantle xenoliths can only provide essential constraints on the nature of the lithospheric mantle if diverse processes that contribute to imparting conflicting geochemical signatures to individual xenoliths can be unraveled. In this regard, microbeam studies involving electron microprobe and laser ablation ICPMS data provide spatial resolutions of major and trace elements among and within individual phases that allow differentiation of these processes. The textures and compositional characteristics of the spinel lherzolite xenoliths from St. George Island provide information on some of the fundamental melting and metasomatic processes that have affected the lithosphere in western Alaska.

Regional and Local Geologic Setting

The Pribilof Islands, Alaska are situated nearly 400–450 km north of the modern-day Aleutian arc front on the southern edge of the Bering Sea shelf near the 180-m depth contour, which represents a sharp break in bottom topography between the shelf region to the northeast and the Aleutian basin to the southwest (Fig. 1; Moll-Stalcup, 1994; Winer et al., 2004; Chang et al., 2009). The Pribilof's are composed of five volcanic islands: three small islets and two principal islands, St. George (~95 km^2) and St. Paul (~104 km^2; Winer et al., 2004). The islands are predominantly constructed of mafic lavas extruded on the Pribilof Ridge, a structural arch trending northwest–southeast on the southern Bering Shelf containing rocks as old as the late Jurassic (Marlow et al., 1976, 1994). The modern-day thickness of the underlying continental crust beneath the islands is 30–35 km (Klemperer et al., 2002).

Intraplate-related volcanism in the BSBP is associated with extension in western Alaska and the Bering shelf region (Marlow et al., 1976, 1994; Worrall, 1991; Cooper at al., 1992; Plafker and Berg, 1994a; Moll-Stalcup, 1995). The Bering shelf was an active convergence zone prior to early Tertiary times (Marlow and Cooper, 1980; Davis et al., 1989; Marlow et al., 1994; Plafker and Berg, 1994a). Motion along this margin halted approximately 50 Ma when subduction shifted to the south causing the Pacific plate to begin subducting beneath Alaska, trapping remnants of the Kula plate behind the developing Aleutian arc in the process (Hillhouse and Coe, 1994). Since, the overriding North American plate and the subducting Pacific plate have experienced dextral-oblique convergence along the northwest–southeast-trending Transition Fault and orthogonal convergence along the northeast–southwest-trending Aleutian arc margin (Fig. 1, Plafker and Berg, 1994a). Present day motion of the Pacific plate is northwest relative to mainland Alaska at rates greater than 4.9 cm/year in southeastern Alaska and upwards of 7.7 cm/year at the western end of the Aleutian arc (Plafker and Berg, 1994a). Interaction between the Pacific–North American plates has resulted in the development of the Aleutian subduction zone and the subsequent magmatic arc; wrench faulting along the margin of the Bering Sea shelf resulting in basin formation; and regional small batch basaltic magmatism of the Bering Sea basalt province (Fig. 1, Plafker and Berg, 1994a, 1994b).

Eruptive activity on St. George Island began as early as 2.8 Ma and continued until at least 1.4 Ma (Feeley et al., 2007; Mukasa et al., 2007). The volcanic center is predominantly influenced by east-west- to northeast-southwest-trending extensional faults, and the topography of the island is now dominated by several similarly trending fault ridges and wave-eroded sea cliffs, the highest of which are greater than 300 m above sea level (Fig. 2; Feeley et al., 2007; Chang et al., 2009). The result is many highly exposed and well-defined stratigraphic sections,

some of which rest directly on pre-Tertiary basement. A serpentinized peridotite body intruded by a garnet-bearing quartz diorite dike with U/Pb zircon age of 52.9±1.5 Ma is exposed on the southeast side of the island (Fig. 2; Davis et al., 1989). Geochemical data in relation to age data indicate no progressive petrologic trends during evolution of the St. George magmatic system, except for late eruption of distinctive plagioclase-phyric basalts with low to moderate MgO contents (5–7 wt.%) beginning at approximately 2.0 Ma (Feeley et al., 2007).

Xenoliths examined in this study were collected from a single large (~0.5 m diameter) boulder sample (SV05-33) along the north-central coast of St. George Island. The boulder was presumed to have originated from an eroded lava flow erupted from the First Bluff eruptive center (Fig. 2). Unfortunately, this is impossible to confirm given that in-place rocks exposed near First Bluff form the Staraya Artil northern fur seal rookery, and is therefore, off limits to sampling.

Methods

Whole Rock Major and Trace Element Analysis. Xenoliths were separated from the host lava flow using a circular diamond blade saw. The cut surfaces were subsequently abraded with quartz in a sand blaster to remove any possible contamination from the saw blade. Whole rock major and minor element analyses were determined by X-Ray fluorescence (XRF) at the GeoAnalytical Lab at Washington State University by the method of Johnson et al., (1999). Trace element compositions of whole rock samples were determined by inductively coupled plasma mass spectrometry (ICP-MS) following the procedures outlined by Knaack et al. (1994).

Mineral Major and Trace Element Analysis. Mineral major and trace element data used in this study were collected during multiple analytical sessions at varying institutions.

Previously obtained and unpublished major element compositions of minerals were obtained using wavelength-dispersive analyses via a Cameca SX50 electron microprobe at the University of Lausanne, Switzerland, using a set of natural and synthetic mineral standards, 15 keV accelerating voltage, 20 nA beam current, and a beam diameter of 2–5 μm. Given the small size of the xenoliths, mineral modes were calculated from least squares regression analyses of mineral proportions and compositions to match whole rock compositions using the IGPET software (Terra Softa, Inc.).

A second dataset of major element compositions of olivine and clinopyroxene were determined using a JEOL JXA-8230 Superprobe electron-probe microanalyzer (EPMA) equipped with five wavelength-dispersive spectrometers and large-formatting diffracting crystals at the University of Iowa, using a 20 keV accelerating voltage and a 20 nA beam current with the beam in spot mode. San Carlos olivine (NMNH 111312-44) was used to calibrate the EPMA for Mg and Ni, and the Astimex Cr pyrope reference material was used to calibrate Si, Fe, Ca, Ti, Mn, Cr, and Al. Prior to each analytical run, peak positions for Ca, Al, Ti, Mn, Cr, and Ni were determined via long dwell times, 200 nA wavelength scans of San Carlos olivine (NMNH 111312-44; Jarosewich et al., 1980) and Kakanui augite (NMNH 122142; Jarosewich et al., 1987), and entered manually into the analytical routine. Major element peak positions were updated before analysis using software peak search routines. The total run-time per spot analysis was 7 minutes, with an on-peak dwell time of 40 seconds for major elements, and 90 seconds for minor and trace elements excluding Al, and a background dwell time of 15 seconds for all elements excluding Al. For Al, on-peak and background dwell times were 360 seconds and 60 seconds, respectively. San Carlos olivine values obtained via EPMA were consistent with

published values with a variability (% r.s.d.; Jarosewich et al., 1980) of <1% for all elements. The detection limit for Al is 10 ppm and 20–30 ppm for Cr, Ni, Ca, and Ti.

Laser ablation measurements on clinopyroxene crystals were determined using an Element XR sector field ICPMS system (ThermoFisher Scientific, Germany and USA) at the Institute of Mineralogy and Geochemistry, University of Lausanne, Switzerland. Operating Conditions of the laser included an output energy of 8 mJ (equivalent to 5 J/cm^2 on-sample fluence), 20 Hz repetition rate, and 75–100 μm pit sizes. Helium was used as a cell gas. The acquisition times for the background and the ablation interval were 70 and 60 seconds, respectively. Almost all isotope masses were scanned using four acquisition points per peak, the mass window having been set at 20% of the peak width. Dwell times per point were 5 ms for ^{42}Ca and ^{27}Al and 10 ms for trace elements. The ThO^+/Th^+ and Ba^{2+}/Ba^+ ratios were optimized to 0.1–0.2% and 1.0–1.4%, respectively. The NIST 612 synthetic glass was used for external standardization. Calcium-42 served as the internal standard. Intensity versus time data were reduced in LAMTRACE. They were checked for the presence of intensity 'spikes' and corrected when necessary. The average element values in the NIST 610 and 612 glasses were taken from Pearce et al., (1997).

Results

Lava Whole Rock Geochemistry. St. George Island lavas comprise a suite of alkali basalts with nearly constant MgO contents (8.2–11.9 wt.%) and a large range of SiO_2 contents (40.9–48.8 wt.%) defining three distinct clusters of whole rock compositions. A detailed discussion of whole rock lava compositions and petrogenesis of the Pribilof Islands is presented in Chang et al. (2009) and therefore, will not be discussed in-depth here. In general, St. George

basalts are classified as basanites, alkali basalts, and marginally subalkali to hawaiites. Whole rock REE trends from St. George show LREE contents that are approximately 50–100 times chondrite normalization values and HREE contents that are approximately 10 times chondrite normalization values. Trace element contents of St. George basalts show more diversification in LREE contents compared to St. Paul basalts, but overall, are similar with no significant Eu or Sm anomalies (Chang et al., 2009).

Petrography and Xenolith Classification. In all St. George rock types, xenoliths and xenocrysts are commonly dispersed throughout the rock. Dunite and spinel lherzolite are the most abundant xenoliths throughout all St. George rocks. The analyzed alkali basalt sample in this study, and xenoliths from other lava flows, host abundant spinel-facies lherzolite xenoliths up to 20 cm in size, which were classified by modal compositions in an olivine–orthopyroxene–clinopyroxene diagram (Fig. 3). Xenocrysts in the observed samples, from most to least abundant, include olivine (54.8–68 vol.%), orthopyroxene (26.6–16.5 vol.%), clinopyroxene (9–20 vol.%), spinel (0.8–3.1 vol. %), plagioclase, and rare amounts of quartz (Fig. 4; Table 1). Melt-reaction textures characterized by glass-bearing, sieved textured rims on clinopyroxene and spinel can be observed in all xenoliths. In many of the samples, clinopyroxene grains show sieve textures and are associated with melt pockets within the xenolith that have compositions of coexisting silicic glass (Na- ± K-rich) and quench-textured olivine, spinel, clinopyroxene, and feldspar (Fig. 4).

Xenolith Whole Rock Geochemistry. Major element and trace element contents for St. George xenoliths and host lava flows are illustrated in Figures 5 and 6 and the full dataset is presented in Table 1. In general, major elements for the xenoliths are restricted with little variability. Major element compositions are compared to St. George lava flows. Silica contents

of the xenolith samples range from 42.70–44.30 wt.% and tend to decrease with increasing MgO content. It should be noted that there is noticeable SiO_2 enrichment in sample SG05-33x9 when compared to the primitive mantle (PM; Fig. 5). Calcium contents range from 2.01–4.20 wt.% and tend to increase with increasing SiO_2 content. It should be noted that xenolith sample SG05-33x2 shows enriched CaO when compared to the primitive mantle (PM; Fig. 5). Aluminum contents range from 1.78–3.92 wt.% and tend to decrease with increasing MgO content. Major element contents are less restricted than Na_2O, K_2O, and TiO_2 which range in contents from 0.24–0.47 wt.%, 0.001–0.047 wt.%, and 0.06–0.22 wt.%, respectively.

Trace element relationships versus Al_2O_3 for St. George xenoliths are illustrated in Figure 6. In general, all the plotted trace elements (i.e., Sr, Rb, Sm, Zr, Th, and Nb) increase with increasing Al_2O_3 (1.78–3.92 wt.%) contents. Strontium contents are variable ranging from 4–28 ppm. Rubidium, Sm, Zr, Th, and Nb are more restricted in their contents ranging from 0.1–0.6 ppm, 0.17–0.65 ppm, 1–9 ppm, 0.01–0.07 ppm, and 0.19–0.61 ppm, respectively. When compared to trace element contents of the primitive mantle (PM), it should be noted that there are enrichments of Sr, Nb, Th, Sm, Rb, and Zr in xenolith sample, SG05-33x9 (Fig. 6).

Major Element Compositions of Minerals. A representative suite of the analyzed minerals clinopyroxene, olivine, and spinel from St. George xenoliths are presented in Tables 2, 3, and 4, respectively. All mineral phases are commonly homogenous in oxides based on the core-to-rim EPMA analysis. Olivine Mg# (Mg#=(MgO/(MgO+FeO))*100, atomic number) range from 78.5–83.4 with an average of 82. In general, Al_2O_3 is tightly restricted in most of the analyzed crystals ranging from 0.02–0.06 wt.%. Calcium, NiO, and Cr_2O_3 contents are slightly more variable ranging from 0.06–0.99 wt.%, 0.03–0.39 wt.%, and 0.02–0.41 wt.%, respectively. The clinopyroxene population has a relatively higher Mg# range of 87.8–90.5 with an average of

90. Major elements Al_2O_3 (4.57–5.66 wt.%), CaO (0.88–1.13 wt.%), Cr_2O_3 (0.37–0.69 wt.%), and Na_2O (0.11–0.21 wt.%) show a small range of content variability. Spinels have a Mg# of 66.4–69.8 and Cr# (Cr#=(Cr/(Cr+Al))*100, atomic number) of 11.3–11.5. All the analyzed spinels are homogenous with very little variability in major element contents.

Trace Element Compositions of CPX. Trace element compositions of clinopyroxenes (Cpx) from St. George lherzolites are reported in Table 5. Rare Earth Element (REE) and multi-trace element distribution patterns are illustrated in Figures 7 and 8. Three clinopyroxene populations are represented in the lherzolite xenoliths. There is a LREE-depleted clinopyroxene population, a LREE-enriched clinopyroxene population, and a population with intermediate REE abundances (Fig. 8). Ratios for LREE/HREE (e.g., La/Yb) range from 0.08–9.63 ppm. MREE ratios for Dy/Yb and La/Sm range from 1.31–2.29 ppm and 0.11–4.46 ppm, respectively.

Discussion

Mantle xenoliths are compositionally influenced by variable degrees of partial melting, melt extraction, and metasomatism. Therefore, their characteristics and chemical contents record deep-earth processes (Pearson et al., 2014). Using major element contents of olivine, equilibrium temperatures for the mantle xenoliths were calculated using Beattie (1993) and Putirka (2008) geothermometers. Overall, the estimated temperatures from the different geothermometers are generally in good agreement with one another. The equilibrium temperatures of the mantle xenoliths range from 1737 °C to 1820 °C, reflecting olivine crystallization temperatures in the mantle. Pribilof Island host lava temperatures were estimated by Chang et al. (2009) ranging from 1268–1427 ± 45°C with an average of 1372 ± 45°C.

Subcontinental lithospheric mantle often experiences complex melt extraction events that cause depletion of basaltic components such as Al_2O_3, CaO, TiO_2, and increasing MgO contents in residues (Xu et al., 2021; Herzberg, 2004). Mantle metasomatism, the process in which a bulk composition of a rock is altered from its original state by the introduction of components from an alternate source, could add Ca, Al, and Fe to peridotites that experience melt extraction (Griffin et al., 2003; Carlson et al., 2004). The St. George mantle xenolith suite comprises fertile to moderately refractory spinel-facies lherzolites resulting from variable degrees of partial melting and metasomatism. Whole-rock lherzolites and clinopyroxene crystals have similar REE trends within a single xenolith, indicating the whole-rock and clinopyroxenes are well-equilibrated, and whole-rock compositions reliably recorded pre-entrainment REE patterns (Fig. 7). Whole-rock and REE trends range from LREE-depleted (SG05-33x11) to LREE-enriched (SG05-33x9), with samples generally having moderate LREE-depleted to flat REE patterns (SG05-33x2 and SG05-33x7). Rare earth elements and other trace elements give detailed insights into the partial melting and metasomatic history of lherzolite xenoliths from St. George Island.

Evidence for Partial Melting. Major and trace element compositional variation diagrams for St. George lherzolite xenoliths are consistent with variable degrees of melt extraction from a primitive mantle source (Figs. 5, 6). Specifically, major elements SiO_2 and Al_2O_3, except for SG05-33x9 regarding SiO_2, tend to decrease with increasing MgO contents, indicative of melt depletion from a primitive mantle source (Fig. 5). Trace elements Th and Nb also show trends consistent with melt depletion, suggesting a control by partial melting (Fig. 6). Plotting the known contents of yttrium (Y) and ytterbium (Yb) of clinopyroxene from the xenoliths on batch and fractional melting models estimate 1-15% melting of a primitive mantle source is needed to reproduce the measured contents (Fig. 9A). Based upon these models, REE

contents for clinopyroxene can be predicted for 1-5% batch melting and 3% fractional melting (Fig. 9B). The predicted REE trend calculated from 1-5% of batch melting fits best to the analyzed clinopyroxene crystals that have moderate LREE-depleted to flat-REE trends (Figs. 8, 9B). The predicted REE trend calculated from 3% of fractional melting fits best to the measured clinopyroxene crystal that has the most LREE-depleted content (Figs. 8, 9B). These models support that at least two episodes of partial melting occurred to produce the REE contents measure in clinopyroxene crystals from the xenoliths, with an exception to the most LREE-enriched clinopyroxene (e.g., SG05-33x9).

Chemical maps of refractory mantle xenoliths (i.e., depleted in incompatible trace elements) further support multiple episodes of partial melting and melt extraction from a primitive mantle source, specifically a spinel-facies primitive mantle source (Fig. 11). This implication is supported by the two generations of spinels present in refractory xenolith sample SG05-33x8. First-generation spinels are characterized by having high Al and low Cr contents, and second-generation spinels are characterized by having lower Al contents and higher Cr contents, relative to the first generation. This is consistent with episodes of melt extraction from a spinel-facies primitive mantle source. Depletions in the incompatible element Al and major element Mg are evident along the grain boundaries of spinel in refractory xenolith sample SG05-33x8, suggesting a spinel reaction occurring during partial melting (Fig. 11). The LREE-enrichment seen in the most refractory xenolith sample, SG05-33x9, indicates that partial melting occurred first to establish the fertile to moderately refractory xenoliths, followed by later metasomatism that enriched the clinopyroxene in REE (Bodinier et al., 1987). Additionally, a portion of the lherzolites have clinopyroxene and whole-rock compositions depleted in LREE, U, and Th, indicating they are likely residues of more recent partial melting (Figs, 7, 8).

Evidence for Metasomatism. Existence of different types of metasomatism (i.e., cryptic and patent), enrichments of incompatible trace elements, and the absence of hydrous minerals (e.g., mica and/or amphibole) suggests St. George xenoliths experienced multiple episodes of metasomatism. Whole-rock xenolith chemical maps show initial evidence for melt-pockets (MP) enriched with the incompatible trace element Al, which indicates a metasomatic event which reintroduced Al into the xenolith (Fig. 4). Fertile mantle xenoliths in host alkali basalts from St. George are characterized by enrichments in incompatible elements, such as Al. Metasomatism can be further investigated by looking closer between the grain boundaries of olivine (Ol) and clinopyroxene (Cpx) in fertile xenolith sample SG05-33x2 (Fig. 10). In addition to Al enrichments, melt pockets also show enrichments in Na, Si, and to a lesser degree Ca, with the presence of secondary olivine phases (i.e., Mg enrichment) forming within the melt pockets (Fig. 10). This indicates a patent metasomatic evident forming secondary mineral phases and enriching the xenolith in incompatible elements. Rare earth element contents of sample SG05-33x9 show steep enrichments in LREE which is further evidence for metasomatism (Fig. 8).

In addition to the chemical maps and LREE enrichments, evidence for metasomatism is present in xenolith whole-rock major and trace element compositional variation diagrams (Figs. 5, 6). Sample SG05-33x9 shows slight enrichments in major element SiO_2, and trace elements Sr, Th, Nb, and to a lesser degree Rb, Sm, and Zr (Figs. 5, 6). Xenolith sample SG05-33x2 shows an enrichment in CaO. These enrichments deviate from the melt-depletion trends seen from a primitive mantle source, indicating metasomatism.

A Model of Partial Melting and Metasomatism. Petrographic and geochemical evidence suggest that St. George lherzolite xenoliths experienced at least two partial melting episodes and two metasomatic episodes before their entrainment in Pribilof Island basalts.

Initially, an ancient partial melting episode established the fertile to moderately refractory xenoliths with variable modal diopside contents and Mg#. Petrographic observations support this must have been an ancient episode because the most refractory xenolith (e.g., SG05-33x9) shows no notable evidence for melting between grain boundaries or melt-reaction textures. In other words, mineral grains that constitute SG05-33x9 are well annealed with distinct boundaries, and the absence of melt-pockets further supports this was an ancient partial melting episode. On major and trace element compositional variation diagrams for St. George lherzolites, trends are consistent with episodes of melt extraction from a primitive mantle source.

Additionally, LREE-enrichment in clinopyroxene from SG05-33x9 is uncharacteristic of mantle residues, suggesting refractory xenoliths experienced partial melting first, followed by later metasomatism (Kourim et al., 2021). A second, more recent partial melting episode best explains petrographic observations and REE trends in the most fertile xenolith sample (e.g., SG05-33x2). The strongest evidence comes from petrographic observations where melt-pockets indicate partial melting occurring moments before the system began to ascend to the surface. This episode of melting would have moderately depleted diopsides in REE, especially LREE, which is observed in fertile xenolith SG05-33x2 (Fig. 8). Batch melting and fractional melting models were used to estimate the degree of partial melting needed to fit the observed REE systematics using trace element Y_n plotted against Yb_n (Fig. 9). These data fit both models for batch and fractional melting suggesting approximately 1–5% batch melting and 3% fractional melting of a fertile source would produce the compositions seen in lherzolite xenoliths from St. George, excluding the LREE-enriched sample SG05-33x9. Batch melting produces the most reasonable fit for moderate REE content samples (e.g., SG05-33x2), while fractional melting best explains LREE-depleted patterns in clinopyroxene (e.g., SG05-33x11).

St. George lherzolite xenoliths provide evidence for at least two different melt-driven metasomatic episodes prior to and during transport to the surface. Diopsides are generally well-equilibrated with the whole-rock, and therefore, accurately record metasomatic enrichment events that pre-date the magmatism responsible for bringing the xenoliths to the surface. The first metasomatic event would have been an ancient or cryptic episode that altered the composition of pre-existing mineral phases, enriching them in LREE and other highly incompatible trace elements (Fig. 8). This event is suggested to be ancient based on the petrography and REE contents of SG05-33x9, which has well-annealed grain boundaries in equilibrium with the whole-rock. Meaning after metasomatism, mineral grains and the whole rock had time to re-equilibrate, supporting this was an ancient event. Sample SG05-33x9, the most refractory lherzolite, is the only sample to shows clear compositional evidence for this metasomatic episode. A second, more recent, patent metasomatic episode involved the infiltration of a Si-, Al-, Na-, ± K-rich melt and the formation of secondary olivine. However, there is no compositional evidence or over-printing of this event in the mineral or whole-rock compositions. Instead, this event was interpreted by the melt-reaction textures between olivine and clinopyroxene grains observable in the chemical map for fertile mantle xenolith SG05-33x2 (Fig. 10). Recent metasomatism likely reflects small amounts of melt infiltration from localized melting of clinopyroxene and spinel producing a Si-, Al-, and Na-rich melt with K-enrichment coming from diffusion of K from the host basalt during transport and residence times in crustal reservoirs during ascent to the surface. Despite this evidence, recent metasomatism is not suggested to be the cause of or related to the ancient metasomatism.

Relationship of Host Alkali Basalts to Mantle Xenoliths. Many of Pribilof Island basalts' major and trace element contents are like ocean island basalts (OIB), such as enriched

alkalis and incompatible trace elements (Chang et al., 2009). After investigation, the geochemical nature of mantle xenoliths from St. George suggests that erupted basalts in the Pribilof Islands are not sourced from melting of lherzolite xenoliths. This is supported when trace element contents for both fertile (SG0533x2) and refractory (SG05-33x9) sources are compared to trace element contents of whole rock sample SG05-33 (Fig. 12). In this regard, both fertile and refractory xenoliths have trace element contents that would be too low to produce the host basalt compositions at low degrees of partial melting (Fig. 12). Instead, a primitive mantle source with residual garnets that strongly partition HREE best fits the trace element contents seen in host alkali basalts from St. George. This suggests St. George Island basalts are extracted from the garnet stability field during partial melting, and the spinel-facies xenoliths are plucked and entrained as the melt migrates upwards toward the surface.

Conclusion

Petrographic and geochemical analysis of spinel-facies lherzolites xenoliths in host alkali basalts from St. George Island show evidence for multiple episodes of partial melting and metasomatism in the underlying mantle lithosphere. Two populations of spinel lherzolite xenoliths were identified as being fertile and refractory based on trace element chemical composition and grain boundary textures. The most refractory lherzolite xenolith analyzed in this study hosts LREE-, Nb-, and Ta-enriched diopside crystals that are well-equilibrated with the whole rock, suggesting that an ancient metasomatic enrichment event occurred that pre-dates the magmatism responsible for entraining the xenoliths and transporting them to the surface. The melt reaction textures observable in the more fertile lherzolite xenoliths indicate that melt infiltration was active in some xenoliths at time of the eruption. However, it should be noted that

this melt infiltration is not responsible for the cause of ancient metasomatism because the samples most heavily infiltrated by melt lack a metasomatic signature in their mineral and whole-rock compositions. Additionally, the infiltrated melt is likely not the same melt responsible for the host alkali basalts but is rather due to localized melting of clinopyroxene and spinel fluxed by an alkali-rich fluid.

Trace element compositions of host alkali basalts compared to both fertile and refractory xenoliths suggest that the mantle xenoliths had no role in sourcing the magmas responsible for the Pribilof Island basalts. The mantle xenoliths host multiple generations of spinels that support they are sourced from the spinel-facies primitive mantle. Both fertile and refractory spinel-facies xenoliths have trace element contents too low to produce the trends seen in host alkali basalts at low degrees of partial melting. Instead, the source responsible for the host alkali basalts is better explained by a primitive mantle source with residual garnets. This implication is supported by trace element systematics and the necessity for melting in the garnet stability field. In this regard, mantle xenoliths were simply plucked and entrained in the host basalts as melt was extracted from the garnet-peridotite portion of the mantle and ascended to the surface.

Acknowledgements

This project was supported by Graduate Student Research grants from the Missouri State University Graduate College and the Bruce L. “Biff” Reed Scholarship Award, Geological Society of America awarded to CLR, and a Missouri Space Grant Affiliate Award to GSM. The authors would like to thank Frank Ramos, Toby Dogwiler, and Matthew McKay for their technical expertise and logistical support during this project and Todd C. Feeley for providing

samples from NSF project EAR-0439676: “Evolution of Intraplate Volcanism in a Diffuse Igneous Province: A Case Study of the Pribilof Islands, Alaska.”

References

Batanova, V.G., Savelieva, G.N., 2009. Melt migration in the mantle beneath spreading zones and formation of replacive dunites: a review. Russian Geology and Geophysics 50, 763–778.

Beattie, P., 1993. On the occurrence of apparent non-Henry's law behaviour in experimental partitioning studies. Geochim Cosmochim Acta 57, 47-55.

Bodinier, J.L., Dupuy, C., Dostal, J., Merlet, C., 1987. Distribution of Trace Transition elements in Olivine and Pyroxenes from Ultramafic Xenoliths - Application of Microprobe Analysis. American Mineralogist 72, 902–913.

Bodinier, J.L., Vasseur, G., Vernieres, J., Dupuy, C., Fabries, J., 1990. Mechanisms of Mantle Metasomatism: Geochemical evidence from the Lherz Orogenic Peridotite. Journal of Petrology 31, 597–628.

Bodinier, J.L., Menzies, M.A., Shimizu, N., Frey, F.A., McPherson, E., 2004. Silicate, hydrous and carbonate metasomatism at Lherz, France: contemporaneous derivatives of silicate melt–harzburgite reaction. Journal of Petrology 45, 299–320.

Chang, J.M., Feeley, T.C., Deraps, M.R., 2009. Petrogenesis of Basaltic Volcanic Rocks from the Pribilof Islands, Alaska, by Melting of Metasomatically Enriched Depleted Lithosphere, Crystallization Differentiation, and Magma Mixing. Journal of Petrology 50, 2249-2286.

Carlson, R.W., Irving, A.J., Schulze, D.J., Hearn, B.C., 2004. Timing of Precambrian melt depletion and Phanerozoic refertilization events in the lithospheric mantle of the Wyoming Craton and adjacent Central Plains Orogen. Lithos 77, 453–472.

Cooper, A.K., Marlow, M.S., Scholl, D.W., Stevenson, A.J., 1992. Evidence for Cenozoic crustal extension in the Bering Sea region. Tectonics 11, 719-731.

Davis, A.S., Pickthorn, L.-B.G., Vallier, T.L., Marlow, M.S., 1989. Petrology and age of volcanic-arc rocks from the continental margin of the Bering Sea: implications for Early Eocene relocation of plate boundaries. Canadian Journal of Earth Sciences 26, 1474-1490.

Feeley, T.C., Cosca, M.A., Hamblock, J.M., Underwood, S.J., 2007. High precision $^{40}Ar/^{39}Ar$ geochronology and geology of St. George Island, Pribilof Islands, Alaska: Implications for eruption rates in the Bering Sea Basalt Province. EOS Transactions, American Geophysical Union 88, Abstract V23B-1433.

Griffin, W.L., O'Reilly, S.Y., Abe, N., Aulbach, S., Davies, R.M., Pearson, N.J., Doyle, B.J., Kivi, K., 2003. The origin and evolution of Archean lithospheric mantle. Precambrian Research 127, 19–41.

Herzberg, C., 2004. Partial crystallization of mid-ocean ridge basalts in the crust and mantle. Journal of Petrology 45, 2389–2405.

Hillhouse, J.W., Coe, R.S., 1994. Paleomagnetic data from Alaska, in: Plafker, G., Berg, H.C. (Eds), The Geology of Alaska. Geological Society of America, The Geology of North America G-1, pp. 797-812.

Jarosewich, E., Nelen, J.A., Norberg, J.A., 1980. Reference Samples for Electron Microprobe Analysis. Geostandards and Geoanalytical Research 4, 43-47.

Jarosewich, E., Clarke, S.R., Barrows N.J., 1987. Allende Meteorite Reference Sample. Smithsonian Contributions to the Earth Sciences, 1-49.

Johnson, D.M., Hooper, P.R., Conrey, R.M., 1999. XRF analysis of rocks and minerals for major and trace elements on a single low dilution Li-tetraborate fused bead. Advances in X-ray Analysis 41, 843-867.

Knaack, C.S., Cornelius, S., Hooper, P.R., 1994. Trace element analyses of rocks and minerals by ICP-MS. Washington State University, Geology Department, Open File Report, 4.

Klemperer, S.L., Miller, E.L., Grantz, A., Scholl, D.W., Group, B.-C.W., 2002. Crustal structure of the Bering and Chukchi shelves: Deep seismic reflection profiles across the North American continent between Alaska and Russia, in: Miller, E.L., Grantz, A., Klemperer, S.L. (Eds) Tectonic Evolution of the Bering Shelf-Chukchi Sea-Arctic Margin and Adjacent landmasses. Geological Society of America, Special Papers 360, pp. 1-24.

Kourim, F., Wang, K.-L., Beinlich, A., Chieh, C.-J., Dygert, N., Lafay, R., Kovach, V., Michibayashi, K., Yarmolyuk, V., Iizuka, Y., 2021. Metasomatism of the off-cratonic lithospheric mantle beneath Hangay Dome, Mongolia: Constraints from trace-element modelling of lherzolite xenoliths. Lithos, 400-401.

Marlow, M.S., Scholl, D.W., Cooper, A.K., Buffington, E.C., 1976. Structure and evolution of Bering Sea shelf south of St. Lawrence Island. AAPG Bulletin 60, 161-183.

Marlow, M.S., Cooper, A.K., 1980. Mesozoic and Cenozoic structural trends under the southern Bering Sea shelf. AAPG Bulletin 64, 2139-2155.

Marlow, M.S., Cooper, A.K., Fisher, M.A., 1994. Geology of the eastern Bering Sea continental shelf, in: Plafker, G., Berg, H.C. (Eds), The Geology of Alaska. Geological Society of America, The Geology of North America, pp. 271-284.

McDonough, W.F., Sun, S.S., 1995. The composition of the Earth. Chemical geology 120 (3–4), 223–253.

Moll-Stalcup, E., Plafker, G., Berg, H., 1994. Latest Cretaceous and Cenozoic magmatism in mainland Alaska, in: Plafker, G., Berg, H.C. (Eds.), The geology of Alaska. Geological Society of America, The Geology of North America, pp. 589-619.

Moll-Stalcup, E.J., 1995. The origin of the Bering Sea basalt province, western Alaska, in: Simakov, K.V., Thurston, D.K. (Eds), Proceedings of the International Conference on Arctic Margins. Magadan: Russian Academy of Sciences Far East Branch North East Science Center, pp. 113-123.

Mukasa, S.B., Andronikov, A.V., Hall, C.M., 2007. The $^{40}Ar/^{39}Ar$ chronology and eruption rates of Cenozoic volcanism in the eastern Bering Sea Volcanic Province, Alaska. Journal of Geophysical Research 112, 1-18.

Pearce, N.J.G., Perkins, W.T., Westgate, J.A., Gorton, M.P., Jackson, S.E., Neal, C.R., Chenery, S.P., 1997. A Compilation of New and Published Major and Trace Element Data for NIST SRM 610 and NIST SRM 612 Glass Reference Materials. Geostandards and Geoanalytic Research 21, 115-144.

Pearson, D.G., Canil, D., Shirey, S.B., 2014. Mantle samples included in volcanic rocks: Xenoliths and diamonds, in: Carlson, R.W. (Eds), Treatise on Geochemistry, 2nd ed. Oxford, UK, Elsevier, pp. 169–253.

Plafker, G., Berg, H.C., 1994a. Introduction, in: Plafker, G., Berg, H.C. (Eds), The Geology of Alaska. Geological Society of America, The Geology of North America G-1, pp. 1-16.

Plafker, G., Berg, H.C., 1994b. Overview of the geology and tectonic evolution of Alaska, in: Plafker, G., Berg, H.C. (Eds), The Geology of Alaska. Geological Society of America, The Geology of North America G-1, pp. 989-1021.

Putirka, K.D., 2008. Thermometers and barometers for volcanic systems. Reviews in Mineralogy and Geochemistry 69, 61–120.

Winer, G.S., Feeley, T.C., Cosca, M.A., 2004. Basaltic volcanism in the Bering Sea: geochronology and volcanic evolution of St. Paul Island, Pribilof Islands, Alaska. Journal of Volcanology and Geothermal Research 134, 277-301.

Wirth, K.R., Grandy, J., Kelley, K., Sadofsky, S., 2002. Evolution of crust and mantle beneath the Bering Sea region: Evidence from xenoliths and late Cenozoic basalts, in: Miller, E. L., Grantz, A. (Eds.), Tectonic Evolution of the Bering Shelf-Chukchi Sea-Arctic Margin and Adjacent landmasses. Geological Society of America, Special Papers 360, pp. 167-193.

Worrall, D.M., 1991.Tectonic history of the Bering Sea and the evolution of Tertiary strike-slip basins of the Bering Shelf. Geological Society of America, Special Papers 257, 120.

Xu, X., Tang, Y., Ying, J., Zhao, X., Xiao, Y., 2021. Three-stage modification of lithospheric mantle: Evidence from petrology, in-situ trace elements, and Sr isotopes of mantle xenoliths in the Cenozoic basalts, northeastern North China Craton. GSA Bulletin.

Table 1. Spinel lherzolite xenolith whole-rock major and trace element contents

	SG05-33x1	SG05-33x2	SG05-33x3	SG05-33x6	SG05-33x7	SG05-33x8	SG05-33x9	SG05-33x11	SG05-33x12	SG05-33x20
	Spinel lherzolite	**Spinel lherzolite**	**Spinel lherzolite**	**Spinel lherzolite**	**Spinel lherzolite**	**Spinel lherzolite**	**Spinel lherzolite**	**Spinel lherzolite**	**Spinel lherzolite**	**Spinel lherzolite**
XRF (wt.%)										
MgO	40.79	37.61	38.80	40.09	40.81	37.42	42.48	39.81	37.73	38.57
SiO2	42.98	44.01	43.63	43.19	42.70	44.30	43.42	43.50	43.80	43.73
TiO2	0.10	0.22	0.14	0.12	0.11	0.17	0.06	0.10	0.10	0.18
Al2O3	2.85	3.92	3.48	2.92	3.11	3.65	1.78	3.10	3.10	3.46
FeO*	8.59	7.99	7.96	8.04	8.68	7.92	8.27	8.18	7.60	8.88
MnO	0.14	0.14	0.14	0.13	0.14	0.13	0.14	0.13	0.13	0.14
CaO	2.40	4.20	3.20	3.02	2.05	4.05	2.01	2.81	3.17	3.43
Na2O	0.32	0.47	0.38	0.33	0.29	0.43	0.24	0.32	0.35	0.44
K2O	0.02	0.03	0.01	0.00	0.00	0.02	0.01	0.01	0.01	0.05
Cr2O3	0.40	0.45	0.34	0.41	0.34	0.38	0.35	0.37	0.56	0.34
NiO	0.27	0.23	0.25	0.26	0.27	0.24	0.28	0.26	0.24	0.23
Total	98.85	99.29	98.32	98.51	98.50	98.72	99.04	98.60	96.78	99.44
XRF (ppm)										
Ni	2113	1829	1954	2082	2084	1850	2225	2061	1862	1783
Cr	2752	3089	2360	2794	2321	2607	2428	2557	3804	2314
Sc	11.90	16.52	13.72	14.28	10.92	16.66	10.36	12.88	14.42	16.10
V	66.64	88.20	74.34	68.04	60.76	89.18	60.20	72.38	74.76	80.50
Ba	8.82	1.82	5.18	2.38	0.00	5.04	8.12	7.00	7.42	1.26
Rb	1.54	0.70	0.98	0.00	0.00	0.00	0.00	0.14	0.56	0.28
Sr	7.56	25.90	12.46	11.06	11.34	19.46	13.30	3.50	11.90	22.26
Zr	9.80	18.20	11.90	11.34	10.36	14.98	8.12	9.38	10.50	18.76
Y	2.80	4.90	3.64	3.92	2.80	5.60	2.10	3.92	3.36	4.76
Nb	1.54	1.26	0.84	2.24	1.40	2.24	2.10	1.12	1.96	2.10
Ga	5.04	5.18	2.94	2.80	3.92	1.96	2.52	2.24	3.36	5.60
Cu	13.44	14.98	14.70	18.48	11.90	23.38	11.34	21.28	14.42	16.10
Zn	58.10	51.10	50.40	53.34	54.32	48.86	52.08	55.30	55.30	57.68
Pb	0.00	0.28	0.00	0.00	0.42	0.00	0.00	0.00	0.00	0.00
La	4.76	2.94	1.40	3.50	2.38	0.14	2.10	4.20	2.24	1.40
Ce	1.12	0.00	5.04	6.86	0.00	4.48	2.52	0.70	1.68	2.80
Th	0.00	0.00	0.00	0.00	0.00	0.00	0.00	0.00	0.00	0.00

Table 1 continued

ICP-MS (ppm)										
La	0.18	0.89	0.26	0.31	0.36	0.49	0.71	0.08	0.37	0.62
Ce	0.45	2.32	0.71	0.67	0.98	1.29	1.50	0.23	0.85	1.59
Pr	0.07	0.35	0.12	0.11	0.14	0.19	0.17	0.05	0.13	0.25
Nd	0.43	1.83	0.72	0.60	0.75	1.10	0.71	0.34	0.68	1.28
Sm	0.20	0.65	0.31	0.27	0.25	0.44	0.17	0.19	0.24	0.47
Eu	0.08	0.25	0.13	0.12	0.10	0.19	0.06	0.08	0.09	0.18
Gd	0.30	0.78	0.48	0.40	0.34	0.63	0.17	0.34	0.34	0.58
Tb	0.06	0.14	0.09	0.08	0.06	0.12	0.03	0.07	0.07	0.11
Dy	0.41	0.91	0.65	0.53	0.42	0.83	0.18	0.50	0.46	0.69
Ho	0.09	0.19	0.14	0.12	0.09	0.18	0.04	0.11	0.10	0.15
Er	0.27	0.49	0.40	0.34	0.26	0.51	0.11	0.31	0.29	0.40
Tm	0.04	0.07	0.06	0.05	0.04	0.08	0.02	0.05	0.04	0.06
Yb	0.25	0.43	0.37	0.30	0.25	0.47	0.11	0.30	0.27	0.36
Lu	0.04	0.07	0.06	0.05	0.04	0.07	0.02	0.05	0.04	0.06
Ba	1.63	1.15	1.42	0.46	0.26	1.83	0.71	1.25	0.82	2.25
Th	0.02	0.07	0.02	0.03	0.04	0.05	0.06	0.01	0.04	0.05
Nb	0.26	0.39	0.19	0.26	0.36	0.49	0.38	0.19	0.29	0.61
Yb	2.38	4.73	3.68	3.03	2.37	4.76	1.01	2.87	2.61	3.80
Hf	0.08	0.25	0.15	0.14	0.10	0.20	0.03	0.08	0.09	0.27
Ta	0.01	0.03	0.01	0.01	0.03	0.03	0.05	0.01	0.02	0.04
U	0.01	0.03	0.01	0.03	0.01	0.04	0.02	0.02	0.01	0.02
Pb	0.07	0.08	0.10	0.06	0.04	0.10	0.06	0.08	0.06	0.11
Rb	0.25	0.39	0.18	0.11	0.09	0.33	0.17	0.23	0.20	0.56
Cs	0.00	0.01	0.00	0.00	0.00	0.00	0.00	0.00	0.00	0.01
Sr	8.77	28.03	13.67	13.30	12.20	20.55	14.70	4.46	13.91	23.95
Sc	11.83	15.64	15.31	13.56	11.02	18.11	13.12	13.53	16.08	15.54
Zr	1.99	8.34	4.28	4.37	2.89	5.76	1.48	1.63	2.83	8.76
Modal phenocrysts (vol. %)†										
OPX	18.50	20.80	22.80	17.40	20.20	23.70	16.50	21.20	26.60	22.00
CPX	11.10	20.00	14.80	14.20	9.30	19.10	9.00	13.00	15.00	16.10
Olivine	68.00	56.10	59.80	66.20	67.80	54.80	73.60	63.60	56.60	59.30
Spinel	2.30	3.10	2.60	2.20	2.70	2.40	0.80	2.30	1.80	2.50
Total	99.90	100.00	100.00	100.00	100.00	100.00	99.90	100.10	100.00	99.90

Table 2. Major element analysis of select clinopyroxene (Cpx) crystals

		SiO_2	TiO_2	Al_2O_3	Cr_2O_3	Fe_2O_3	FeO	MnO	MgO	CaO	Na_2O	Sum wt.%	Mg#
SG0533x8	Cpx6c	54.75	0.20	5.53	0.41	0.00	6.46	0.17	31.81	0.94	0.17	100.45	0.90
SG0533x8	Cpx6r	54.53	0.18	5.66	0.41	0.32	6.33	0.14	31.87	0.98	0.18	100.61	0.90
SG0533X2	Cpx6c	53.88	0.19	5.38	0.43	0.54	6.20	0.14	31.59	0.90	0.17	99.41	0.90
SG0533X2	Cpx6r	54.23	0.25	5.51	0.45	0.49	6.17	0.14	31.75	0.95	0.21	100.14	0.90
SG0533X11	Cpx10c	54.00	0.13	5.46	0.47	0.00	6.26	0.13	31.43	1.03	0.16	99.06	0.90
SG0533X11	Cpx10r	54.13	0.14	5.58	0.53	0.00	6.39	0.14	31.39	1.08	0.15	99.54	0.90
SG0533X9	Cpx8c	54.62	0.10	4.57	0.66	0.23	6.05	0.10	32.18	1.08	0.11	99.70	0.91
SG0533X9	Cpx8r	54.57	0.11	4.63	0.66	0.19	6.04	0.11	31.96	1.13	0.17	99.58	0.90
SG0533X7	Cpx6c	54.48	0.19	5.52	0.37	0.00	6.67	0.16	31.61	0.90	0.17	100.06	0.89
SG0533X7	Cpx7c	54.49	0.19	5.34	0.38	0.00	6.59	0.14	31.66	0.95	0.18	99.91	0.90
SG0533X20	Cpx6c	53.97	0.21	5.66	0.39	0.00	7.59	0.14	30.69	1.08	0.15	99.89	0.88
SG0533X20	Cpx6r	53.68	0.19	5.63	0.40	0.79	7.09	0.18	30.76	1.07	0.19	99.99	0.89

Mg# = Mg/(Mg + Fe) cationic ratio.

Table 3. Major element analysis of select olivine (OL) crystals

		SiO_2	TiO_2	Al_2O_3	FeO	MnO	MgO	CaO	Cr2O3	NiO	Sum wt.%	Fa	Fo	Mg#
SG0533x2	OL1c	40.69	0.02	0.02	10.40	0.16	48.50	0.10	0.03	0.32	100.23	0.11	0.89	0.82
SG0533x2	OL1r	40.87	0.02	0.04	10.47	0.15	48.38	0.08	0.04	0.30	100.36	0.11	0.89	0.82
SG0533X7	OL5c	40.63	0.03	0.04	10.45	0.21	47.93	0.12	0.02	0.33	99.75	0.11	0.89	0.82
SG0533X7	OL5r	40.99	0.01	0.02	10.27	0.16	48.13	0.11	0.05	0.28	100.03	0.11	0.89	0.82
SG0533x8	OL3c	41.08	0.02	0.03	10.19	0.16	48.22	0.11	0.03	0.35	100.19	0.11	0.89	0.83
SG0533x8	OL3r	40.54	0.00	0.03	10.45	0.12	47.84	0.08	0.08	0.30	99.43	0.11	0.89	0.82
SG0533X9	OL1c	40.41	0.02	0.04	10.06	0.13	48.78	0.10	0.04	0.32	99.91	0.10	0.90	0.83
SG0533X9	OL1r	40.74	0.02	0.04	9.93	0.18	48.71	0.10	0.04	0.30	100.07	0.10	0.90	0.83
SG0533x11	OL4c	40.74	0.01	0.05	9.80	0.10	48.23	0.10	0.02	0.33	99.39	0.10	0.90	0.83
SG0533x11	OL4r	40.86	0.02	0.03	9.96	0.17	48.14	0.14	0.06	0.30	99.67	0.10	0.90	0.83
SG0533X20	OL1c	40.13	0.01	0.03	12.62	0.13	46.53	0.11	0.04	0.29	99.89	0.13	0.87	0.79
SG0533X20	OL1r	40.44	0.02	0.04	12.70	0.20	46.59	0.14	0.03	0.27	100.42	0.13	0.87	0.79

Mg# = Mg/(Mg + Fe) cationic ratio.

Table 4. Major element analysis of spinel (SP)

		SiO_2	TiO_2	Al_2O_3	Cr_2O_3	Fe_2O_3	FeO	Mn	MgO	ZnO	Sum wt.%	Mg#	Cr#
SG0533X2	SP1c	0.06	0.32	55.08	10.45	2.82	9.61	0.11	20.22	0.00	98.67	67.78	11.29
SG0533X2	SP1r	0.07	0.34	54.09	10.42	3.16	8.80	0.12	20.37	0.00	97.37	69.83	11.44
SG0533X2	SP1s	0.07	0.31	53.90	10.43	3.11	9.02	0.11	20.14	0.00	97.10	69.07	11.49
SG0533X2	SP1t	0.07	0.31	54.37	10.45	2.48	9.52	0.10	19.89	0.00	97.19	67.63	11.43
SG0533X2	SP1d	0.07	0.33	54.45	10.51	2.71	9.52	0.13	20.01	0.00	97.75	67.76	11.46
SG0533X2	SP2c	0.07	0.34	53.53	10.36	2.99	8.99	0.09	20.01	0.00	96.39	69.00	11.49
SG0533X2	SP2c	0.05	0.35	54.17	10.40	3.32	9.18	0.13	20.18	0.06	97.85	68.73	11.41
SG0533X2	SP2d	0.09	0.34	54.05	10.42	3.06	9.30	0.10	20.04	0.10	97.49	68.30	11.45
SG0533X2	SP3c	0.07	0.23	54.14	10.29	2.96	9.00	0.12	20.03	0.12	96.96	69.00	11.30
SG0533X2	SP4	0.05	0.33	53.38	10.38	3.26	9.20	0.08	19.86	0.00	96.55	68.34	11.54
SG0533X2	SP5	0.05	0.34	53.91	10.45	3.15	9.39	0.14	19.95	0.00	97.37	68.00	11.50
SG0533X2	SP6	0.07	0.33	54.31	10.33	2.47	9.94	0.15	19.60	0.00	97.20	66.35	11.31
SG0533X2	SP7	0.07	0.33	54.76	10.46	3.43	9.03	0.16	20.56	0.00	98.79	69.48	11.36
SG0533X2	SP8	0.07	0.32	54.60	10.45	3.21	9.13	0.12	20.39	0.00	98.28	69.07	11.38
SG0533X2	SP9	0.06	0.33	54.49	10.47	3.29	9.07	0.11	20.41	0.00	98.25	69.23	11.42
SG0533X2	SP10	0.06	0.33	54.86	10.43	2.69	9.68	0.03	20.10	0.00	98.18	67.49	11.31

Mg# = Mg/(Mg + Fe) cationic ratio.
Cr# = Cr/(Cr+Al) cationic ratio.

Table 5. Trace element analysis of select clinopyroxene (Cpx) crystals

	SG05-33x11	**SG05-33x11**	**SG05-33x9**	**SG05-33x9**	**SG05-33x7**	**SG05-33x7**	**SG05-33x2**
	Cpx 6	Cpx 2	Cpx 2	Cpx 4	Cpx 5	Cpx 1	Cpx 3
Cs	0.01	0.01	0.01	0.01	0.01	0.01	0.01
Rb	0.04	0.08	0.02	0.02	0.02	1.31	0.04
Ba	0.28	0.53	0.11	0.08	0.10	1.04	0.21
Th	0.03	0.05	0.66	0.59	0.07	0.31	0.18
U	0.03	0.02	0.19	0.19	0.06	0.08	0.08
Nb	0.55	0.42	2.40	2.40	2.85	2.96	1.05
Ta	0.03	0.04	0.25	0.35	0.29	0.28	0.07
La	0.21	0.16	6.23	7.17	2.06	3.64	3.88
Ce	0.79	0.87	13.02	14.69	7.63	10.84	9.56
Pb	0.04	0.04	0.19	0.08	0.04	0.08	0.10
Pr	0.25	0.28	1.36	1.72	1.34	1.69	1.39
Sr	22.77	20.50	132	155	48.01	95.61	122
Nd	2.63	2.45	6.38	6.84	7.16	8.24	7.34
Zr	13.29	13.88	9.62	8.78	31.82	39.79	39.44
Hf	0.90	0.86	0.09	0.12	1.05	1.37	1.22
Sm	1.91	1.25	1.83	1.61	2.20	2.55	3.24
Eu	0.62	0.59	0.59	0.60	0.81	0.77	0.85
Gd	2.41	2.53	1.65	1.66	2.74	3.39	3.57
Tb	0.60	0.50	0.26	0.23	0.54	0.57	0.53
Dy	3.49	3.68	1.63	1.52	3.77	3.60	3.99
Ho	0.81	0.75	0.37	0.27	0.77	0.90	0.78
Y	20.18	19.52	8.49	7.45	20.88	22.85	22.06
Er	2.27	2.30	0.85	0.79	2.33	2.57	2.36
Tm	0.31	0.20	0.14	0.15	0.37	0.35	0.36
Yb	2.49	1.91	1.02	0.74	2.14	2.75	1.84
Lu	0.27	0.28	0.13	0.12	0.32	0.42	0.29
Sc	68.05	62.86	67.69	57.79	76.18	78.68	77.56
V	299	266	302	275	308	324	298
Ni	462	449	447	399	403	367	449
Li	4.80	3.55	3.27	2.46	1.97	8.71	2.81
Cr	8387	5637	8008	7704	5887	6195	6235
Co	30.08	25.88	27.70	26.24	23.09	23.16	29.72
Zn	21.31	13.88	13.69	13.51	10.18	11.02	12.49

Table 5 continued

	SG05-33x2	SG05-33x2	SG05-33x2	SG05-33x20	SG05-33x20	SG05-33x8	SG05-33x8
	Cpx 3	Cpx 3	Cpx3	Cpx 1	Cpx 1	Cpx 2	Cpx 3
Cs	0.01	0.01	0.02	0.01	0.01	0.01	0.01
Rb	0.03	0.04	0.06	0.24	0.19	0.06	0.04
Ba	0.27	0.22	0.32	0.10	0.12	0.08	0.15
Th	0.21	0.16	0.38	0.02	0.02	0.02	0.07
U	0.05	0.05	0.10	0.02	0.01	0.01	0.06
Nb	0.70	0.42	1.59	0.12	0.03	0.17	1.12
Ta	0.05	0.04	0.12	0.05	0.03	0.03	0.10
La	3.98	3.18	4.51	0.86	0.93	0.86	1.78
Ce	10.12	9.04	11.80	3.89	3.99	3.49	5.15
Pb	0.10	0.07	0.09	0.03	0.03	0.03	0.07
Pr	1.47	1.40	1.63	0.82	0.86	0.71	0.92
Sr	131	103	114	30.20	35.13	41.03	98.42
Nd	7.38	7.47	8.88	4.58	5.58	4.41	5.15
Zr	39.22	37.31	47.77	27.85	26.44	26.27	34.85
Hf	1.26	1.13	1.38	0.93	0.84	1.03	1.32
Sm	2.11	2.22	2.55	1.96	2.21	1.78	2.37
Eu	0.95	0.90	1.00	0.76	0.63	0.64	0.88
Gd	3.04	3.20	3.60	2.70	3.23	2.96	3.37
Tb	0.51	0.57	0.51	0.41	0.49	0.53	0.51
Dy	3.93	3.67	4.31	3.48	3.24	4.15	4.27
Ho	0.93	0.76	0.81	0.72	0.70	0.77	0.84
Y	22.01	20.94	22.68	18.48	18.97	20.41	22.36
Er	2.45	2.18	2.17	1.90	2.02	2.09	2.47
Tm	0.30	0.29	0.30	0.32	0.30	0.35	0.33
Yb	2.14	2.05	2.11	1.52	1.99	2.30	2.25
Lu	0.27	0.27	0.27	0.28	0.21	0.29	0.28
Sc	70.64	65.36	70.34	55.74	54.87	68.30	64.92
V	292	284	304	248	258	281	296
Ni	449	392	412	299	314	379	453
Li	2.00	2.24	2.50	6.42	6.49	3.39	8.15
Cr	6041	5880	6184	4853	4978	5395	5258
Co	26.65	23.12	22.49	22.78	25.11	22.61	26.73
Zn	14.10	11.07	11.34	12.40	11.30	10.46	13.92

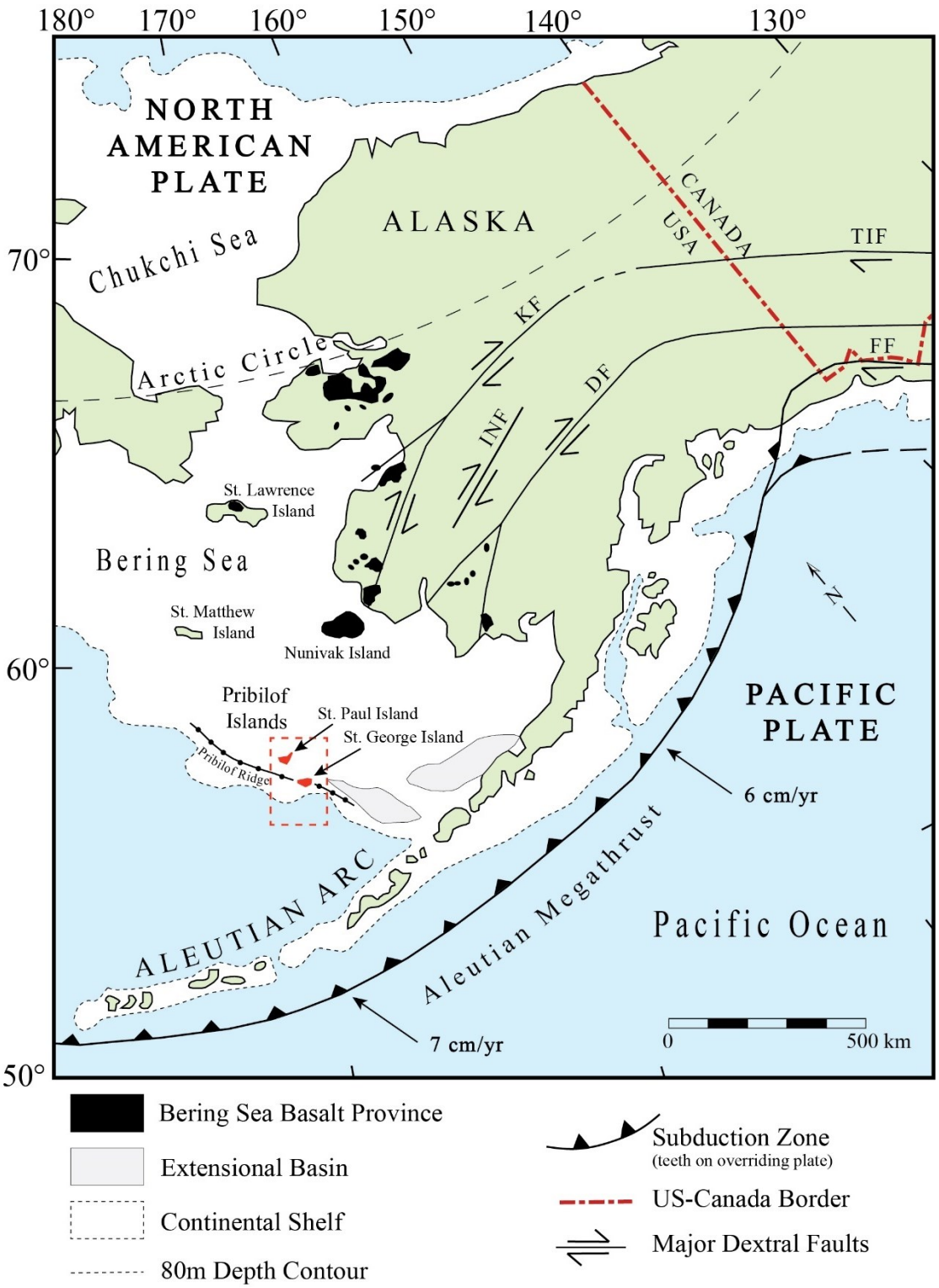

Figure 1. Location and regional tectonic setting of mainland Alaska and the Bering Sea basalt province with the Pribilof Islands shaded red with a dashed box around their location modified from Chang et al. (2009).

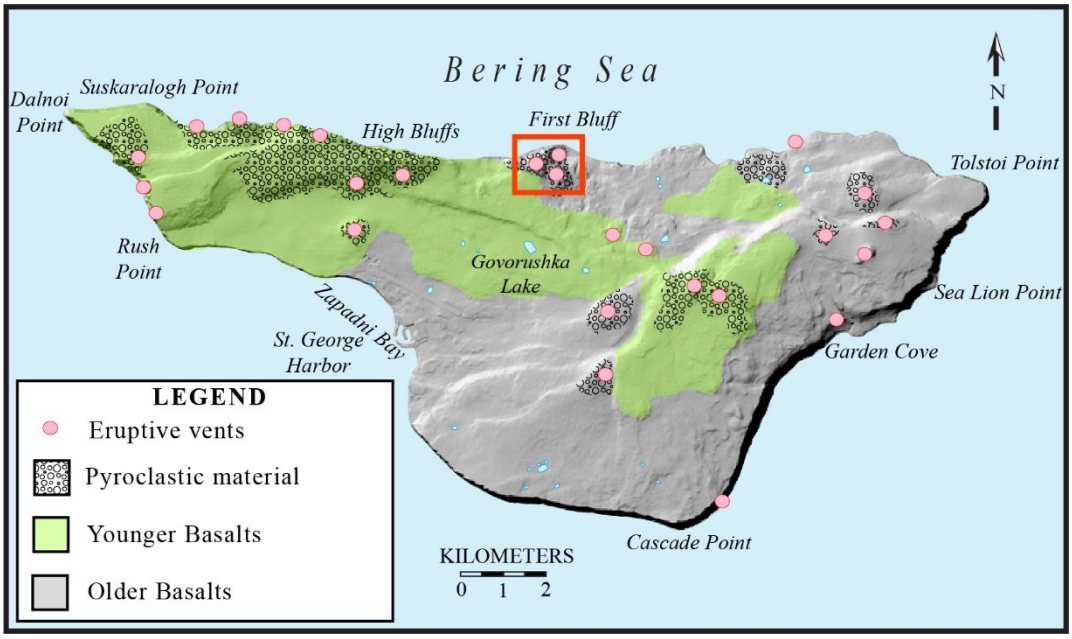

Figure 2. Simplified geologic map of St. George Island and location of xenolith sample from First Bluff (north-central coast, red box) modified from Chang et al. (2009).

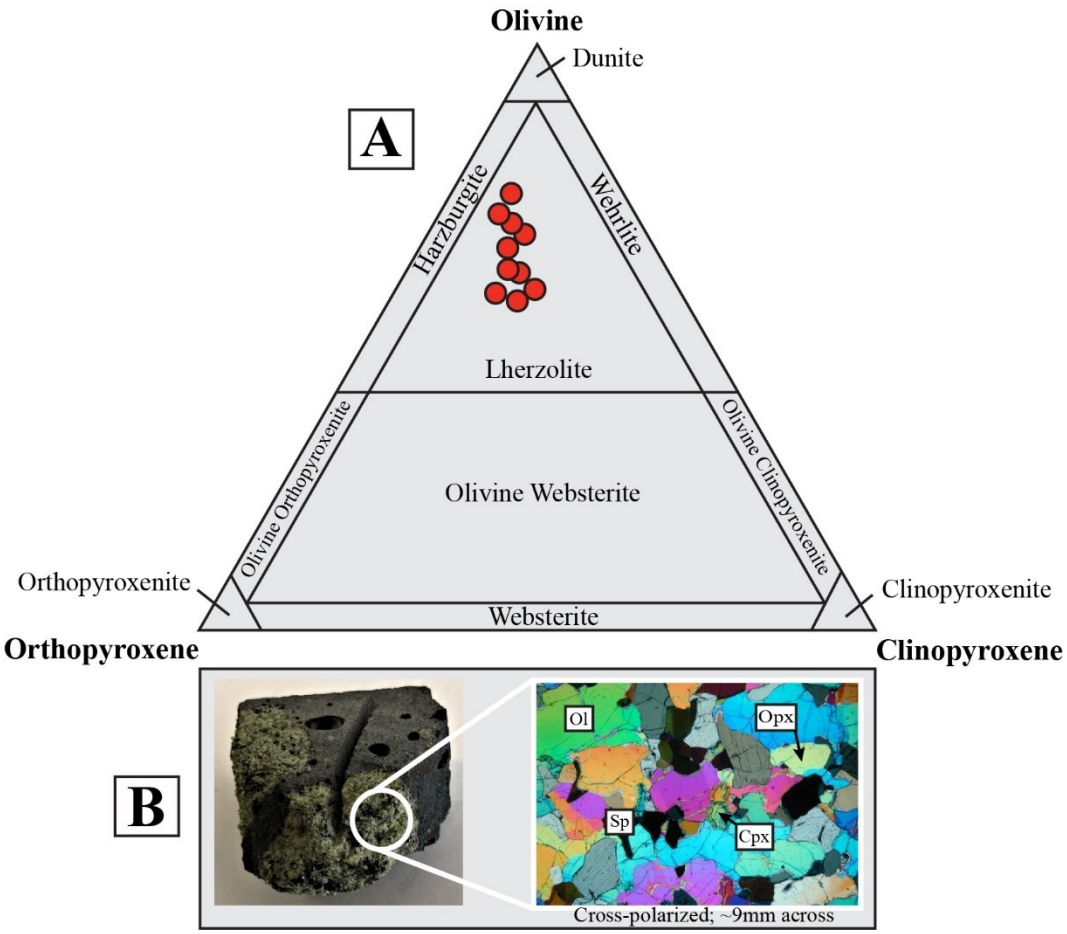

Figure 3. A. Petrological classification of St. George xenoliths based on modal percentages of olivine, orthopyroxene, and clinopyroxene. All xenoliths are lherzolite in modal composition. **B.** Xenolith sample with a microscopic view of grains in cross-polarized light. Ol=olivine, Opx=orthopyroxene; Sp=spinel; Cpx=clinopyroxene.

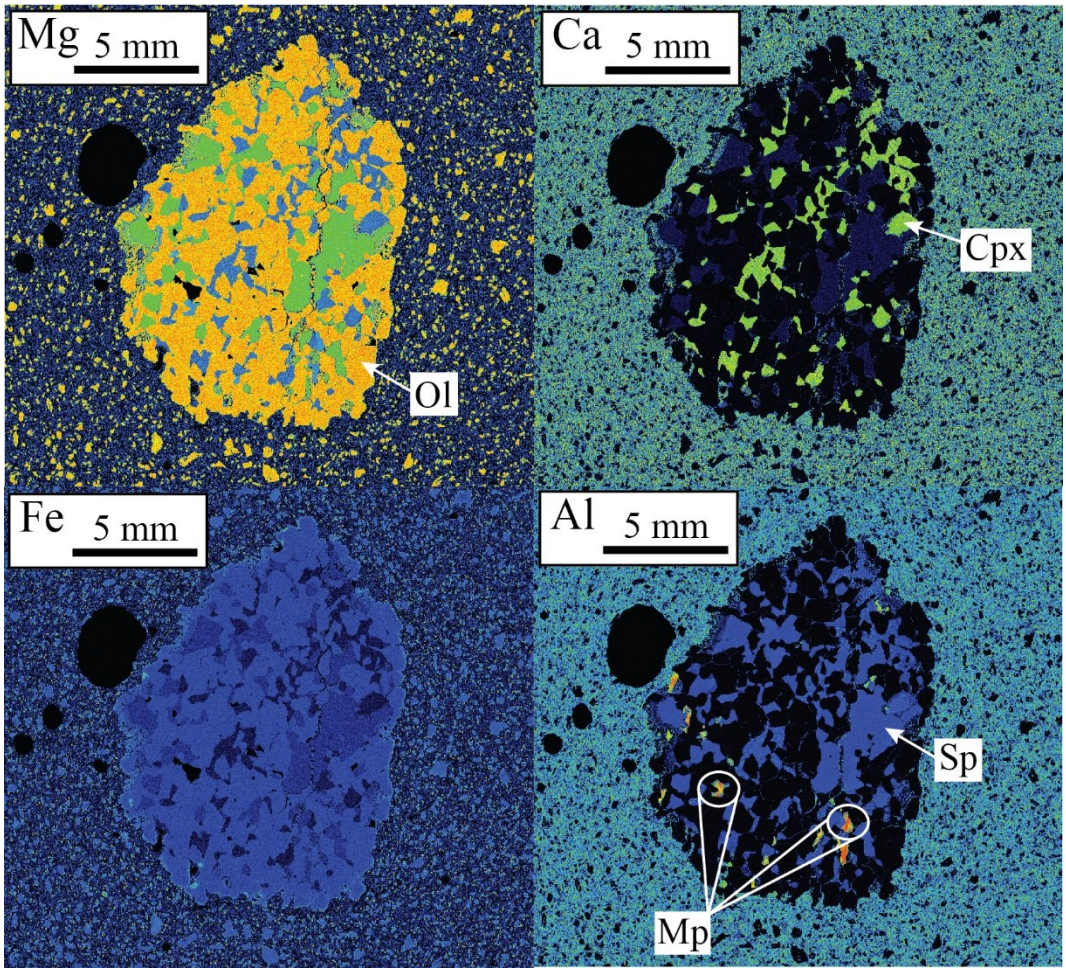

Figure 4. Whole rock chemical maps of St. George xenoliths showing abundances of olivine (Ol), clinopyroxene (Cpx), and spinel (Sp). Melt pockets (Mp) are evident in the Al chemical map.

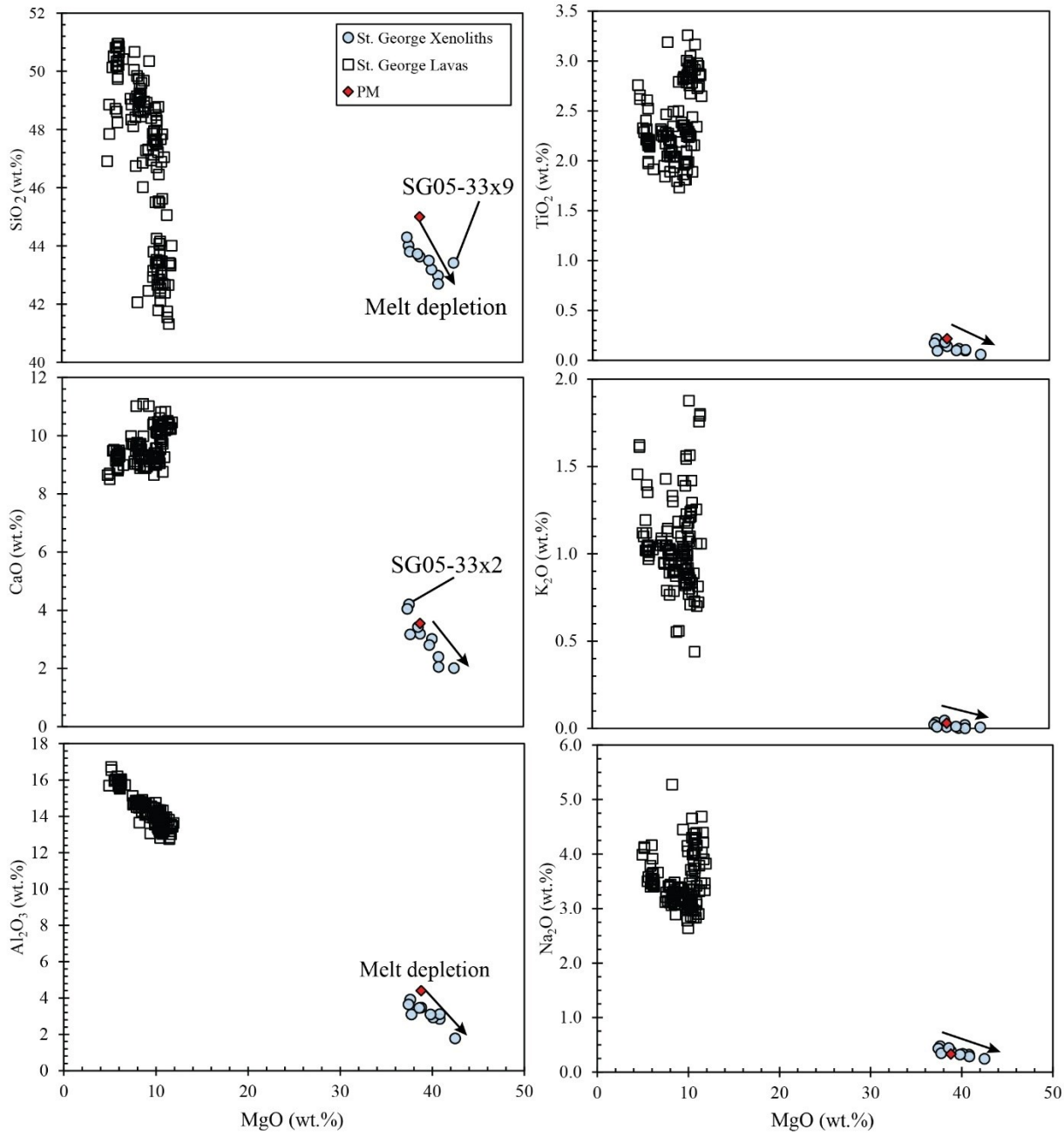

Figure 5. Major element compositional variation diagrams plotted against MgO (wt.%) for St. George lherzolite xenoliths and compared to whole rock basalt compositions. Primitive mantle (PM) major element values from McDonough and Sun (1995).

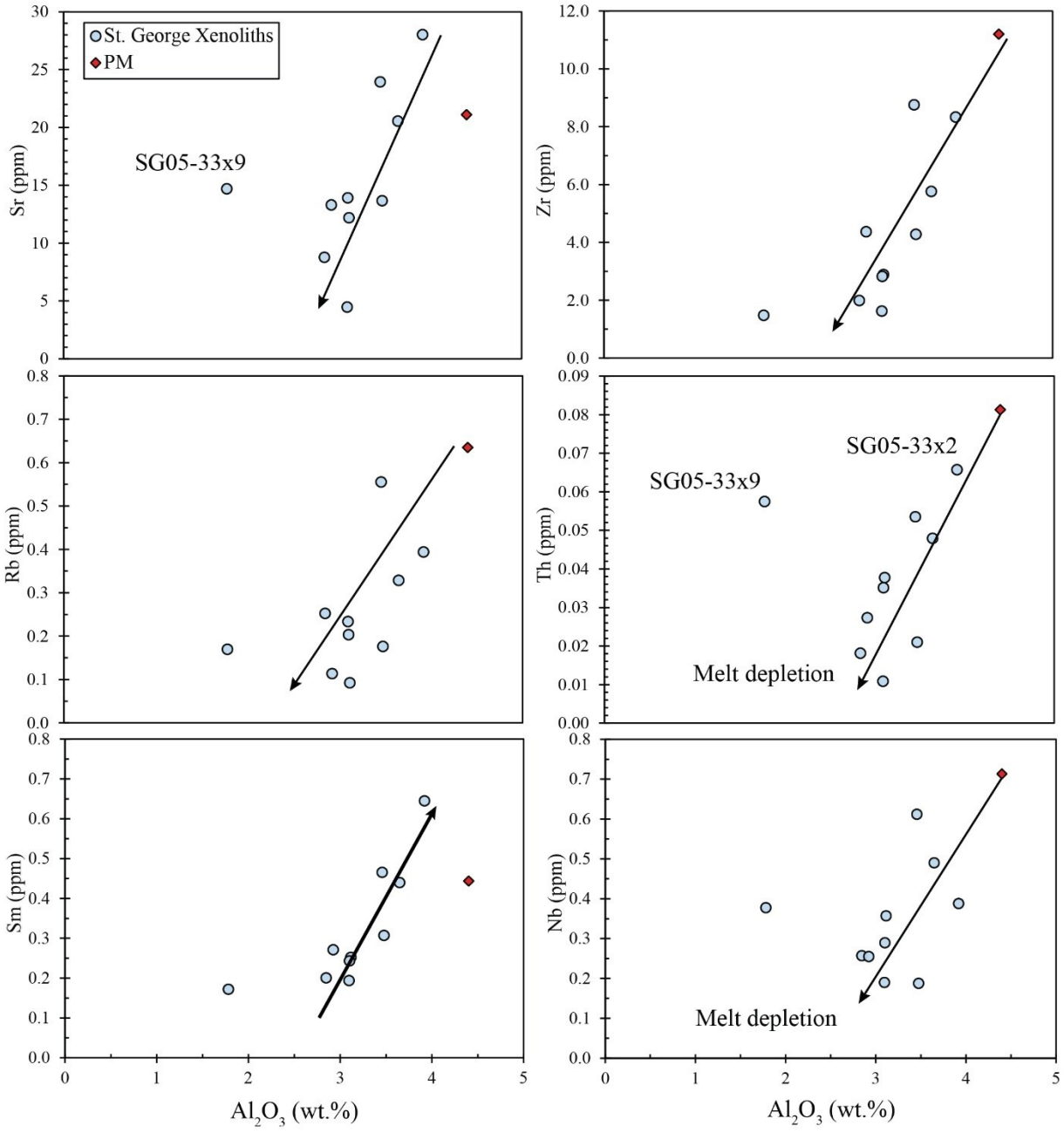

Figure 6. Trace element compositional variation diagrams plotted against Al_2O_3 (wt.%) for St. George lherzolite xenoliths compared to primitive mantle (PM) trace element contents from McDonough and Sun (1995).

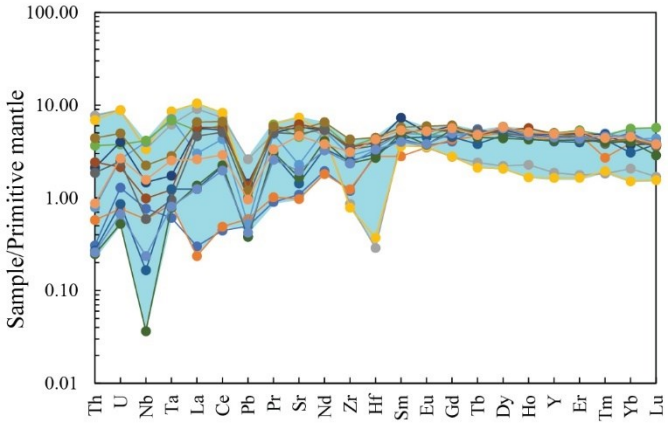

Figure 7. Primitive mantle normalized trace element patterns of clinopyroxene in lherzolite xenoliths from St. George. Normalizing values from McDonough and Sun (1995).

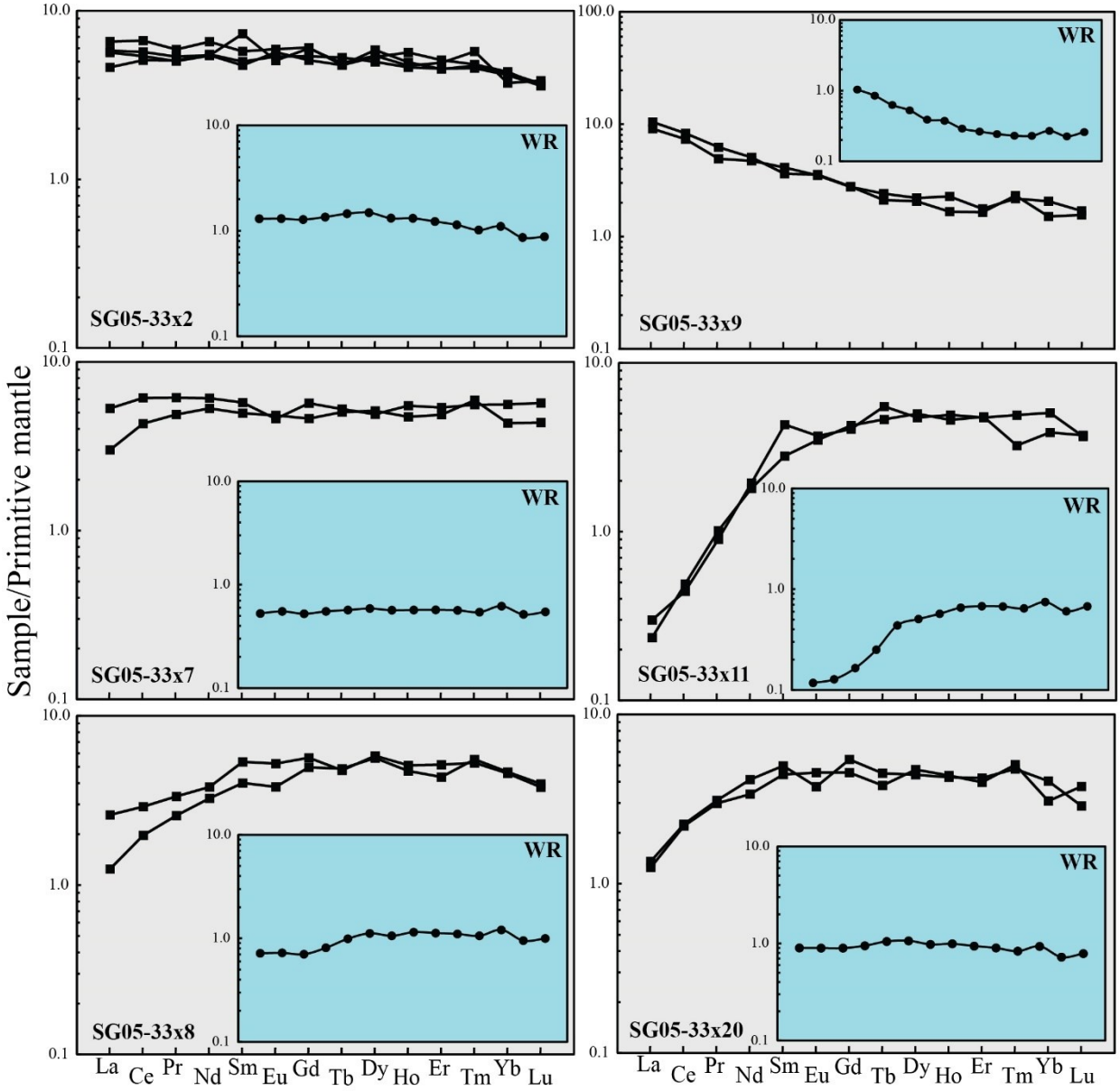

Figure 8. Primitive mantle normalized REE patterns of clinopyroxene. Whole rock (WR) REE values are in the blue inset maps of each sample. Normalization values from McDonough and Sun (1995).

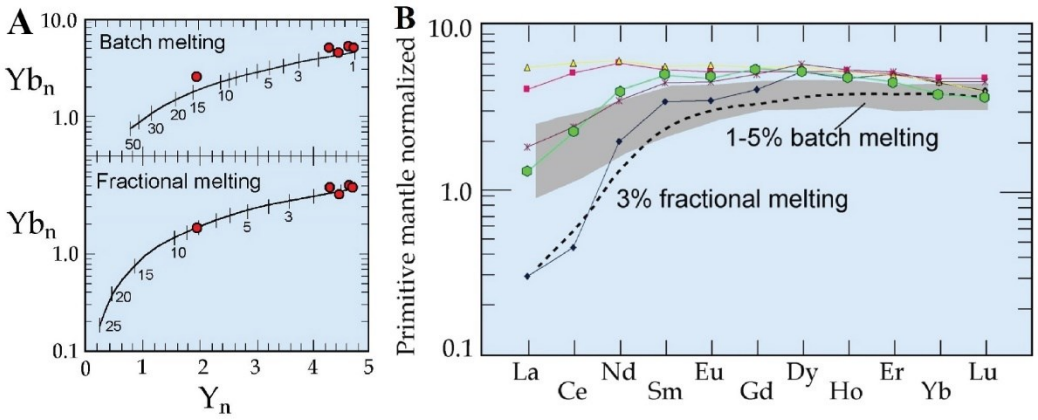

Figure 9. (A) Batch and fractional melting models with Y and Yb contents of clinopyroxene from St. George lherzolites. (B) Comparison of REE compositions estimated for residual clinopyroxene formed by 1–5% batch melting (grey field) and 3% fractional melting (dashed line) of a fertile mantle source with the compositions of fertile St. George lherzolites superimposed.

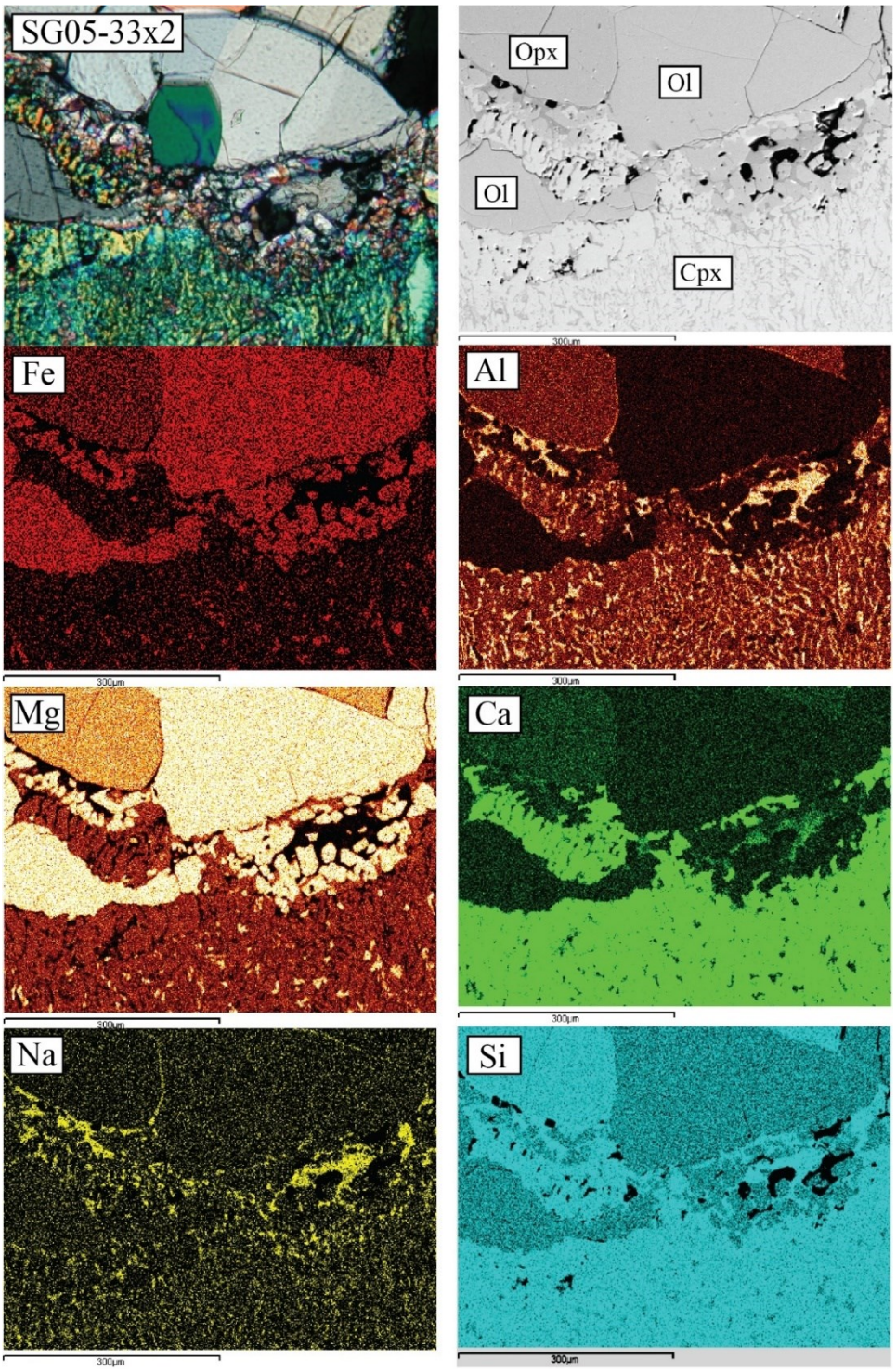

Figure 10. Chemical maps between grain boundaries of fertile mantle xenolith sample SG05-33x2. Chemical maps reveal melt-reaction textures and enrichments of Al, Na, Si, and Ca along clinopyroxene (Cpx) grain boundaries where secondary olivine are developing as a result of metasomatism.

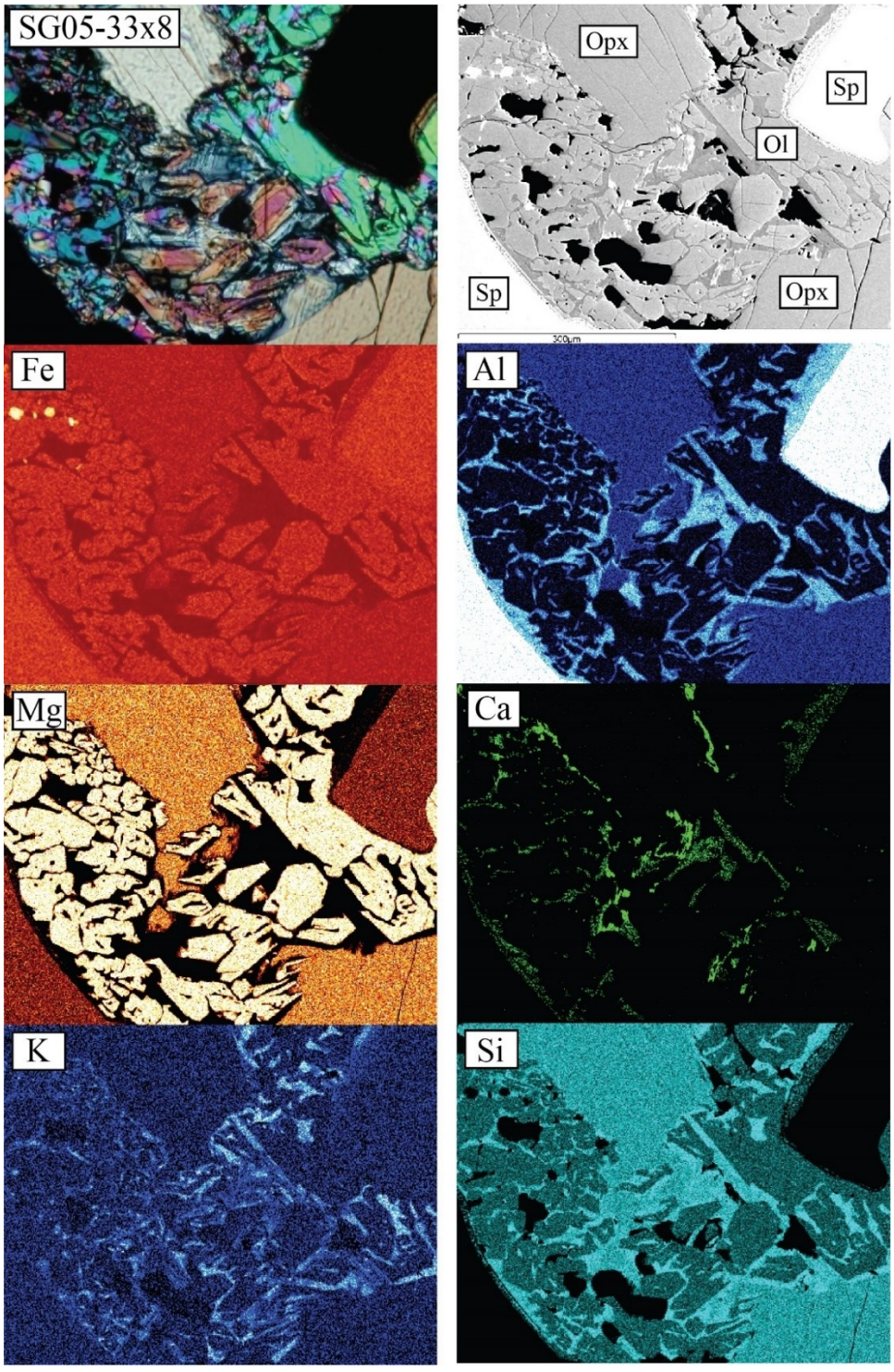

Figure 11. Chemical maps between grain boundaries of refractory mantle xenolith sample SG05-33x8. Partial melting has caused depletions of Mg and Al along the rims of spinel (Sp). Bright areas in Ca map are concentrated around orthopyroxene (Opx).

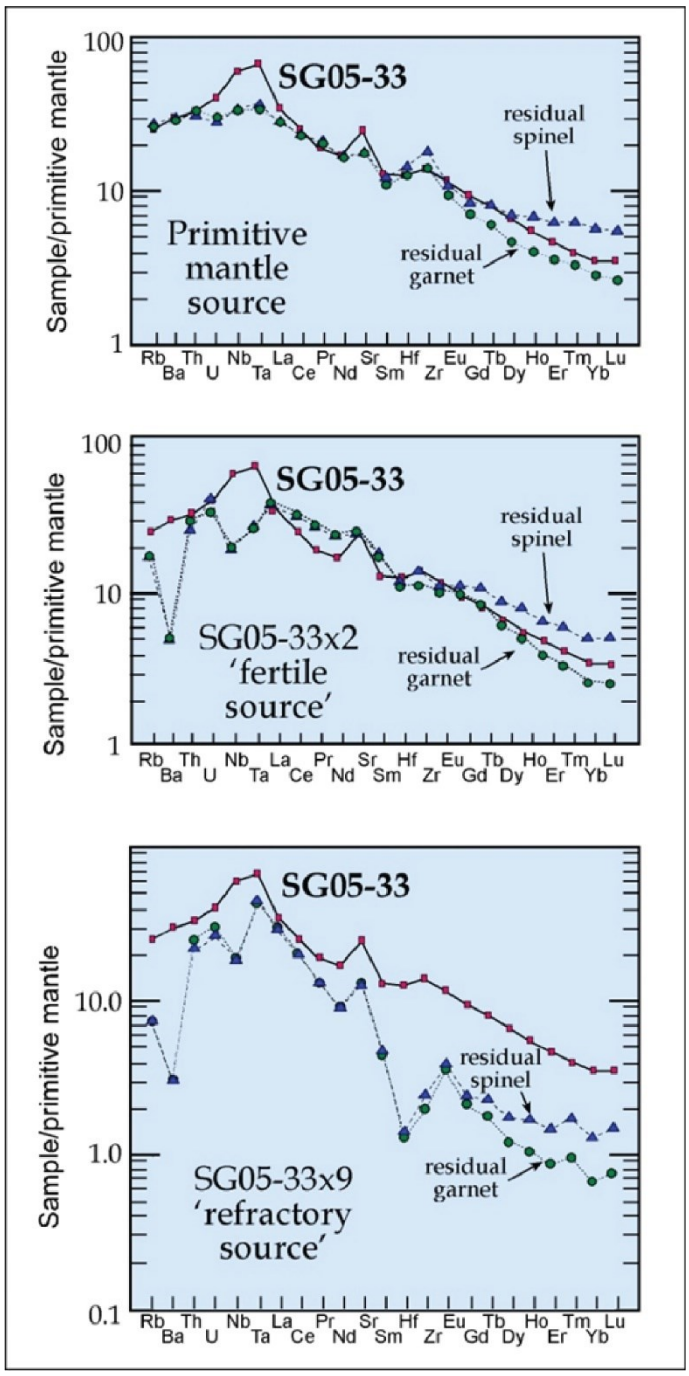

Figure 12. Batch melting model showing the relationship of lherzolites xenoliths to host basalts from St. George Island. Trace element contents are for whole-rock SG05-33, fertile xenolith SG05-33x2, and refractory xenolith SG05-33x9.

CONCLUSIONS

Monogenetic volcanic fields are the most abundant form of volcanism on the planet. The small volume nature of these systems requires magma to rapidly ascend to reach the surface of Earth. Therefore, basaltic compositions and in situ mineral compositions carry the signature of deep-Earth processes that give rise to them (McGee and Smith, 2016). Combining physical petrological observations with compositional data has proven to be an indispensable tool in determining magma source and time constraints for volcanic processes responsible for eruptions on St. Paul and St. George islands. The results of the studies that constitute this thesis have aided in resolving the magmatic system that underpins the Pribilof Islands, Alaska. These data have contributed to a regional understanding of volcanism in the Bering Sea basalt province and a broader, more overarching understanding of ocean islands and continental intraplate volcanism.

The first manuscript, *Resolving the Magmatic Plumbing System of Monogenetic Volcanoes from St. Paul Island, Alaska: Insights from Diffusion Chronometry*, revealed three populations of olivine phenocrysts resided within the host lava prior to the system erupting. This observation indicates that the magmatic plumbing system underlying St. Paul Island is more complex than previously assumed. These data suggest that a mantle-derived melt (~Fo_{86}) hosting chemically homogenous olivine type 1A crystal cores was injected into a shallower level, more evolved melt (~Fo_{77}) hosting type 1B olivine crystal cores which triggered a magma mixing episode. The normal-zoned core-to-rim nature of type 1A phenocrysts suggests crystallization of the core occurred following mixing. The magma mixing event was recorded in the reverse zoning patterns in type 1B core-to-rim compositional profiles. Time scales were calculated by modeling Fe–Mg interdiffusion. Results revealed that the system resided for approximately 20

days before the ascent to the surface from the onset of magma mixing. The rapid ascent and subsequent degassing of the magma developed type 2 skeletal olivine phenocrysts. These observations support that the volcanic system underlying St. Paul involves a multi-stage process that does not reflect a single, compositionally distinct batch of magma with little to no residence time in crustal reservoirs. Groundmass isotopic signatures of St. Paul basalts show a relationship to alkali basalts hosting mantle xenoliths from St. George, indicating each island developed from the same magmatic source, which was investigated in the second manuscript.

The results of the second manuscript, *Lithospheric Melting and Metasomatism Beneath the Pribilof Islands: Insights from Spinel Peridotite Xenoliths from St. George Island, Alaska*, highlighted key aspects of melt generation in the lithospheric mantle beneath the Pribilof Islands. Petrological and chemical observations identified both fertile and refractory xenoliths present in host alkali basalts. This evidence revealed spinel-facies lherzolite xenoliths from St. George experienced at least two episodes of partial melting and two episodes of metasomatism. The most refractory xenolith sample analyzed hosts LREE-, Nb-, and Ta-enriched diopside crystals that are well-equilibrated with the whole rock, suggesting that ancient metasomatism enrichment had to occur prior to the magmatism responsible for entraining and transporting the xenoliths to the surface. The melt reaction textures seen in more fertile xenoliths signify melt infiltration was active in some of the samples prior to or at the time of the eruption. However, melt infiltration is not the cause of ancient metasomatism because the most heavily infiltrated samples lack a metasomatic signature in their mineral and whole-rock compositions.

Furthermore, the infiltrated melt is not the same source of magma responsible for the host alkali basalts but is relatively localized melting of clinopyroxene and spinel, fluxed by an alkali-rich fluid. Modeling of whole-rock and trace element contents support St. George basalts are

sourced from a primitive mantle melt rather than melting of preexisting lherzolite xenoliths. Although it is evident mantle xenoliths experienced a small degree of partial melting, the important implication from this study is that the spinel lherzolites are not the primary source of magma for the Pribilof Islands, nor do they have any significant influence on compositional changes within the system over time.

These data, together with previously reported petrological and geochemical evidence (Change et al., 2009; Winer et al., 2004; Feeley and Winer, 1999), confirm that partial melting and primary basalt formation in the Pribilof Islands, and likely throughout the BSBP, resulted from the lithospheric extension which induced decompression melting of a metasomatized mantle. This observation implies that episodes of volcanism on the Pribilof Islands are not indicative of a mantle plume upwelling from the lower mantle but are a direct result of partial melting in the upper mantle exploiting preexisting fractures as conduits for magma ascent.

REFERENCES

Chang, J.M., Feeley, T.C., and Deraps, M.R., 2009, Petrogenesis of Basaltic Volcanic Rocks from the Pribilof Islands, Alaska, by Melting of Metasomatically Enriched Depleted Lithosphere, Crystallization Differentiation, and Magma Mixing: Journal of Petrology, v. 50, no. 12, p. 2249-2286.

Cañón-Tapia, E., and Walker, G.P.L., 2004, Global aspects of volcanism: the perspectives of "plate tectonics" and "volcanic systems": Earth-Science Reviews, v. 66, p. 163-182.

Cañón-Tapia, E., 2016, Reappraisal of the significance of volcanic fields: Journal of Volcanology and Geothermal Research, v. 310, p. 26-38.

Feeley, T.C., and Winer, G.S., 1999, Evidence for fractionation of Quaternary basalts on St. Paul Island, Alaska, with implications for the development of shallow magma chambers beneath Bering Sea volcanoes: Lithos, v. 46, p. 661-676.

McGee, L.E., and Smith, I.E.M., 2016, Interpreting chemical compositions of small-scale basaltic systems: A review. Journal of Volcanology and Geothermal Research, v. 325, p. 45-60.

Moll-Stalcup, E., Plafker, G., and Berg, H., 1994, Latest Cretaceous and Cenozoic magmatism in mainland Alaska, *in* Plafker, G., and Berg, H.C., eds., The geology of Alaska: Geological Society of America, The Geology of North America, p. 589-619.

Németh, K., and Kereszturi, G., 2015, Monogenetic volcanism: personal views and discussion: International Journal of Earth Sciences, v. 104, p. 2131-2146.

Winer, G.S., Feeley, T.C., and Cosca, M.A., 2004, Basaltic volcanism in the Bering Sea: geochronology and volcanic evolution of St. Paul Island, Pribilof Islands, Alaska: Journal of Volcanology and Geothermal Research, v. 134, p. 277-301.

Wirth, K. R., Grandy, J., Kelley, K., and Sadofsky, S., 2002, Evolution of crust and mantle beneath the Bering Sea region: Evidence from xenoliths and late Cenozoic basalts: Special Papers-Geological Society of America, v. 360, p. 167-194.

APPENDIX

Appendix. *Manuscript 1.* Major element data for St. Paul Island olivine (wt.%); core (C)-rim (R) transects

Sample	SiO_2	MgO	Al_2O_3	CaO	TiO_2	FeO	MnO	Cr_2O_3	NiO	Total	Mg#	%Fo
SP98-39_OL1-C	39.625	45.518	0.064	0.247	0.022	13.840	0.167	0.019	0.214	99.717	0.767	85.424
SP98-39_OL1	39.692	45.693	0.068	0.245	0.014	13.594	0.163	0.021	0.213	99.703	0.771	85.693
SP98-39_OL1	39.803	46.076	0.074	0.265	0.014	13.435	0.159	0.036	0.217	100.079	0.774	85.939
SP98-39_OL1	39.867	46.222	0.068	0.253	0.015	13.177	0.162	0.047	0.250	100.061	0.778	86.209
SP98-39_OL1-R	39.213	44.230	0.045	0.329	0.022	15.200	0.207	0.024	0.206	99.474	0.744	83.832
SP98-39_OL2-C	39.357	44.163	0.057	0.238	0.019	15.306	0.194	0.018	0.210	99.560	0.743	83.718
SP98-39_OL2	39.444	44.145	0.610	0.246	0.020	15.353	0.185	0.015	0.214	100.231	0.742	83.671
SP98-39_OL2	39.438	44.229	0.059	0.237	0.022	15.382	0.188	0.012	0.221	99.788	0.742	83.671
SP98-39_OL2	39.333	44.313	0.059	0.241	0.025	15.119	0.184	0.014	0.218	99.506	0.746	83.930
SP98-39_OL2-R	37.900	37.451	0.037	0.402	0.022	23.106	0.315	0.010	0.131	99.374	0.618	74.282
SP98-39_OL3-C	39.885	46.205	0.065	0.232	0.012	13.428	0.158	0.035	0.257	100.277	0.775	85.978
SP98-39_OL3	39.730	45.879	0.068	0.231	0.015	13.354	0.158	0.038	0.254	99.726	0.775	85.960
SP98-39_OL3	39.722	45.952	0.068	0.235	0.013	13.402	0.163	0.051	0.250	99.855	0.774	85.935
SP98-39_OL3	39.705	45.666	0.074	0.251	0.012	13.660	0.167	0.041	0.256	99.831	0.770	85.627
SP98-39_OL3-R	37.003	33.450	0.037	0.428	0.033	28.441	0.415	0.010	0.092	99.908	0.540	67.699
SP98-39_OL4-C	39.184	43.068	0.058	0.249	0.019	16.892	0.202	0.018	0.179	99.871	0.718	81.960
SP98-39_OL4	39.274	43.067	0.052	0.209	0.021	17.095	0.208	0.010	0.169	100.104	0.716	81.783
SP98-39_OL4	39.330	43.126	0.057	0.208	0.023	16.857	0.203	0.009	0.172	99.985	0.719	82.011
SP98-39_OL4	38.902	41.817	0.049	0.238	0.023	18.161	0.238	0.016	0.167	99.612	0.697	80.404
SP98-39_OL4-R	35.370	25.745	0.028	0.588	0.058	37.017	0.668	0.000	0.048	99.523	0.410	55.344
SP98-39_OL5-C	39.569	44.567	0.067	0.303	0.019	15.331	0.194	0.036	0.212	100.297	0.744	83.819
SP98-39_OL5	39.451	44.548	0.062	0.299	0.017	15.134	0.194	0.034	0.211	99.949	0.746	83.988
SP98-39_OL5	39.510	44.558	0.059	0.300	0.017	15.169	0.196	0.029	0.213	100.049	0.746	83.960
SP98-39_OL5	39.549	44.561	0.060	0.301	0.018	15.152	0.200	0.030	0.212	100.082	0.746	83.976

SP98-39_OL5	39.566	44.610	0.059	0.305	0.018	15.193	0.202	0.032	0.210	100.195	0.746	83.955
SP98-39_OL5	39.573	44.523	0.057	0.304	0.020	15.194	0.200	0.027	0.212	100.109	0.746	83.928
SP98-39_OL5	39.462	44.454	0.056	0.304	0.019	15.228	0.200	0.025	0.211	99.960	0.745	83.876
SP98-39_OL5	39.528	44.418	0.058	0.309	0.020	15.322	0.202	0.031	0.213	100.099	0.744	83.782
SP98-39_OL5	39.512	44.287	0.049	0.311	0.019	15.354	0.205	0.034	0.208	99.979	0.743	83.713
SP98-39_OL5	39.542	44.239	0.047	0.315	0.014	15.432	0.201	0.026	0.209	100.025	0.741	83.629
SP98-39_OL5	39.472	44.223	0.049	0.320	0.019	15.519	0.205	0.027	0.203	100.036	0.740	83.547
SP98-39_OL5	39.434	44.072	0.047	0.326	0.019	15.629	0.212	0.027	0.197	99.963	0.738	83.402
SP98-39_OL5	39.464	43.953	0.046	0.350	0.020	15.758	0.211	0.022	0.192	100.016	0.736	83.251
SP98-39_OL5	39.390	43.788	0.046	0.371	0.023	15.936	0.224	0.024	0.183	99.986	0.733	83.040
SP98-39_OL5	39.358	43.571	0.044	0.384	0.024	16.455	0.227	0.016	0.179	100.259	0.726	82.513
SP98-39_OL5	39.155	42.606	0.042	0.403	0.025	17.473	0.246	0.022	0.164	100.136	0.709	81.291
SP98-39_OL5	38.738	40.878	0.038	0.428	0.027	19.438	0.272	0.022	0.145	99.987	0.678	78.936
SP98-39_OL5	38.289	38.613	0.035	0.456	0.035	22.245	0.320	0.016	0.129	100.137	0.634	75.570
SP98-39_OL5-R	37.317	34.325	0.036	0.502	0.044	27.340	0.421	0.009	0.098	100.091	0.557	69.109
SP98-39_OL6-C	39.603	44.493	0.041	0.215	0.014	15.203	0.186	0.021	0.222	99.998	0.745	83.910
SP98-39_OL6	39.640	44.582	0.040	0.217	0.017	15.187	0.189	0.022	0.222	100.114	0.746	83.951
SP98-39_OL6	39.740	44.778	0.040	0.213	0.017	15.168	0.185	0.021	0.220	100.383	0.747	84.027
SP98-39_OL6	39.750	44.694	0.038	0.213	0.014	15.161	0.190	0.020	0.219	100.298	0.747	84.008
SP98-39_OL6	39.818	44.756	0.037	0.213	0.012	15.159	0.188	0.022	0.222	100.427	0.747	84.029
SP98-39_OL6	39.690	44.760	0.039	0.214	0.014	15.126	0.187	0.021	0.218	100.268	0.747	84.059
SP98-39_OL6	39.646	44.623	0.039	0.215	0.011	15.129	0.183	0.022	0.217	100.085	0.747	84.016
SP98-39_OL6	39.715	44.746	0.038	0.214	0.010	15.167	0.186	0.016	0.218	100.310	0.747	84.018
SP98-39_OL6	40.006	45.107	0.054	0.216	0.015	15.146	0.186	0.024	0.222	100.975	0.749	84.145
SP98-39_OL6	39.607	44.713	0.040	0.216	0.015	15.158	0.186	0.020	0.218	100.174	0.747	84.017
SP98-39_OL6	39.597	44.701	0.036	0.214	0.012	15.081	0.186	0.017	0.219	100.062	0.748	84.081
SP98-39_OL6	39.663	44.549	0.036	0.218	0.010	15.053	0.190	0.020	0.221	99.960	0.747	84.061
SP98-39_OL6	39.468	44.833	0.036	0.216	0.011	15.082	0.189	0.020	0.223	100.078	0.748	84.120
SP98-39_OL6	39.684	44.725	0.036	0.216	0.016	15.116	0.189	0.022	0.226	100.228	0.747	84.058

SP98-39_OL6	39.689	44.717	0.051	0.218	0.018	15.150	0.190	0.022	0.224	100.279	0.747	84.025
SP98-39_OL6	39.474	44.421	0.043	0.217	0.015	15.066	0.189	0.025	0.221	99.670	0.747	84.011
SP98-39_OL6	39.632	44.776	0.042	0.217	0.017	15.166	0.191	0.020	0.218	100.277	0.747	84.029
SP98-39_OL6	39.456	44.861	0.047	0.217	0.014	15.060	0.184	0.017	0.218	100.074	0.749	84.148
SP98-39_OL6	39.677	44.698	0.048	0.220	0.014	15.103	0.193	0.021	0.216	100.190	0.747	84.061
SP98-39_OL6	39.479	44.735	0.045	0.215	0.017	15.093	0.187	0.024	0.217	100.012	0.748	84.081
SP98-39_OL6	39.582	44.733	0.048	0.220	0.018	15.080	0.186	0.018	0.218	100.103	0.748	84.091
SP98-39_OL6	39.654	44.850	0.042	0.217	0.016	15.044	0.187	0.020	0.217	100.248	0.749	84.158
SP98-39_OL6	39.676	44.796	0.043	0.215	0.014	15.080	0.186	0.014	0.222	100.244	0.748	84.111
SP98-39_OL6	39.658	44.754	0.043	0.220	0.015	15.021	0.188	0.024	0.222	100.144	0.749	84.151
SP98-39_OL6	39.709	44.860	0.040	0.217	0.018	15.087	0.185	0.017	0.219	100.351	0.748	84.123
SP98-39_OL6	39.561	44.797	0.042	0.224	0.013	15.029	0.188	0.017	0.219	100.091	0.749	84.156
SP98-39_OL6	39.671	44.868	0.041	0.220	0.016	15.060	0.189	0.017	0.226	100.307	0.749	84.150
SP98-39_OL6	39.745	44.815	0.041	0.222	0.014	15.028	0.190	0.021	0.225	100.301	0.749	84.162
SP98-39_OL6	39.793	44.877	0.039	0.223	0.014	15.025	0.193	0.024	0.224	100.411	0.749	84.184
SP98-39_OL6	39.777	44.900	0.042	0.221	0.011	15.025	0.190	0.016	0.223	100.404	0.749	84.190
SP98-39_OL6	39.698	44.881	0.042	0.226	0.015	15.038	0.186	0.017	0.219	100.321	0.749	84.173
SP98-39_OL6	39.786	44.823	0.042	0.228	0.015	15.020	0.188	0.019	0.216	100.336	0.749	84.172
SP98-39_OL6	39.755	44.929	0.040	0.227	0.016	15.019	0.187	0.018	0.218	100.408	0.749	84.204
SP98-39_OL6	39.849	45.018	0.042	0.229	0.013	15.019	0.186	0.019	0.223	100.597	0.750	84.231
SP98-39_OL6	39.895	45.032	0.043	0.232	0.013	14.998	0.186	0.022	0.222	100.644	0.750	84.253
SP98-39_OL6	39.819	44.949	0.040	0.231	0.013	15.007	0.190	0.030	0.220	100.498	0.750	84.220
SP98-39_OL6	39.655	44.807	0.045	0.233	0.015	14.955	0.190	0.015	0.221	100.137	0.750	84.225
SP98-39_OL6	39.731	44.913	0.042	0.241	0.015	15.006	0.189	0.020	0.223	100.379	0.750	84.211
SP98-39_OL6	39.840	44.907	0.043	0.245	0.013	14.914	0.193	0.028	0.219	100.401	0.751	84.291
SP98-39_OL6	39.534	44.791	0.042	0.248	0.017	14.978	0.191	0.023	0.221	100.045	0.749	84.200
SP98-39_OL6	39.712	44.929	0.047	0.252	0.017	14.943	0.189	0.021	0.222	100.331	0.750	84.272
SP98-39_OL6	39.794	45.006	0.043	0.253	0.015	14.988	0.192	0.023	0.223	100.537	0.750	84.254
SP98-39_OL6	39.915	45.022	0.044	0.256	0.015	15.002	0.192	0.024	0.227	100.696	0.750	84.247

SP98-39_OL6	39.662	44.929	0.047	0.261	0.019	14.974	0.187	0.025	0.223	100.327	0.750	84.244
SP98-39_OL6	39.655	44.974	0.052	0.268	0.019	15.002	0.196	0.027	0.227	100.419	0.750	84.233
SP98-39_OL6	39.754	44.847	0.053	0.275	0.020	15.018	0.194	0.024	0.221	100.405	0.749	84.180
SP98-39_OL6	39.599	44.850	0.051	0.282	0.024	15.028	0.194	0.025	0.220	100.273	0.749	84.173
SP98-39_OL6	39.634	44.797	0.055	0.287	0.024	15.010	0.191	0.029	0.215	100.243	0.749	84.173
SP98-39_OL6	39.955	44.991	0.054	0.296	0.020	15.038	0.192	0.030	0.214	100.790	0.749	84.206
SP98-39_OL6	39.827	44.907	0.053	0.297	0.021	15.080	0.202	0.028	0.209	100.624	0.749	84.144
SP98-39_OL6	39.863	44.773	0.051	0.301	0.019	15.107	0.194	0.028	0.212	100.547	0.748	84.080
SP98-39_OL6	39.827	44.593	0.050	0.310	0.020	15.151	0.204	0.024	0.216	100.396	0.746	83.986
SP98-39_OL6	39.807	44.506	0.048	0.322	0.020	15.453	0.208	0.026	0.205	100.594	0.742	83.693
SP98-39_OL6	39.702	43.962	0.047	0.337	0.027	16.138	0.218	0.026	0.196	100.653	0.731	82.919
SP98-39_OL6	39.341	42.412	0.043	0.375	0.025	17.739	0.247	0.023	0.181	100.384	0.705	80.991
SP98-39_OL6	38.757	39.439	0.044	0.434	0.034	21.064	0.305	0.022	0.144	100.244	0.652	76.940
SP98-39_OL6-R	40.336	37.298	1.526	0.729	0.055	24.269	0.387	0.010	0.075	104.684	0.606	73.253
SP98-39_OL7-C	39.599	44.497	0.064	0.228	0.021	15.463	0.193	0.014	0.191	100.269	0.742	83.681
SP98-39_OL7	39.621	44.510	0.058	0.233	0.023	15.315	0.192	0.012	0.190	100.152	0.744	83.817
SP98-39_OL7	39.695	44.803	0.054	0.252	0.020	15.193	0.187	0.020	0.195	100.419	0.747	84.012
SP98-39_OL7	39.641	44.821	0.051	0.293	0.018	15.124	0.199	0.027	0.207	100.380	0.748	84.079
SP98-39_OL7-R	37.456	34.165	0.050	0.462	0.030	27.540	0.410	0.011	0.104	100.227	0.554	68.854
SP98-39_OL8-C	39.580	44.711	0.067	0.309	0.027	15.045	0.197	0.035	0.219	100.189	0.748	84.117
SP98-39_OL8	39.605	44.714	0.069	0.302	0.025	15.044	0.197	0.037	0.222	100.215	0.748	84.118
SP98-39_OL8	39.335	44.661	0.071	0.302	0.022	14.991	0.196	0.034	0.212	99.825	0.749	84.149
SP98-39_OL8	39.435	44.638	0.069	0.300	0.019	15.005	0.192	0.039	0.221	99.917	0.748	84.130
SP98-39_OL8	39.489	44.636	0.067	0.300	0.022	15.049	0.196	0.034	0.224	100.017	0.748	84.091
SP98-39_OL8	39.398	44.681	0.063	0.302	0.022	15.042	0.195	0.034	0.220	99.958	0.748	84.110
SP98-39_OL8	39.713	44.613	0.062	0.309	0.022	15.133	0.197	0.034	0.220	100.303	0.747	84.009
SP98-39_OL8	39.617	44.592	0.062	0.311	0.026	15.183	0.194	0.038	0.217	100.239	0.746	83.958
SP98-39_OL8	39.541	44.288	0.059	0.320	0.023	15.353	0.204	0.027	0.207	100.020	0.743	83.714
SP98-39_OL8	39.168	43.251	0.056	0.330	0.022	16.350	0.221	0.028	0.206	99.633	0.726	82.499

SP98-39_OL8	38.526	40.090	0.051	0.361	0.030	20.472	0.292	0.027	0.187	100.034	0.662	77.727
SP98-39_OL8	36.672	31.809	0.043	0.469	0.055	30.096	0.499	0.006	0.098	99.746	0.514	65.319
SP98-39_OL8	35.926	24.864	0.210	3.293	0.316	34.357	0.649	0.002	0.036	99.651	0.420	56.324
SP98-39_OL8-R	32.961	19.424	2.718	0.830	0.101	42.398	0.860	0.000	0.032	99.322	0.314	44.945
SP98-39_OL9-C	39.893	45.779	0.068	0.238	0.018	13.982	0.171	0.033	0.242	100.424	0.766	85.369
SP98-39_OL9	35.037	39.028	4.606	0.255	0.017	12.804	0.160	0.032	0.233	92.170	0.753	84.452
SP98-39_OL9	39.813	45.653	0.067	0.235	0.014	13.937	0.170	0.039	0.243	100.171	0.766	85.374
SP98-39_OL9	39.706	45.308	0.059	0.249	0.011	14.034	0.173	0.036	0.245	99.819	0.764	85.192
SP98-39_OL9-R	39.189	43.109	0.048	0.359	0.024	16.751	0.231	0.025	0.199	99.936	0.720	82.098
SP98-39_OL10-C	38.932	42.104	0.054	0.217	0.022	18.189	0.230	0.001	0.099	99.847	0.698	80.487
SP98-39_OL10	38.979	42.147	0.053	0.213	0.023	18.180	0.234	0.004	0.098	99.930	0.699	80.512
SP98-39_OL10	38.997	42.195	0.052	0.215	0.025	18.245	0.224	0.003	0.099	100.055	0.698	80.473
SP98-39_OL10	38.865	42.116	0.055	0.212	0.020	18.100	0.227	0.002	0.100	99.696	0.699	80.569
SP98-39_OL10	38.925	42.234	0.052	0.213	0.019	18.202	0.234	0.003	0.097	99.979	0.699	80.525
SP98-39_OL10	38.927	42.212	0.054	0.215	0.021	18.170	0.227	0.003	0.098	99.927	0.699	80.544
SP98-39_OL10	38.912	42.112	0.054	0.213	0.024	18.158	0.228	0.004	0.094	99.800	0.699	80.518
SP98-39_OL10	38.967	42.271	0.052	0.214	0.024	18.299	0.227	0.001	0.100	100.154	0.698	80.455
SP98-39_OL10	38.930	42.284	0.054	0.212	0.019	18.235	0.228	0.004	0.098	100.064	0.699	80.515
SP98-39_OL10	38.977	42.387	0.054	0.214	0.022	18.272	0.228	0.003	0.103	100.259	0.699	80.521
SP98-39_OL10	38.931	42.273	0.055	0.213	0.024	18.263	0.233	0.001	0.101	100.093	0.698	80.487
SP98-39_OL10	38.954	42.366	0.053	0.218	0.024	18.273	0.231	0.004	0.098	100.222	0.699	80.513
SP98-39_OL10	38.985	42.304	0.054	0.213	0.020	18.217	0.232	0.000	0.103	100.127	0.699	80.538
SP98-39_OL10	38.947	42.246	0.052	0.214	0.027	18.210	0.227	0.005	0.098	100.026	0.699	80.523
SP98-39_OL10	38.974	42.342	0.053	0.212	0.022	18.258	0.222	0.006	0.100	100.189	0.699	80.516
SP98-39_OL10	38.930	42.372	0.054	0.217	0.021	18.203	0.231	0.007	0.099	100.132	0.700	80.576
SP98-39_OL10	38.775	42.273	0.055	0.213	0.022	18.226	0.233	0.001	0.102	99.899	0.699	80.519
SP98-39_OL10	39.170	42.547	0.054	0.216	0.021	18.300	0.226	0.002	0.097	100.633	0.699	80.556
SP98-39_OL10	38.759	42.250	0.052	0.217	0.023	18.167	0.232	0.000	0.103	99.802	0.699	80.561
SP98-39_OL10	38.791	42.232	0.053	0.215	0.023	18.156	0.231	0.006	0.097	99.803	0.699	80.564

SP98-39_OL10	38.736	42.529	0.051	0.213	0.021	18.154	0.228	0.005	0.102	100.039	0.701	80.675
SP98-39_OL10	38.854	42.292	0.052	0.216	0.021	18.102	0.227	0.000	0.103	99.867	0.700	80.632
SP98-39_OL10	38.859	42.371	0.054	0.214	0.025	18.106	0.226	0.001	0.103	99.958	0.701	80.658
SP98-39_OL10	38.745	42.368	0.055	0.218	0.021	18.154	0.220	0.002	0.105	99.888	0.700	80.615
SP98-39_OL10	38.935	42.461	0.059	0.217	0.022	18.057	0.227	0.005	0.097	100.078	0.702	80.734
SP98-39_OL10	38.425	41.805	0.439	0.219	0.022	18.079	0.231	0.004	0.100	99.324	0.698	80.471
SP98-39_OL10	38.807	42.559	0.052	0.218	0.026	18.054	0.228	0.007	0.105	100.057	0.702	80.772
SP98-39_OL10	39.061	42.547	0.053	0.219	0.022	18.024	0.226	0.003	0.106	100.261	0.702	80.794
SP98-39_OL10	39.042	42.513	0.053	0.219	0.022	18.033	0.229	0.002	0.098	100.210	0.702	80.773
SP98-39_OL10	38.971	42.520	0.054	0.219	0.022	18.010	0.227	0.000	0.094	100.117	0.702	80.795
SP98-39_OL10	38.968	42.481	0.051	0.222	0.024	17.942	0.229	0.003	0.096	100.016	0.703	80.840
SP98-39_OL10	38.906	42.526	0.056	0.219	0.021	17.943	0.226	0.002	0.106	100.004	0.703	80.855
SP98-39_OL10	38.964	42.466	0.054	0.223	0.021	17.889	0.222	0.003	0.107	99.950	0.704	80.881
SP98-39_OL10	39.029	42.437	0.054	0.220	0.021	17.886	0.218	0.000	0.101	99.966	0.703	80.872
SP98-39_OL10	38.978	42.445	0.054	0.221	0.024	17.840	0.220	0.005	0.105	99.891	0.704	80.915
SP98-39_OL10	38.970	42.586	0.055	0.225	0.023	17.854	0.228	0.004	0.111	100.056	0.705	80.954
SP98-39_OL10	39.006	42.673	0.053	0.224	0.023	17.818	0.223	0.007	0.103	100.131	0.705	81.016
SP98-39_OL10	39.060	42.562	0.052	0.228	0.027	17.729	0.222	0.001	0.102	99.983	0.706	81.054
SP98-39_OL10	39.009	42.614	0.059	0.224	0.026	17.718	0.221	0.003	0.100	99.974	0.706	81.082
SP98-39_OL10	39.018	42.629	0.059	0.227	0.027	17.708	0.220	0.000	0.109	99.997	0.707	81.096
SP98-39_OL10	38.899	42.468	0.058	0.228	0.028	17.659	0.221	0.003	0.109	99.672	0.706	81.081
SP98-39_OL10	39.010	42.697	0.059	0.231	0.029	17.670	0.216	0.005	0.110	100.026	0.707	81.153
SP98-39_OL10	39.017	42.729	0.058	0.230	0.028	17.665	0.217	0.002	0.113	100.058	0.708	81.169
SP98-39_OL10	39.038	42.699	0.056	0.229	0.027	17.606	0.220	0.004	0.110	99.990	0.708	81.209
SP98-39_OL10	39.027	42.785	0.057	0.229	0.024	17.622	0.219	0.007	0.110	100.081	0.708	81.226
SP98-39_OL10	39.105	42.754	0.057	0.232	0.026	17.607	0.221	0.005	0.115	100.120	0.708	81.229
SP98-39_OL10	39.026	42.789	0.057	0.232	0.022	17.567	0.221	0.005	0.120	100.038	0.709	81.275
SP98-39_OL10	39.096	42.803	0.054	0.233	0.022	17.522	0.225	0.000	0.118	100.074	0.710	81.319
SP98-39_OL10	39.059	42.865	0.056	0.233	0.024	17.518	0.218	0.000	0.125	100.097	0.710	81.345

SP98-39_OL10	39.009	42.890	0.053	0.235	0.022	17.493	0.220	0.002	0.119	100.043	0.710	81.375
SP98-39_OL10	39.113	42.953	0.053	0.238	0.021	17.491	0.219	0.006	0.127	100.220	0.711	81.399
SP98-39_OL10	39.034	42.901	0.052	0.237	0.020	17.456	0.218	0.008	0.123	100.049	0.711	81.411
SP98-39_OL10	39.125	42.979	0.050	0.240	0.017	17.462	0.218	0.008	0.134	100.231	0.711	81.433
SP98-39_OL10	39.198	43.106	0.051	0.241	0.022	17.459	0.217	0.000	0.125	100.419	0.712	81.480
SP98-39_OL10	39.123	42.990	0.049	0.242	0.018	17.387	0.220	0.004	0.130	100.162	0.712	81.502
SP98-39_OL10	39.058	42.948	0.051	0.246	0.017	17.408	0.223	0.004	0.133	100.089	0.712	81.469
SP98-39_OL10	39.020	42.958	0.052	0.242	0.023	17.382	0.217	0.005	0.140	100.039	0.712	81.496
SP98-39_OL10	38.991	42.854	0.050	0.245	0.018	17.293	0.218	0.006	0.139	99.813	0.712	81.536
SP98-39_OL10	39.014	42.997	0.052	0.245	0.022	17.322	0.215	0.007	0.133	100.005	0.713	81.561
SP98-39_OL10	39.119	43.067	0.052	0.248	0.018	17.228	0.217	0.001	0.140	100.090	0.714	81.667
SP98-39_OL10	38.757	43.118	0.051	0.251	0.022	17.213	0.221	0.005	0.148	99.785	0.715	81.698
SP98-39_OL10	39.088	43.230	0.052	0.253	0.016	17.144	0.222	0.003	0.141	100.150	0.716	81.796
SP98-39_OL10	39.120	43.334	0.050	0.259	0.019	17.104	0.223	0.000	0.145	100.253	0.717	81.867
SP98-39_OL10	39.184	43.255	0.051	0.259	0.020	17.035	0.217	0.008	0.145	100.174	0.717	81.900
SP98-39_OL10	39.104	43.202	0.051	0.265	0.021	16.966	0.220	0.009	0.153	99.990	0.718	81.942
SP98-39_OL10	39.008	43.231	0.050	0.274	0.020	16.977	0.229	0.004	0.154	99.947	0.718	81.942
SP98-39_OL10	38.810	43.069	0.049	0.286	0.022	17.120	0.230	0.009	0.163	99.757	0.716	81.762
SP98-39_OL10	39.151	42.844	0.049	0.296	0.024	17.316	0.241	0.012	0.167	100.098	0.712	81.513
SP98-39_OL10	39.019	42.570	0.046	0.309	0.020	17.729	0.249	0.022	0.170	100.135	0.706	81.056
SP98-39_OL10	38.921	42.218	0.049	0.319	0.026	18.177	0.264	0.018	0.173	100.165	0.699	80.541
SP98-39_OL10	38.873	41.728	0.044	0.323	0.029	18.635	0.271	0.018	0.171	100.091	0.691	79.961
SP98-39_OL10	38.828	41.381	0.043	0.338	0.026	19.188	0.294	0.018	0.168	100.283	0.683	79.352
SP98-39_OL10	38.546	40.548	0.042	0.359	0.033	19.877	0.310	0.016	0.158	99.888	0.671	78.425
SP98-39_OL10	38.489	39.965	0.044	0.387	0.032	20.704	0.333	0.016	0.155	100.124	0.659	77.476
SP98-39_OL10	38.378	39.250	0.042	0.423	0.030	21.546	0.347	0.018	0.138	100.171	0.646	76.450
SP98-39_OL10	38.164	38.419	0.039	0.476	0.042	22.399	0.354	0.009	0.117	100.019	0.632	75.348
SP98-39_OL10	37.909	37.114	0.035	0.533	0.058	23.959	0.383	0.007	0.101	100.098	0.608	73.407
SP98-39_OL10	37.381	34.792	0.037	0.588	0.079	26.563	0.431	0.007	0.096	99.974	0.567	70.007

SP98-39_OL10-R	36.468	30.461	0.046	0.734	0.115	31.743	0.556	0.009	0.064	100.195	0.490	63.100
SP98-25_OL1-C	40.242	46.899	0.062	0.230	0.016	13.022	0.160	0.043	0.256	100.930	0.783	86.519
SP98-25_OL1	40.155	46.814	0.062	0.229	0.016	13.026	0.150	0.045	0.248	100.745	0.782	86.495
SP98-25_OL1	40.181	46.816	0.062	0.234	0.012	13.029	0.159	0.047	0.252	100.791	0.782	86.492
SP98-25_OL1	40.185	46.892	0.064	0.231	0.015	13.022	0.158	0.040	0.255	100.861	0.783	86.518
SP98-25_OL1	40.179	46.748	0.067	0.231	0.016	13.023	0.161	0.040	0.254	100.718	0.782	86.480
SP98-25_OL1	40.131	46.757	0.063	0.231	0.016	13.014	0.152	0.046	0.255	100.665	0.782	86.491
SP98-25_OL1	40.091	46.790	0.064	0.231	0.016	13.064	0.157	0.041	0.255	100.708	0.782	86.455
SP98-25_OL1	40.055	46.754	0.067	0.230	0.017	13.025	0.154	0.041	0.252	100.594	0.782	86.480
SP98-25_OL1	40.072	46.776	0.068	0.233	0.012	13.043	0.157	0.044	0.254	100.658	0.782	86.470
SP98-25_OL1	40.133	46.777	0.068	0.232	0.017	13.060	0.156	0.045	0.258	100.745	0.782	86.454
SP98-25_OL1	40.120	46.860	0.069	0.232	0.015	13.046	0.156	0.042	0.252	100.792	0.782	86.488
SP98-25_OL1	40.141	46.888	0.067	0.231	0.013	13.042	0.159	0.044	0.258	100.843	0.782	86.498
SP98-25_OL1	40.106	46.798	0.065	0.234	0.015	13.027	0.159	0.050	0.253	100.706	0.782	86.489
SP98-25_OL1	40.132	46.849	0.067	0.232	0.017	13.059	0.163	0.042	0.259	100.818	0.782	86.474
SP98-25_OL1	40.059	46.689	0.066	0.231	0.017	13.065	0.160	0.046	0.248	100.581	0.781	86.429
SP98-25_OL1	40.185	46.817	0.067	0.232	0.016	13.045	0.159	0.038	0.253	100.810	0.782	86.478
SP98-25_OL1	40.115	46.808	0.063	0.234	0.018	13.044	0.159	0.045	0.252	100.739	0.782	86.476
SP98-25_OL1	40.061	46.882	0.063	0.229	0.018	13.012	0.162	0.045	0.253	100.725	0.783	86.524
SP98-25_OL1	40.069	46.822	0.067	0.230	0.013	13.056	0.156	0.041	0.249	100.702	0.782	86.469
SP98-25_OL1	40.049	46.800	0.066	0.232	0.017	13.042	0.160	0.039	0.253	100.659	0.782	86.476
SP98-25_OL1	40.093	46.733	0.065	0.229	0.015	13.049	0.160	0.043	0.257	100.643	0.782	86.454
SP98-25_OL1	40.088	46.745	0.067	0.233	0.016	13.028	0.160	0.045	0.258	100.640	0.782	86.475
SP98-25_OL1	40.039	46.783	0.066	0.231	0.020	13.035	0.158	0.044	0.254	100.629	0.782	86.478
SP98-25_OL1	40.086	46.804	0.065	0.231	0.016	13.043	0.152	0.045	0.257	100.700	0.782	86.477
SP98-25_OL1	40.079	46.871	0.066	0.231	0.018	13.026	0.162	0.044	0.255	100.751	0.783	86.508
SP98-25_OL1	40.208	46.855	0.065	0.234	0.017	13.018	0.158	0.047	0.252	100.853	0.783	86.512
SP98-25_OL1	40.170	46.812	0.067	0.229	0.021	13.032	0.163	0.047	0.257	100.798	0.782	86.489
SP98-25_OL1	40.159	46.774	0.065	0.230	0.018	13.009	0.158	0.043	0.260	100.715	0.782	86.500

SP98-25_OL1	40.027	46.653	0.064	0.233	0.017	13.009	0.154	0.045	0.253	100.454	0.782	86.470
SP98-25_OL1	40.083	46.744	0.065	0.231	0.015	13.001	0.158	0.045	0.255	100.597	0.782	86.499
SP98-25_OL1	40.031	46.723	0.066	0.235	0.017	13.012	0.158	0.044	0.251	100.536	0.782	86.485
SP98-25_OL1	40.102	46.765	0.066	0.232	0.015	13.032	0.157	0.050	0.257	100.677	0.782	86.476
SP98-25_OL1	40.059	46.776	0.066	0.232	0.013	13.006	0.161	0.047	0.256	100.615	0.782	86.503
SP98-25_OL1	40.149	46.841	0.064	0.233	0.018	13.024	0.157	0.050	0.258	100.793	0.782	86.503
SP98-25_OL1	40.078	46.827	0.066	0.232	0.014	13.002	0.158	0.042	0.259	100.679	0.783	86.519
SP98-25_OL1	40.208	46.902	0.065	0.233	0.015	13.033	0.159	0.045	0.257	100.916	0.783	86.510
SP98-25_OL1	40.137	46.831	0.065	0.234	0.017	12.985	0.156	0.047	0.253	100.725	0.783	86.535
SP98-25_OL1	40.149	46.784	0.066	0.232	0.013	12.997	0.155	0.045	0.254	100.696	0.783	86.513
SP98-25_OL1	40.071	46.860	0.066	0.239	0.016	13.038	0.157	0.045	0.253	100.745	0.782	86.495
SP98-25_OL1	40.131	46.791	0.065	0.235	0.018	13.014	0.162	0.042	0.258	100.715	0.782	86.500
SP98-25_OL1	40.102	46.814	0.066	0.234	0.015	13.096	0.162	0.048	0.256	100.793	0.781	86.432
SP98-25_OL1	40.215	46.922	0.066	0.234	0.014	13.020	0.163	0.047	0.262	100.942	0.783	86.527
SP98-25_OL1	40.233	46.880	0.065	0.234	0.018	13.012	0.158	0.051	0.256	100.907	0.783	86.523
SP98-25_OL1	40.210	46.884	0.063	0.235	0.020	13.045	0.161	0.040	0.256	100.914	0.782	86.495
SP98-25_OL1	40.170	46.922	0.066	0.237	0.013	13.039	0.160	0.045	0.260	100.912	0.783	86.509
SP98-25_OL1	40.255	46.891	0.065	0.237	0.013	13.025	0.158	0.041	0.257	100.942	0.783	86.514
SP98-25_OL1	40.120	46.882	0.067	0.234	0.017	13.015	0.157	0.044	0.255	100.790	0.783	86.521
SP98-25_OL1	40.139	46.754	0.067	0.237	0.016	13.011	0.155	0.041	0.261	100.681	0.782	86.493
SP98-25_OL1	40.097	46.858	0.063	0.233	0.016	12.986	0.159	0.052	0.256	100.720	0.783	86.541
SP98-25_OL1	40.135	46.865	0.065	0.237	0.017	13.028	0.158	0.042	0.260	100.808	0.782	86.505
SP98-25_OL1	40.155	46.845	0.063	0.236	0.016	13.005	0.156	0.050	0.259	100.785	0.783	86.521
SP98-25_OL1	40.175	46.894	0.066	0.233	0.017	13.014	0.159	0.049	0.256	100.861	0.783	86.525
SP98-25_OL1	40.093	46.771	0.064	0.237	0.016	12.987	0.157	0.047	0.258	100.629	0.783	86.518
SP98-25_OL1	40.095	46.853	0.064	0.236	0.013	12.975	0.155	0.047	0.257	100.695	0.783	86.550
SP98-25_OL1	40.118	46.963	0.064	0.235	0.013	13.003	0.155	0.052	0.259	100.861	0.783	86.552
SP98-25_OL1	40.235	46.774	0.066	0.234	0.020	12.947	0.153	0.046	0.256	100.730	0.783	86.555
SP98-25_OL1	40.145	46.750	0.065	0.239	0.015	12.984	0.155	0.050	0.255	100.657	0.783	86.516

SP98-25_OL1	40.135	46.742	0.065	0.238	0.015	12.960	0.163	0.041	0.256	100.616	0.783	86.535
SP98-25_OL1	40.187	46.790	0.066	0.239	0.016	12.971	0.159	0.046	0.256	100.730	0.783	86.538
SP98-25_OL1	40.156	46.791	0.065	0.235	0.017	12.979	0.161	0.044	0.260	100.708	0.783	86.531
SP98-25_OL1	40.101	46.794	0.065	0.240	0.016	12.961	0.154	0.047	0.261	100.639	0.783	86.548
SP98-25_OL1	40.121	46.605	0.068	0.242	0.013	13.000	0.157	0.047	0.263	100.515	0.782	86.466
SP98-25_OL1	40.171	46.854	0.070	0.240	0.019	12.933	0.160	0.051	0.263	100.760	0.784	86.587
SP98-25_OL1	40.146	46.894	0.066	0.237	0.016	12.996	0.154	0.051	0.263	100.823	0.783	86.541
SP98-25_OL1	40.138	46.835	0.066	0.239	0.013	12.924	0.158	0.054	0.258	100.685	0.784	86.591
SP98-25_OL1	40.122	46.767	0.065	0.240	0.014	12.942	0.150	0.050	0.258	100.608	0.783	86.558
SP98-25_OL1	40.026	46.802	0.066	0.239	0.013	12.982	0.157	0.050	0.265	100.599	0.783	86.530
SP98-25_OL1	40.133	46.882	0.064	0.237	0.016	12.979	0.155	0.048	0.262	100.777	0.783	86.553
SP98-25_OL1	40.134	46.855	0.066	0.237	0.013	13.007	0.161	0.052	0.267	100.792	0.783	86.522
SP98-25_OL1	40.089	46.904	0.064	0.240	0.015	13.018	0.158	0.054	0.261	100.802	0.783	86.524
SP98-25_OL1	40.198	46.927	0.061	0.238	0.016	13.015	0.153	0.049	0.263	100.920	0.783	86.532
SP98-25_OL1	40.073	46.902	0.063	0.238	0.014	13.025	0.159	0.052	0.272	100.797	0.783	86.517
SP98-25_OL1	40.078	46.895	0.063	0.239	0.012	13.027	0.154	0.051	0.263	100.783	0.783	86.514
SP98-25_OL1	39.938	46.823	0.063	0.241	0.014	13.008	0.157	0.051	0.265	100.560	0.783	86.513
SP98-25_OL1	39.892	46.821	0.060	0.240	0.014	13.026	0.159	0.047	0.268	100.527	0.782	86.496
SP98-25_OL1	40.258	46.912	0.063	0.240	0.013	12.980	0.155	0.047	0.270	100.937	0.783	86.560
SP98-25_OL1	40.220	46.878	0.064	0.240	0.017	12.985	0.157	0.053	0.268	100.881	0.783	86.547
SP98-25_OL1	40.179	46.828	0.065	0.240	0.014	12.971	0.158	0.052	0.267	100.772	0.783	86.547
SP98-25_OL1	40.088	46.787	0.067	0.241	0.015	12.984	0.158	0.050	0.263	100.652	0.783	86.525
SP98-25_OL1	40.172	46.778	0.065	0.238	0.013	12.977	0.155	0.054	0.265	100.715	0.783	86.530
SP98-25_OL1	40.170	46.749	0.065	0.241	0.013	13.021	0.154	0.047	0.264	100.722	0.782	86.483
SP98-25_OL1	40.201	46.758	0.065	0.238	0.014	13.018	0.159	0.053	0.267	100.773	0.782	86.488
SP98-25_OL1	40.164	46.863	0.066	0.239	0.014	13.059	0.158	0.047	0.273	100.883	0.782	86.477
SP98-25_OL1	40.225	46.825	0.064	0.240	0.016	13.042	0.158	0.048	0.265	100.883	0.782	86.482
SP98-25_OL1	40.175	46.838	0.065	0.241	0.010	13.051	0.157	0.055	0.273	100.864	0.782	86.478
SP98-25_OL1	40.194	46.721	0.066	0.238	0.013	13.111	0.159	0.055	0.269	100.825	0.781	86.395

SP98-25_OL1	40.073	46.725	0.066	0.242	0.014	13.080	0.159	0.054	0.264	100.676	0.781	86.423
SP98-25_OL1	40.104	46.719	0.068	0.242	0.016	13.116	0.154	0.054	0.270	100.743	0.781	86.390
SP98-25_OL1	40.149	46.738	0.061	0.240	0.015	13.162	0.156	0.052	0.269	100.842	0.780	86.353
SP98-25_OL1	40.132	46.722	0.060	0.243	0.014	13.137	0.156	0.050	0.268	100.782	0.781	86.372
SP98-25_OL1	40.183	46.820	0.063	0.242	0.014	13.166	0.162	0.047	0.268	100.964	0.781	86.370
SP98-25_OL1	40.103	46.745	0.061	0.237	0.013	13.173	0.157	0.047	0.265	100.802	0.780	86.346
SP98-25_OL1	40.225	46.742	0.058	0.241	0.009	13.199	0.157	0.047	0.264	100.943	0.780	86.322
SP98-25_OL1	40.217	46.697	0.082	0.241	0.012	13.191	0.160	0.060	0.263	100.923	0.780	86.317
SP98-25_OL1	40.198	46.702	0.065	0.238	0.011	13.228	0.159	0.048	0.263	100.911	0.779	86.285
SP98-25_OL1	40.170	46.532	0.062	0.242	0.012	13.233	0.159	0.052	0.264	100.726	0.779	86.237
SP98-25_OL1	40.072	46.665	0.064	0.242	0.013	13.274	0.164	0.049	0.270	100.811	0.779	86.235
SP98-25_OL1	40.016	46.703	0.070	0.245	0.014	13.290	0.161	0.047	0.264	100.809	0.778	86.230
SP98-25_OL1	40.105	46.397	0.158	0.242	0.016	13.259	0.158	0.068	0.265	100.668	0.778	86.180
SP98-25_OL1	40.123	46.501	0.111	0.244	0.012	13.302	0.162	0.057	0.263	100.774	0.778	86.168
SP98-25_OL1	40.058	46.516	0.069	0.249	0.015	13.320	0.167	0.055	0.261	100.710	0.777	86.156
SP98-25_OL1	40.114	46.571	0.068	0.248	0.010	13.359	0.163	0.052	0.254	100.838	0.777	86.134
SP98-25_OL1	40.074	46.397	0.073	0.245	0.011	13.397	0.163	0.055	0.260	100.675	0.776	86.055
SP98-25_OL1	40.094	46.450	0.068	0.246	0.014	13.450	0.160	0.048	0.259	100.788	0.775	86.022
SP98-25_OL1	40.121	46.415	0.067	0.249	0.010	13.445	0.161	0.048	0.254	100.770	0.775	86.018
SP98-25_OL1	40.251	46.632	0.064	0.250	0.012	13.479	0.169	0.050	0.256	101.163	0.776	86.043
SP98-25_OL1	40.098	46.477	0.065	0.254	0.014	13.475	0.165	0.050	0.252	100.848	0.775	86.007
SP98-25_OL1	40.096	46.438	0.065	0.254	0.014	13.531	0.166	0.045	0.250	100.861	0.774	85.947
SP98-25_OL1	39.852	46.274	0.066	0.258	0.013	13.556	0.172	0.042	0.250	100.484	0.773	85.881
SP98-25_OL1	39.833	46.193	0.066	0.260	0.011	13.602	0.170	0.050	0.248	100.431	0.773	85.819
SP98-25_OL1	40.020	46.301	0.068	0.267	0.015	13.651	0.172	0.046	0.246	100.785	0.772	85.804
SP98-25_OL1	40.109	46.449	0.066	0.269	0.017	13.694	0.165	0.043	0.250	101.063	0.772	85.804
SP98-25_OL1	40.018	46.340	0.063	0.272	0.015	13.747	0.173	0.048	0.250	100.925	0.771	85.728
SP98-25_OL1	40.062	46.343	0.066	0.276	0.018	13.798	0.162	0.046	0.242	101.012	0.771	85.684
SP98-25_OL1	40.144	46.386	0.063	0.282	0.016	13.866	0.174	0.044	0.240	101.213	0.770	85.635

SP98-25_OL1	40.083	46.162	0.057	0.287	0.016	13.900	0.175	0.038	0.238	100.956	0.769	85.545
SP98-25_OL1	40.016	46.072	0.057	0.291	0.014	13.970	0.169	0.037	0.238	100.862	0.767	85.459
SP98-25_OL1	39.936	45.874	0.054	0.299	0.015	14.158	0.178	0.037	0.233	100.784	0.764	85.238
SP98-25_OL1	39.833	45.770	0.053	0.299	0.015	14.352	0.177	0.033	0.222	100.752	0.761	85.037
SP98-25_OL1	39.870	45.437	0.047	0.307	0.017	14.689	0.182	0.031	0.222	100.802	0.756	84.644
SP98-25_OL1	39.793	45.003	0.047	0.308	0.015	15.253	0.193	0.028	0.215	100.854	0.747	84.020
SP98-25_OL1	39.452	44.139	0.048	0.316	0.025	16.266	0.213	0.025	0.202	100.685	0.731	82.864
SP98-25_OL1	39.342	42.878	0.046	0.323	0.020	17.858	0.232	0.021	0.175	100.894	0.706	81.056
SP98-25_OL1	38.910	41.017	0.042	0.346	0.022	19.988	0.265	0.016	0.158	100.764	0.672	78.526
SP98-25_OL1	38.388	37.923	0.039	0.393	0.024	23.602	0.330	0.009	0.133	100.840	0.616	74.115
SP98-25_OL1	37.328	32.538	0.036	0.494	0.043	30.060	0.470	0.004	0.085	101.056	0.520	65.857
SP98-25_OL1-R	36.121	27.965	0.030	0.622	0.063	35.262	0.620	0.001	0.059	100.745	0.442	58.562
SP98-25_OL2-C	39.757	44.914	0.065	0.233	0.015	15.398	0.183	0.022	0.216	100.801	0.745	83.866
SP98-25_OL2	39.623	44.674	0.064	0.229	0.018	15.406	0.186	0.021	0.218	100.439	0.744	83.786
SP98-25_OL2	39.477	44.687	0.062	0.228	0.019	15.581	0.185	0.020	0.218	100.476	0.741	83.636
SP98-25_OL2	39.339	44.621	0.060	0.228	0.029	15.513	0.185	0.012	0.212	100.199	0.742	83.675
SP98-25_OL2-R	37.745	37.379	0.033	0.480	0.037	23.666	0.356	0.007	0.118	99.821	0.612	73.784
SP98-25_OL3-C	39.510	45.276	0.053	0.236	0.015	14.721	0.178	0.022	0.205	100.215	0.755	84.569
SP98-25_OL3	39.879	45.865	0.572	0.241	0.013	14.678	0.180	0.026	0.206	101.660	0.758	84.776
SP98-25_OL3	39.759	45.573	0.057	0.236	0.013	14.738	0.180	0.019	0.217	100.790	0.756	84.640
SP98-25_OL3	39.902	45.470	0.056	0.236	0.012	14.703	0.180	0.024	0.210	100.791	0.756	84.642
SP98-25_OL3	39.822	45.456	0.059	0.237	0.015	14.730	0.181	0.026	0.212	100.740	0.755	84.613
SP98-25_OL3	39.839	45.419	0.056	0.238	0.014	14.695	0.178	0.024	0.207	100.669	0.756	84.634
SP98-25_OL3	39.803	45.388	0.056	0.238	0.013	14.712	0.178	0.025	0.217	100.630	0.755	84.609
SP98-25_OL3	39.807	45.448	0.058	0.238	0.016	14.712	0.174	0.027	0.214	100.694	0.755	84.627
SP98-25_OL3	39.807	45.463	0.056	0.241	0.013	14.674	0.178	0.027	0.205	100.664	0.756	84.665
SP98-25_OL3	39.777	45.383	0.056	0.235	0.013	14.727	0.177	0.025	0.215	100.608	0.755	84.596
SP98-25_OL3	39.808	45.459	0.055	0.239	0.014	14.697	0.178	0.025	0.213	100.687	0.756	84.643
SP98-25_OL3	39.873	45.529	0.055	0.239	0.016	14.706	0.182	0.027	0.208	100.835	0.756	84.655

SP98-25_OL3	39.761	45.432	0.055	0.239	0.014	14.677	0.177	0.025	0.213	100.592	0.756	84.654
SP98-25_OL3	39.858	45.446	0.056	0.238	0.013	14.646	0.176	0.019	0.208	100.661	0.756	84.685
SP98-25_OL3	39.759	45.156	0.053	0.239	0.014	14.615	0.174	0.029	0.212	100.252	0.755	84.629
SP98-25_OL3	39.829	45.513	0.055	0.239	0.013	14.707	0.178	0.023	0.213	100.769	0.756	84.650
SP98-25_OL3	39.781	45.426	0.056	0.239	0.017	14.658	0.179	0.025	0.206	100.586	0.756	84.668
SP98-25_OL3	39.797	45.480	0.055	0.240	0.017	14.633	0.177	0.026	0.216	100.641	0.757	84.706
SP98-25_OL3	39.814	45.409	0.056	0.241	0.014	14.668	0.178	0.025	0.207	100.612	0.756	84.655
SP98-25_OL3	39.848	45.494	0.057	0.239	0.014	14.690	0.177	0.025	0.211	100.753	0.756	84.660
SP98-25_OL3	39.865	45.536	0.056	0.240	0.012	14.643	0.176	0.029	0.213	100.770	0.757	84.713
SP98-25_OL3	39.851	45.430	0.057	0.242	0.014	14.591	0.176	0.025	0.213	100.599	0.757	84.729
SP98-25_OL3	39.820	45.531	0.055	0.241	0.014	14.590	0.178	0.027	0.209	100.665	0.757	84.759
SP98-25_OL3	39.850	45.489	0.055	0.242	0.013	14.550	0.175	0.026	0.210	100.609	0.758	84.783
SP98-25_OL3	39.803	45.633	0.057	0.245	0.016	14.624	0.178	0.021	0.212	100.789	0.757	84.757
SP98-25_OL3	39.782	45.494	0.057	0.242	0.020	14.570	0.173	0.026	0.211	100.574	0.757	84.766
SP98-25_OL3	39.742	45.539	0.057	0.244	0.014	14.553	0.184	0.025	0.210	100.568	0.758	84.793
SP98-25_OL3	39.762	45.573	0.057	0.249	0.016	14.529	0.175	0.027	0.211	100.599	0.758	84.825
SP98-25_OL3	39.584	45.577	0.057	0.249	0.013	14.553	0.180	0.028	0.214	100.452	0.758	84.805
SP98-25_OL3	39.646	45.555	0.055	0.246	0.016	14.474	0.177	0.032	0.211	100.412	0.759	84.868
SP98-25_OL3	39.733	45.523	0.056	0.252	0.013	14.513	0.176	0.026	0.210	100.503	0.758	84.824
SP98-25_OL3	39.842	45.539	0.055	0.250	0.015	14.450	0.181	0.031	0.208	100.570	0.759	84.885
SP98-25_OL3	39.768	45.611	0.054	0.255	0.017	14.427	0.175	0.031	0.209	100.546	0.760	84.925
SP98-25_OL3	39.887	45.619	0.055	0.252	0.014	14.438	0.173	0.027	0.208	100.673	0.760	84.918
SP98-25_OL3	39.773	45.643	0.052	0.255	0.014	14.440	0.177	0.028	0.211	100.594	0.760	84.923
SP98-25_OL3	39.827	45.712	0.052	0.259	0.014	14.415	0.178	0.037	0.212	100.706	0.760	84.965
SP98-25_OL3	39.831	45.723	0.050	0.264	0.015	14.391	0.181	0.027	0.209	100.692	0.761	84.989
SP98-25_OL3	39.839	45.756	0.047	0.266	0.011	14.384	0.179	0.031	0.213	100.726	0.761	85.004
SP98-25_OL3	39.823	45.702	0.047	0.268	0.010	14.342	0.179	0.024	0.213	100.606	0.761	85.027
SP98-25_OL3	39.855	45.682	0.044	0.268	0.012	14.363	0.177	0.024	0.213	100.637	0.761	85.002
SP98-25_OL3	39.769	45.687	0.044	0.276	0.015	14.375	0.181	0.030	0.216	100.594	0.761	84.993

SP98-25_OL3	39.750	45.545	0.047	0.274	0.013	14.397	0.181	0.033	0.219	100.458	0.760	84.934
SP98-25_OL3	39.730	45.541	0.047	0.281	0.012	14.454	0.181	0.034	0.220	100.500	0.759	84.882
SP98-25_OL3	39.834	45.439	0.049	0.286	0.016	14.535	0.189	0.037	0.223	100.608	0.758	84.781
SP98-25_OL3	39.729	45.381	0.055	0.291	0.013	14.677	0.186	0.038	0.221	100.589	0.756	84.639
SP98-25_OL3	39.612	45.172	0.053	0.294	0.014	14.899	0.190	0.038	0.220	100.491	0.752	84.382
SP98-25_OL3	39.577	44.701	0.053	0.297	0.018	15.215	0.201	0.043	0.218	100.323	0.746	83.963
SP98-25_OL3	39.549	44.441	0.049	0.301	0.012	15.562	0.210	0.034	0.216	100.373	0.741	83.576
SP98-25_OL3	39.392	44.053	0.047	0.304	0.018	16.120	0.221	0.031	0.210	100.395	0.732	82.964
SP98-25_OL3	39.214	43.465	0.050	0.310	0.018	16.710	0.233	0.031	0.193	100.223	0.722	82.254
SP98-25_OL3	39.067	43.020	0.049	0.314	0.020	17.308	0.239	0.028	0.191	100.236	0.713	81.582
SP98-25_OL3	38.905	42.379	0.044	0.320	0.021	18.037	0.260	0.028	0.177	100.172	0.701	80.720
SP98-25_OL3	38.764	41.530	0.042	0.343	0.022	18.954	0.276	0.022	0.166	100.119	0.687	79.610
SP98-25_OL3	38.751	40.859	0.039	0.361	0.020	19.714	0.289	0.020	0.149	100.202	0.675	78.693
SP98-25_OL3	38.511	39.930	0.043	0.395	0.024	20.665	0.308	0.017	0.139	100.033	0.659	77.494
SP98-25_OL3	38.283	39.177	0.038	0.421	0.024	21.637	0.325	0.014	0.132	100.052	0.644	76.340
SP98-25_OL3	37.903	37.775	0.036	0.455	0.027	23.099	0.349	0.009	0.119	99.773	0.621	74.452
SP98-25_OL3-R	37.344	35.659	0.038	0.488	0.032	25.426	0.393	0.007	0.112	99.500	0.584	71.422
SP98-25_OL4-C	39.619	44.660	0.061	0.218	0.016	15.531	0.182	0.021	0.224	100.533	0.742	83.671
SP98-25_OL4	39.598	44.602	0.065	0.220	0.019	15.551	0.180	0.018	0.219	100.473	0.741	83.636
SP98-25_OL4	39.498	44.352	0.062	0.214	0.019	15.750	0.186	0.014	0.218	100.314	0.738	83.383
SP98-25_OL4	39.933	44.881	0.060	0.221	0.022	15.708	0.191	0.020	0.210	101.245	0.741	83.584
SP98-25_OL4-R	39.179	44.068	0.048	0.311	0.018	15.518	0.198	0.022	0.202	99.563	0.740	83.500
SP98-25_OL5-C	39.714	44.894	0.061	0.209	0.017	15.189	0.176	0.026	0.219	100.503	0.747	84.044
SP98-25_OL5	39.725	44.962	0.059	0.209	0.017	15.259	0.177	0.021	0.223	100.651	0.747	84.002
SP98-25_OL5	39.672	44.872	0.059	0.208	0.013	15.192	0.182	0.026	0.221	100.445	0.747	84.034
SP98-25_OL5	39.781	44.951	0.059	0.211	0.020	15.221	0.181	0.017	0.217	100.657	0.747	84.033
SP98-25_OL5	39.731	44.908	0.059	0.208	0.015	15.207	0.182	0.020	0.221	100.550	0.747	84.032
SP98-25_OL5	39.674	44.804	0.059	0.209	0.013	15.228	0.180	0.018	0.229	100.412	0.746	83.983
SP98-25_OL5	39.647	44.995	0.060	0.212	0.017	15.302	0.184	0.021	0.218	100.655	0.746	83.974

SP98-25_OL5	39.687	44.939	0.058	0.207	0.014	15.231	0.187	0.022	0.224	100.569	0.747	84.020
SP98-25_OL5	39.720	44.975	0.059	0.212	0.020	15.218	0.178	0.021	0.221	100.624	0.747	84.042
SP98-25_OL5	39.559	44.775	0.061	0.208	0.017	15.216	0.182	0.021	0.220	100.259	0.746	83.984
SP98-25_OL5	39.720	44.879	0.057	0.207	0.015	15.213	0.183	0.017	0.221	100.511	0.747	84.017
SP98-25_OL5	39.757	45.006	0.059	0.214	0.015	15.242	0.185	0.021	0.222	100.720	0.747	84.030
SP98-25_OL5	39.832	45.170	0.061	0.209	0.013	15.274	0.180	0.022	0.222	100.984	0.747	84.050
SP98-25_OL5	37.739	42.407	0.118	0.217	0.015	15.135	0.181	0.019	0.219	96.048	0.737	83.313
SP98-25_OL5	39.856	44.864	0.141	0.218	0.017	15.242	0.179	0.019	0.221	100.756	0.746	83.988
SP98-25_OL5	40.560	46.222	0.204	0.218	0.015	15.247	0.182	0.020	0.225	102.894	0.752	84.381
SP98-25_OL5	38.257	42.861	1.285	0.233	0.017	15.133	0.185	0.018	0.215	98.205	0.739	83.463
SP98-25_OL5	39.632	44.901	0.063	0.209	0.016	15.227	0.185	0.016	0.216	100.465	0.747	84.013
SP98-25_OL5	39.742	44.954	0.064	0.212	0.015	15.272	0.182	0.019	0.219	100.680	0.746	83.988
SP98-25_OL5	39.647	44.889	0.062	0.210	0.016	15.224	0.182	0.019	0.225	100.473	0.747	84.011
SP98-25_OL5	39.793	44.929	0.066	0.209	0.017	15.168	0.176	0.023	0.221	100.600	0.748	84.072
SP98-25_OL5	39.726	44.942	0.064	0.210	0.015	15.150	0.180	0.017	0.219	100.522	0.748	84.093
SP98-25_OL5	39.766	44.990	0.065	0.210	0.014	15.177	0.179	0.023	0.225	100.648	0.748	84.083
SP98-25_OL5	39.703	44.956	0.065	0.209	0.018	15.184	0.178	0.021	0.225	100.559	0.748	84.066
SP98-25_OL5	39.655	44.911	0.067	0.207	0.015	15.174	0.177	0.016	0.220	100.440	0.747	84.062
SP98-25_OL5	39.711	44.872	0.067	0.210	0.020	15.158	0.181	0.019	0.221	100.459	0.747	84.064
SP98-25_OL5	39.642	44.887	0.068	0.210	0.018	15.133	0.182	0.025	0.217	100.382	0.748	84.091
SP98-25_OL5	39.665	44.926	0.064	0.209	0.018	15.154	0.178	0.019	0.221	100.454	0.748	84.084
SP98-25_OL5	39.743	44.932	0.068	0.209	0.019	15.138	0.182	0.021	0.216	100.529	0.748	84.100
SP98-25_OL5	39.659	44.871	0.066	0.208	0.016	15.190	0.181	0.023	0.216	100.430	0.747	84.036
SP98-25_OL5	39.796	44.941	0.067	0.209	0.016	15.162	0.180	0.016	0.219	100.607	0.748	84.081
SP98-25_OL5	39.791	45.105	0.067	0.208	0.020	15.261	0.181	0.020	0.221	100.874	0.747	84.043
SP98-25_OL5	39.803	45.133	0.067	0.208	0.014	15.213	0.183	0.020	0.216	100.857	0.748	84.093
SP98-25_OL5	39.727	45.010	0.066	0.207	0.017	15.189	0.181	0.022	0.223	100.642	0.748	84.078
SP98-25_OL5	39.780	44.900	0.065	0.208	0.018	15.223	0.187	0.020	0.223	100.625	0.747	84.015
SP98-25_OL5	39.753	44.956	0.067	0.207	0.018	15.180	0.181	0.020	0.222	100.604	0.748	84.070

SP98-25_OL5	39.732	44.912	0.067	0.209	0.020	15.222	0.182	0.015	0.222	100.580	0.747	84.020
SP98-25_OL5	39.733	44.959	0.067	0.209	0.021	15.216	0.182	0.017	0.222	100.624	0.747	84.039
SP98-25_OL5	39.629	44.783	0.067	0.208	0.018	15.205	0.181	0.021	0.214	100.326	0.747	83.996
SP98-25_OL5	39.708	44.919	0.067	0.212	0.014	15.233	0.182	0.015	0.219	100.567	0.747	84.012
SP98-25_OL5	39.772	44.830	0.067	0.209	0.016	15.186	0.180	0.020	0.219	100.499	0.747	84.027
SP98-25_OL5	39.682	44.914	0.067	0.208	0.014	15.247	0.181	0.016	0.215	100.544	0.747	83.998
SP98-25_OL5	39.741	44.951	0.067	0.208	0.015	15.253	0.184	0.017	0.215	100.651	0.747	84.004
SP98-25_OL5	39.817	45.052	0.077	0.210	0.018	15.223	0.180	0.016	0.218	100.809	0.747	84.061
SP98-25_OL5	39.907	45.242	0.064	0.212	0.016	15.271	0.183	0.018	0.219	101.131	0.748	84.075
SP98-25_OL5	39.626	44.855	0.059	0.207	0.015	15.218	0.180	0.018	0.221	100.398	0.747	84.007
SP98-25_OL5	39.722	44.882	0.058	0.211	0.016	15.239	0.178	0.022	0.215	100.542	0.747	83.996
SP98-25_OL5	39.726	44.974	0.059	0.213	0.019	15.238	0.180	0.016	0.219	100.643	0.747	84.024
SP98-25_OL5	39.638	44.937	0.060	0.215	0.016	15.245	0.180	0.020	0.220	100.530	0.747	84.007
SP98-25_OL5	39.807	44.930	0.059	0.215	0.018	15.315	0.187	0.017	0.218	100.767	0.746	83.943
SP98-25_OL5	39.831	44.860	0.061	0.230	0.014	15.366	0.188	0.019	0.217	100.786	0.745	83.878
SP98-25_OL5	39.791	45.100	0.054	0.267	0.023	15.350	0.181	0.012	0.212	100.989	0.746	83.964
SP98-25_OL5	41.106	45.043	0.313	0.477	0.055	15.504	0.184	0.006	0.181	102.868	0.744	83.812
SP98-25_OL5	39.609	43.554	0.481	0.708	0.059	15.314	0.178	0.003	0.174	100.082	0.740	83.520
SP98-25_OL5	39.701	44.821	0.060	0.258	0.017	15.276	0.182	0.019	0.218	100.551	0.746	83.945
SP98-25_OL5	39.694	44.929	0.060	0.227	0.017	15.282	0.186	0.015	0.222	100.631	0.746	83.972
SP98-25_OL5	39.737	44.871	0.062	0.215	0.017	15.216	0.182	0.021	0.218	100.538	0.747	84.013
SP98-25_OL5	39.724	44.900	0.062	0.213	0.015	15.251	0.182	0.018	0.221	100.585	0.746	83.990
SP98-25_OL5	39.761	44.909	0.061	0.210	0.018	15.270	0.179	0.019	0.214	100.639	0.746	83.977
SP98-25_OL5	39.805	45.076	0.059	0.210	0.014	15.257	0.181	0.019	0.212	100.834	0.747	84.038
SP98-25_OL5	39.836	44.946	0.062	0.211	0.014	15.253	0.182	0.019	0.217	100.737	0.747	84.003
SP98-25_OL5	39.766	44.862	0.060	0.208	0.016	15.278	0.184	0.018	0.218	100.608	0.746	83.956
SP98-25_OL5	39.650	44.841	0.059	0.212	0.015	15.249	0.181	0.021	0.217	100.445	0.746	83.975
SP98-25_OL5	39.660	44.837	0.061	0.209	0.015	15.251	0.181	0.020	0.221	100.454	0.746	83.971
SP98-25_OL5	39.766	44.914	0.059	0.211	0.017	15.262	0.182	0.019	0.218	100.648	0.746	83.985

SP98-25_OL5	39.747	44.867	0.061	0.208	0.014	15.267	0.177	0.022	0.222	100.584	0.746	83.966
SP98-25_OL5	39.785	44.892	0.060	0.209	0.015	15.268	0.182	0.019	0.223	100.651	0.746	83.973
SP98-25_OL5	39.757	44.911	0.060	0.207	0.016	15.280	0.184	0.014	0.222	100.650	0.746	83.968
SP98-25_OL5	39.816	44.947	0.062	0.207	0.016	15.284	0.179	0.019	0.217	100.746	0.746	83.975
SP98-25_OL5	39.702	44.992	0.060	0.211	0.018	15.251	0.181	0.022	0.222	100.659	0.747	84.018
SP98-25_OL5	39.892	44.972	0.060	0.210	0.015	15.231	0.182	0.024	0.216	100.803	0.747	84.029
SP98-25_OL5	39.887	44.971	0.060	0.210	0.014	15.279	0.185	0.018	0.215	100.838	0.746	83.987
SP98-25_OL5	39.764	44.963	0.062	0.207	0.017	15.280	0.185	0.022	0.213	100.713	0.746	83.984
SP98-25_OL5	39.796	44.898	0.061	0.209	0.012	15.290	0.183	0.022	0.215	100.686	0.746	83.956
SP98-25_OL5	39.800	44.908	0.062	0.207	0.016	15.255	0.181	0.017	0.217	100.662	0.746	83.990
SP98-25_OL5	39.854	44.847	0.061	0.206	0.017	15.269	0.181	0.014	0.217	100.667	0.746	83.959
SP98-25_OL5	39.795	44.923	0.062	0.207	0.016	15.243	0.184	0.016	0.216	100.662	0.747	84.004
SP98-25_OL5	39.862	45.074	0.061	0.208	0.014	15.287	0.187	0.021	0.219	100.931	0.747	84.011
SP98-25_OL5	39.960	45.127	0.063	0.207	0.015	15.244	0.186	0.019	0.217	101.038	0.747	84.065
SP98-25_OL5	39.745	44.701	0.062	0.207	0.018	15.292	0.184	0.027	0.216	100.454	0.745	83.894
SP98-25_OL5	39.839	44.900	0.063	0.207	0.014	15.271	0.182	0.015	0.220	100.712	0.746	83.973
SP98-25_OL5	39.837	45.042	0.062	0.208	0.017	15.260	0.183	0.021	0.223	100.853	0.747	84.025
SP98-25_OL5	39.861	45.090	0.061	0.206	0.016	15.274	0.184	0.018	0.216	100.927	0.747	84.027
SP98-25_OL5	39.809	45.109	0.061	0.208	0.016	15.245	0.183	0.020	0.215	100.866	0.747	84.058
SP98-25_OL5	39.870	45.107	0.062	0.208	0.017	15.253	0.181	0.019	0.218	100.935	0.747	84.050
SP98-25_OL5	39.921	45.251	0.063	0.208	0.019	15.325	0.185	0.019	0.219	101.209	0.747	84.030
SP98-25_OL5	39.833	45.006	0.066	0.209	0.015	15.246	0.182	0.021	0.214	100.792	0.747	84.027
SP98-25_OL5	39.893	45.198	0.065	0.205	0.016	15.276	0.182	0.020	0.210	101.064	0.747	84.057
SP98-25_OL5	39.875	45.067	0.065	0.206	0.017	15.192	0.182	0.021	0.221	100.844	0.748	84.092
SP98-25_OL5	39.853	45.055	0.064	0.207	0.017	15.229	0.182	0.017	0.214	100.836	0.747	84.056
SP98-25_OL5	39.965	45.054	0.063	0.207	0.017	15.178	0.177	0.021	0.217	100.898	0.748	84.100
SP98-25_OL5	39.837	45.173	0.059	0.206	0.015	15.231	0.180	0.020	0.216	100.936	0.748	84.089
SP98-25_OL5	39.912	45.236	0.077	0.206	0.019	15.167	0.182	0.021	0.216	101.035	0.749	84.164
SP98-25_OL5	39.768	44.916	0.058	0.208	0.016	15.194	0.181	0.017	0.212	100.570	0.747	84.045

SP98-25_OL5	39.884	45.054	0.060	0.206	0.017	15.214	0.184	0.015	0.220	100.854	0.748	84.069
SP98-25_OL5	39.954	45.167	0.060	0.205	0.016	15.206	0.185	0.012	0.220	101.024	0.748	84.110
SP98-25_OL5	39.866	45.066	0.059	0.208	0.014	15.156	0.183	0.015	0.214	100.781	0.748	84.124
SP98-25_OL5	39.881	45.190	0.059	0.208	0.020	15.153	0.184	0.019	0.214	100.927	0.749	84.164
SP98-25_OL5	39.938	45.178	0.059	0.208	0.014	15.174	0.180	0.022	0.212	100.982	0.749	84.141
SP98-25_OL5	39.882	45.123	0.059	0.205	0.015	15.155	0.177	0.013	0.218	100.848	0.749	84.141
SP98-25_OL5	39.971	45.194	0.061	0.209	0.014	15.168	0.183	0.021	0.213	101.033	0.749	84.151
SP98-25_OL5	39.811	45.083	0.059	0.205	0.013	15.169	0.184	0.019	0.208	100.751	0.748	84.117
SP98-25_OL5	39.955	45.256	0.061	0.211	0.017	15.153	0.185	0.018	0.214	101.069	0.749	84.182
SP98-25_OL5	40.052	45.352	0.064	0.208	0.015	15.077	0.179	0.012	0.211	101.169	0.751	84.278
SP98-25_OL5	40.338	45.809	0.117	0.213	0.016	15.079	0.184	0.024	0.211	101.990	0.752	84.408
SP98-25_OL5	39.829	45.046	0.208	0.211	0.021	15.071	0.182	0.018	0.213	100.799	0.749	84.193
SP98-25_OL5	39.889	45.256	0.063	0.211	0.016	15.099	0.184	0.018	0.210	100.944	0.750	84.230
SP98-25_OL5	39.922	45.237	0.062	0.209	0.016	15.052	0.182	0.020	0.218	100.916	0.750	84.266
SP98-25_OL5	39.975	45.233	0.056	0.212	0.019	14.992	0.184	0.010	0.215	100.894	0.751	84.317
SP98-25_OL5	39.743	45.288	0.058	0.213	0.017	15.052	0.179	0.018	0.212	100.781	0.751	84.280
SP98-25_OL5	40.008	45.304	0.058	0.215	0.013	14.988	0.182	0.021	0.216	101.004	0.751	84.342
SP98-25_OL5	39.861	45.177	0.059	0.213	0.016	15.008	0.179	0.017	0.214	100.744	0.751	84.287
SP98-25_OL5	39.951	45.232	0.060	0.216	0.013	14.982	0.179	0.017	0.211	100.860	0.751	84.326
SP98-25_OL5	40.098	45.404	0.057	0.218	0.016	14.996	0.181	0.020	0.213	101.203	0.752	84.364
SP98-25_OL5	40.211	45.535	0.061	0.219	0.014	14.962	0.182	0.018	0.215	101.417	0.753	84.432
SP98-25_OL5	39.957	45.317	0.059	0.218	0.018	14.926	0.182	0.017	0.212	100.907	0.752	84.400
SP98-25_OL5	40.017	45.351	0.061	0.217	0.016	14.913	0.184	0.021	0.210	100.989	0.753	84.421
SP98-25_OL5	40.053	45.335	0.060	0.220	0.017	14.902	0.183	0.017	0.213	100.999	0.753	84.427
SP98-25_OL5	40.030	45.467	0.059	0.222	0.015	14.859	0.180	0.021	0.213	101.065	0.754	84.503
SP98-25_OL5	40.042	45.521	0.065	0.222	0.015	14.839	0.178	0.018	0.212	101.112	0.754	84.536
SP98-25_OL5	40.071	45.380	0.063	0.228	0.021	14.742	0.183	0.026	0.214	100.928	0.755	84.581
SP98-25_OL5	40.086	45.506	0.062	0.227	0.017	14.796	0.179	0.019	0.213	101.106	0.755	84.569
SP98-25_OL5	40.079	45.592	0.062	0.224	0.019	14.711	0.179	0.021	0.210	101.097	0.756	84.669

SP98-25_OL5	40.052	45.613	0.057	0.228	0.016	14.664	0.182	0.013	0.212	101.036	0.757	84.716
SP98-25_OL5	40.136	45.674	0.057	0.230	0.013	14.695	0.183	0.021	0.214	101.223	0.757	84.706
SP98-25_OL5	40.106	45.610	0.055	0.235	0.015	14.613	0.177	0.021	0.216	101.047	0.757	84.761
SP98-25_OL5	40.011	45.501	0.057	0.235	0.015	14.623	0.181	0.026	0.216	100.864	0.757	84.721
SP98-25_OL5	39.963	45.381	0.056	0.235	0.016	14.601	0.181	0.025	0.215	100.672	0.757	84.706
SP98-25_OL5	39.946	45.510	0.056	0.236	0.014	14.612	0.177	0.021	0.220	100.792	0.757	84.733
SP98-25_OL5	40.026	45.700	0.055	0.237	0.015	14.625	0.180	0.022	0.221	101.080	0.758	84.775
SP98-25_OL5	40.083	45.690	0.053	0.243	0.011	14.635	0.176	0.030	0.221	101.142	0.757	84.764
SP98-25_OL5	40.033	45.725	0.054	0.246	0.015	14.654	0.176	0.028	0.222	101.153	0.757	84.757
SP98-25_OL5	39.743	45.664	0.054	0.249	0.016	14.645	0.185	0.024	0.220	100.800	0.757	84.747
SP98-25_OL5	39.911	45.702	0.053	0.252	0.018	14.667	0.182	0.025	0.226	101.035	0.757	84.739
SP98-25_OL5	40.146	45.666	0.054	0.255	0.016	14.700	0.180	0.027	0.221	101.265	0.756	84.700
SP98-25_OL5	40.083	45.565	0.053	0.261	0.019	14.728	0.188	0.030	0.226	101.153	0.756	84.646
SP98-25_OL5	40.089	45.646	0.055	0.264	0.016	14.799	0.189	0.030	0.219	101.306	0.755	84.607
SP98-25_OL5	39.979	45.585	0.054	0.265	0.014	14.826	0.185	0.031	0.220	101.158	0.755	84.566
SP98-25_OL5	40.052	45.570	0.058	0.268	0.016	14.860	0.190	0.036	0.222	101.270	0.754	84.531
SP98-25_OL5	39.979	45.411	0.057	0.273	0.016	14.859	0.187	0.033	0.221	101.036	0.753	84.486
SP98-25_OL5	40.068	45.392	0.055	0.276	0.012	14.924	0.193	0.032	0.219	101.170	0.753	84.424
SP98-25_OL5	40.093	45.438	0.053	0.282	0.013	15.039	0.189	0.033	0.221	101.362	0.751	84.336
SP98-25_OL5	40.086	45.349	0.051	0.286	0.018	15.125	0.194	0.033	0.219	101.361	0.750	84.234
SP98-25_OL5	40.034	45.481	0.051	0.289	0.020	15.254	0.199	0.029	0.217	101.574	0.749	84.160
SP98-25_OL5	39.858	44.953	0.053	0.296	0.018	15.379	0.201	0.033	0.210	101.001	0.745	83.894
SP98-25_OL5	39.829	44.683	0.051	0.306	0.021	15.821	0.209	0.025	0.208	101.152	0.739	83.424
SP98-25_OL5	39.625	43.883	0.046	0.324	0.022	16.732	0.225	0.028	0.199	101.084	0.724	82.375
SP98-25_OL5	39.235	42.566	0.043	0.348	0.027	18.184	0.251	0.025	0.178	100.855	0.701	80.663
SP98-25_OL5-R	39.175	40.657	0.041	0.402	0.028	20.858	0.295	0.019	0.154	101.630	0.661	77.646
SP98-25_OL6-C	40.116	45.713	0.064	0.209	0.018	14.519	0.176	0.023	0.239	101.077	0.759	84.873
SP98-25_OL6	40.193	45.674	0.067	0.204	0.018	14.473	0.175	0.022	0.238	101.064	0.759	84.903
SP98-25_OL6	40.090	45.672	0.065	0.214	0.016	14.381	0.175	0.023	0.237	100.872	0.761	84.983

SP98-25_OL6	40.133	45.867	0.065	0.229	0.017	14.219	0.172	0.025	0.237	100.962	0.763	85.182
SP98-25_OL6-R	38.636	39.006	0.038	0.421	0.069	22.547	0.334	0.036	0.138	101.226	0.634	75.507
SP98-25_OL7-C	39.680	44.368	0.060	0.227	0.017	16.112	0.195	0.013	0.185	100.857	0.734	83.071
SP98-25_OL7	39.443	44.152	0.066	0.230	0.018	16.115	0.197	0.016	0.188	100.426	0.733	83.000
SP98-25_OL7	39.475	44.235	0.060	0.225	0.018	15.940	0.199	0.015	0.190	100.356	0.735	83.180
SP98-25_OL7	39.303	44.225	0.101	0.239	0.021	15.656	0.192	0.019	0.192	99.947	0.739	83.426
SP98-25_OL7-R	38.680	39.295	0.044	0.362	0.023	22.049	0.295	0.009	0.135	100.892	0.641	76.053
SP98-25_OL8-C	40.528	46.490	0.105	0.220	0.016	14.356	0.172	0.028	0.223	102.138	0.764	85.231
SP98-25_OL8	40.205	45.966	0.059	0.222	0.015	14.322	0.167	0.027	0.231	101.213	0.762	85.117
SP98-25_OL8	41.105	47.238	0.079	0.233	0.016	14.275	0.173	0.032	0.230	103.380	0.768	85.501
SP98-25_OL8	40.211	46.075	0.060	0.246	0.016	14.140	0.174	0.032	0.225	101.178	0.765	85.309
SP98-25_OL8-R	39.374	36.866	0.059	0.500	0.045	26.468	0.418	0.009	0.109	103.847	0.582	71.281
SP98-25_OL9-C	39.869	45.876	0.060	0.241	0.019	14.289	0.170	0.034	0.237	100.795	0.762	85.121
SP98-25_OL9	39.919	45.876	0.059	0.240	0.018	14.230	0.172	0.035	0.229	100.777	0.763	85.174
SP98-25_OL9	39.811	46.000	0.062	0.251	0.019	14.234	0.174	0.033	0.236	100.821	0.764	85.205
SP98-25_OL9	39.888	45.695	0.055	0.278	0.017	14.617	0.186	0.044	0.236	101.014	0.758	84.781
SP98-25_OL9-R	37.870	35.648	0.075	0.452	0.031	26.033	0.407	0.013	0.116	100.644	0.578	70.931
SP98-25_OL10-C	40.235	46.521	0.065	0.231	0.014	13.711	0.167	0.034	0.242	101.219	0.772	85.809
SP98-25_OL10	40.269	46.357	0.065	0.230	0.018	13.691	0.167	0.040	0.246	101.084	0.772	85.783
SP98-25_OL10	40.204	46.463	0.067	0.233	0.015	13.694	0.165	0.040	0.243	101.124	0.772	85.808
SP98-25_OL10	40.109	46.444	0.067	0.231	0.015	13.709	0.162	0.038	0.243	101.017	0.772	85.790
SP98-25_OL10	40.216	46.510	0.065	0.234	0.015	13.725	0.165	0.034	0.246	101.209	0.772	85.793
SP98-25_OL10	40.206	46.348	0.066	0.231	0.012	13.708	0.166	0.035	0.250	101.022	0.772	85.765
SP98-25_OL10	40.174	46.351	0.066	0.232	0.014	13.711	0.161	0.037	0.244	100.990	0.772	85.763
SP98-25_OL10	40.004	46.392	0.066	0.233	0.018	13.682	0.168	0.041	0.243	100.846	0.772	85.800
SP98-25_OL10	40.236	46.414	0.065	0.233	0.013	13.686	0.170	0.037	0.253	101.106	0.772	85.802
SP98-25_OL10	40.004	46.401	0.065	0.231	0.017	13.690	0.166	0.036	0.246	100.856	0.772	85.795
SP98-25_OL10	40.190	46.373	0.067	0.235	0.014	13.689	0.169	0.034	0.246	101.017	0.772	85.789
SP98-25_OL10	40.299	46.371	0.066	0.232	0.017	13.663	0.161	0.034	0.242	101.084	0.772	85.811

SP98-25_OL10	40.225	46.352	0.067	0.235	0.013	13.692	0.159	0.034	0.250	101.026	0.772	85.780
SP98-25_OL10	40.327	46.435	0.068	0.231	0.013	13.665	0.166	0.032	0.251	101.188	0.773	85.826
SP98-25_OL10	40.179	46.402	0.067	0.236	0.014	13.711	0.163	0.038	0.244	101.055	0.772	85.777
SP98-25_OL10	40.270	46.307	0.070	0.232	0.018	13.675	0.166	0.038	0.244	101.020	0.772	85.784
SP98-25_OL10	40.155	46.415	0.068	0.235	0.014	13.689	0.165	0.037	0.242	101.021	0.772	85.800
SP98-25_OL10	40.221	46.417	0.068	0.234	0.013	13.721	0.166	0.028	0.245	101.113	0.772	85.772
SP98-25_OL10	40.201	46.331	0.068	0.237	0.016	13.684	0.168	0.036	0.240	100.980	0.772	85.782
SP98-25_OL10	39.776	45.828	0.068	0.562	0.013	13.571	0.158	0.037	0.247	100.261	0.772	85.751
SP98-25_OL10	40.223	46.480	0.067	0.236	0.011	13.692	0.163	0.032	0.245	101.149	0.772	85.814
SP98-25_OL10	40.249	46.366	0.066	0.232	0.013	13.663	0.168	0.032	0.246	101.035	0.772	85.810
SP98-25_OL10	40.157	46.318	0.066	0.232	0.012	13.726	0.167	0.031	0.243	100.952	0.771	85.741
SP98-25_OL10	40.161	46.283	0.069	0.239	0.013	13.697	0.165	0.033	0.248	100.907	0.772	85.758
SP98-25_OL10	40.210	46.477	0.070	0.231	0.015	13.712	0.165	0.037	0.246	101.163	0.772	85.796
SP98-25_OL10	40.223	46.499	0.068	0.236	0.018	13.711	0.166	0.029	0.247	101.197	0.772	85.802
SP98-25_OL10	40.142	46.275	0.066	0.237	0.013	13.720	0.166	0.031	0.245	100.894	0.771	85.736
SP98-25_OL10	40.163	46.380	0.067	0.233	0.019	13.715	0.168	0.030	0.244	101.018	0.772	85.767
SP98-25_OL10	40.302	46.525	0.067	0.233	0.019	13.719	0.164	0.025	0.244	101.297	0.772	85.802
SP98-25_OL10	40.163	46.356	0.069	0.232	0.016	13.725	0.165	0.035	0.239	101.001	0.772	85.753
SP98-25_OL10	40.413	46.708	0.072	0.232	0.017	13.719	0.164	0.037	0.244	101.605	0.773	85.850
SP98-25_OL10	40.521	46.606	0.068	0.235	0.014	13.650	0.169	0.034	0.246	101.542	0.773	85.884
SP98-25_OL10	40.314	46.443	0.067	0.233	0.014	13.655	0.168	0.032	0.243	101.170	0.773	85.837
SP98-25_OL10	40.297	46.527	0.069	0.233	0.019	13.641	0.167	0.028	0.245	101.224	0.773	85.872
SP98-25_OL10	40.118	46.270	0.067	0.232	0.017	13.646	0.167	0.033	0.246	100.794	0.772	85.800
SP98-25_OL10	40.207	46.440	0.067	0.232	0.018	13.657	0.165	0.033	0.236	101.055	0.773	85.835
SP98-25_OL10	40.275	46.339	0.067	0.235	0.015	13.677	0.170	0.030	0.242	101.050	0.772	85.791
SP98-25_OL10	40.242	46.358	0.064	0.234	0.014	13.655	0.167	0.029	0.242	101.005	0.772	85.816
SP98-25_OL10	40.216	46.290	0.069	0.235	0.014	13.676	0.167	0.031	0.245	100.941	0.772	85.779
SP98-25_OL10	40.358	46.445	0.066	0.237	0.016	13.681	0.169	0.034	0.241	101.247	0.772	85.815
SP98-25_OL10	40.260	46.365	0.066	0.235	0.013	13.604	0.165	0.029	0.245	100.982	0.773	85.862

SP98-25_OL10	40.260	46.353	0.065	0.238	0.015	13.751	0.168	0.028	0.246	101.124	0.771	85.729
SP98-25_OL10	40.214	46.301	0.069	0.240	0.017	13.634	0.164	0.030	0.245	100.914	0.773	85.819
SP98-25_OL10	40.172	46.385	0.066	0.244	0.016	13.680	0.166	0.024	0.244	100.996	0.772	85.800
SP98-25_OL10	40.193	46.436	0.064	0.240	0.014	13.729	0.161	0.033	0.247	101.116	0.772	85.769
SP98-25_OL10	40.170	46.390	0.066	0.239	0.015	13.747	0.168	0.032	0.251	101.078	0.771	85.742
SP98-25_OL10	40.224	46.284	0.062	0.240	0.014	13.716	0.165	0.037	0.244	100.985	0.771	85.742
SP98-25_OL10	40.223	46.421	0.064	0.236	0.012	13.766	0.168	0.042	0.244	101.176	0.771	85.733
SP98-25_OL10	40.131	46.417	0.065	0.240	0.019	13.723	0.169	0.039	0.243	101.046	0.772	85.770
SP98-25_OL10	40.199	46.391	0.065	0.241	0.017	13.754	0.169	0.041	0.246	101.123	0.771	85.736
SP98-25_OL10	40.116	46.434	0.065	0.239	0.014	13.778	0.163	0.044	0.242	101.094	0.771	85.726
SP98-25_OL10	40.233	46.294	0.064	0.236	0.017	13.721	0.163	0.041	0.241	101.009	0.771	85.739
SP98-25_OL10	40.259	46.457	0.064	0.235	0.015	13.775	0.168	0.047	0.235	101.253	0.771	85.735
SP98-25_OL10	40.261	46.449	0.066	0.240	0.018	13.753	0.165	0.040	0.246	101.237	0.772	85.752
SP98-25_OL10	40.258	46.427	0.066	0.241	0.014	13.773	0.166	0.036	0.240	101.220	0.771	85.729
SP98-25_OL10	40.254	46.414	0.066	0.240	0.016	13.758	0.165	0.034	0.246	101.193	0.771	85.738
SP98-25_OL10	40.282	46.400	0.066	0.239	0.013	13.784	0.165	0.040	0.245	101.233	0.771	85.712
SP98-25_OL10	40.266	46.425	0.067	0.239	0.016	13.759	0.166	0.036	0.244	101.217	0.771	85.741
SP98-25_OL10	40.325	46.428	0.068	0.238	0.016	13.773	0.162	0.035	0.244	101.288	0.771	85.728
SP98-25_OL10	40.200	46.416	0.067	0.237	0.014	13.789	0.163	0.034	0.243	101.164	0.771	85.711
SP98-25_OL10	40.273	46.423	0.066	0.239	0.016	13.806	0.168	0.037	0.243	101.271	0.771	85.698
SP98-25_OL10	40.431	46.490	0.067	0.239	0.016	13.771	0.165	0.033	0.246	101.457	0.771	85.746
SP98-25_OL10	40.344	46.391	0.064	0.239	0.016	13.752	0.172	0.038	0.244	101.259	0.771	85.737
SP98-25_OL10	40.048	46.317	0.065	0.239	0.016	13.762	0.168	0.041	0.246	100.901	0.771	85.709
SP98-25_OL10	40.253	46.333	0.065	0.239	0.013	13.748	0.168	0.040	0.250	101.108	0.771	85.726
SP98-25_OL10	40.234	46.370	0.065	0.240	0.016	13.765	0.168	0.038	0.241	101.136	0.771	85.720
SP98-25_OL10	40.348	46.472	0.065	0.241	0.010	13.810	0.167	0.037	0.245	101.394	0.771	85.707
SP98-25_OL10	40.285	46.403	0.065	0.238	0.015	13.832	0.169	0.036	0.247	101.290	0.770	85.670
SP98-25_OL10	40.266	46.463	0.064	0.241	0.013	13.827	0.166	0.032	0.243	101.315	0.771	85.690
SP98-25_OL10	40.222	46.502	0.066	0.243	0.013	13.867	0.168	0.039	0.242	101.362	0.770	85.665

SP98-25_OL10	40.204	46.463	0.065	0.238	0.013	13.856	0.170	0.036	0.249	101.294	0.770	85.664
SP98-25_OL10	40.317	46.444	0.067	0.241	0.015	13.880	0.165	0.036	0.248	101.412	0.770	85.638
SP98-25_OL10	40.241	46.447	0.083	0.239	0.014	13.839	0.165	0.046	0.250	101.323	0.770	85.675
SP98-25_OL10	40.212	46.450	0.069	0.238	0.016	13.881	0.169	0.044	0.243	101.320	0.770	85.639
SP98-25_OL10	40.251	46.325	0.068	0.238	0.013	13.889	0.166	0.039	0.248	101.237	0.769	85.598
SP98-25_OL10	40.255	46.313	0.093	0.242	0.013	13.873	0.165	0.051	0.250	101.254	0.770	85.610
SP98-25_OL10	40.216	46.373	0.064	0.239	0.013	13.911	0.166	0.037	0.251	101.268	0.769	85.592
SP98-25_OL10	40.230	46.312	0.064	0.239	0.013	13.940	0.171	0.038	0.246	101.252	0.769	85.550
SP98-25_OL10	40.183	46.373	0.063	0.245	0.014	13.932	0.168	0.037	0.246	101.260	0.769	85.573
SP98-25_OL10	40.284	46.362	0.062	0.240	0.015	13.948	0.168	0.046	0.248	101.373	0.769	85.556
SP98-25_OL10	40.270	46.408	0.063	0.239	0.012	13.942	0.164	0.037	0.248	101.382	0.769	85.573
SP98-25_OL10	40.257	46.317	0.061	0.239	0.013	13.938	0.169	0.038	0.249	101.280	0.769	85.553
SP98-25_OL10	40.256	46.317	0.061	0.240	0.014	13.948	0.167	0.043	0.246	101.291	0.769	85.544
SP98-25_OL10	40.227	46.328	0.063	0.241	0.017	13.961	0.164	0.046	0.245	101.292	0.768	85.535
SP98-25_OL10	40.282	46.294	0.066	0.244	0.012	13.980	0.171	0.035	0.247	101.331	0.768	85.510
SP98-25_OL10	40.278	46.285	0.063	0.241	0.014	13.954	0.168	0.039	0.247	101.288	0.768	85.530
SP98-25_OL10	40.237	46.288	0.064	0.240	0.011	14.005	0.163	0.042	0.247	101.296	0.768	85.486
SP98-25_OL10	40.193	46.287	0.066	0.243	0.014	13.968	0.167	0.040	0.241	101.217	0.768	85.518
SP98-25_OL10	40.249	46.314	0.066	0.245	0.014	13.981	0.169	0.041	0.240	101.318	0.768	85.514
SP98-25_OL10	40.219	46.132	0.067	0.242	0.015	13.978	0.167	0.041	0.242	101.102	0.767	85.468
SP98-25_OL10	40.211	46.159	0.067	0.246	0.012	14.034	0.171	0.040	0.249	101.190	0.767	85.425
SP98-25_OL10	40.232	46.241	0.067	0.245	0.011	14.009	0.173	0.040	0.246	101.265	0.767	85.469
SP98-25_OL10	40.216	46.288	0.066	0.255	0.013	14.020	0.170	0.036	0.247	101.310	0.768	85.472
SP98-25_OL10	40.188	46.102	0.066	0.248	0.014	14.007	0.168	0.046	0.240	101.078	0.767	85.434
SP98-25_OL10	40.222	46.270	0.066	0.245	0.010	14.016	0.175	0.033	0.247	101.282	0.768	85.471
SP98-25_OL10	40.270	46.196	0.066	0.247	0.013	14.015	0.173	0.034	0.243	101.256	0.767	85.452
SP98-25_OL10	40.243	46.229	0.065	0.248	0.009	14.062	0.173	0.041	0.242	101.311	0.767	85.419
SP98-25_OL10	40.240	46.160	0.064	0.249	0.012	14.069	0.169	0.038	0.246	101.246	0.766	85.394
SP98-25_OL10	40.211	46.165	0.069	0.247	0.012	14.096	0.174	0.038	0.242	101.254	0.766	85.372

SP98-25_OL10	40.227	46.142	0.068	0.249	0.014	14.091	0.169	0.042	0.244	101.246	0.766	85.370
SP98-25_OL10	40.180	46.132	0.066	0.251	0.015	14.135	0.174	0.038	0.241	101.231	0.765	85.328
SP98-25_OL10	40.238	46.062	0.065	0.248	0.009	14.130	0.175	0.039	0.238	101.204	0.765	85.313
SP98-25_OL10	40.182	46.118	0.065	0.254	0.014	14.204	0.174	0.041	0.237	101.288	0.765	85.263
SP98-25_OL10	39.961	45.985	0.065	0.254	0.013	14.218	0.173	0.041	0.232	100.942	0.764	85.215
SP98-25_OL10	40.040	45.930	0.064	0.255	0.010	14.259	0.178	0.032	0.238	101.006	0.763	85.163
SP98-25_OL10	40.030	45.892	0.066	0.257	0.017	14.261	0.180	0.033	0.239	100.974	0.763	85.152
SP98-25_OL10	40.127	45.958	0.059	0.260	0.012	14.299	0.179	0.037	0.241	101.171	0.763	85.135
SP98-25_OL10	40.141	45.824	0.059	0.261	0.012	14.362	0.182	0.035	0.235	101.111	0.761	85.043
SP98-25_OL10	40.141	45.870	0.062	0.262	0.014	14.424	0.180	0.043	0.236	101.232	0.761	85.001
SP98-25_OL10	39.768	45.661	0.060	0.265	0.014	14.437	0.182	0.032	0.235	100.654	0.760	84.930
SP98-25_OL10	39.905	45.774	0.058	0.263	0.012	14.473	0.188	0.034	0.235	100.941	0.760	84.931
SP98-25_OL10	40.121	45.741	0.057	0.267	0.011	14.538	0.186	0.035	0.228	101.184	0.759	84.864
SP98-25_OL10	40.074	45.703	0.059	0.272	0.010	14.603	0.189	0.036	0.228	101.174	0.758	84.796
SP98-25_OL10	40.038	45.632	0.057	0.271	0.012	14.685	0.180	0.031	0.229	101.134	0.757	84.704
SP98-25_OL10	39.959	45.440	0.060	0.278	0.015	14.718	0.183	0.035	0.224	100.911	0.755	84.619
SP98-25_OL10	40.036	45.513	0.058	0.278	0.015	14.824	0.190	0.038	0.227	101.178	0.754	84.547
SP98-25_OL10	40.068	45.454	0.057	0.279	0.014	14.862	0.190	0.036	0.220	101.179	0.754	84.496
SP98-25_OL10	39.924	45.319	0.058	0.285	0.015	14.943	0.189	0.033	0.217	100.982	0.752	84.386
SP98-25_OL10	39.948	45.366	0.057	0.288	0.012	15.022	0.194	0.036	0.217	101.140	0.751	84.330
SP98-25_OL10	40.029	45.287	0.054	0.292	0.016	15.105	0.195	0.040	0.212	101.229	0.750	84.234
SP98-25_OL10	39.896	45.147	0.054	0.294	0.020	15.158	0.194	0.032	0.213	101.006	0.749	84.146
SP98-25_OL10	39.955	45.082	0.051	0.299	0.017	15.218	0.198	0.026	0.210	101.058	0.748	84.074
SP98-25_OL10	39.898	45.145	0.049	0.301	0.019	15.311	0.198	0.028	0.211	101.158	0.747	84.011
SP98-25_OL10	39.923	45.048	0.050	0.305	0.018	15.357	0.200	0.024	0.207	101.129	0.746	83.942
SP98-25_OL10	39.887	44.911	0.052	0.305	0.018	15.373	0.202	0.028	0.209	100.985	0.745	83.886
SP98-25_OL10	39.761	44.919	0.046	0.311	0.019	15.434	0.201	0.023	0.209	100.924	0.744	83.835
SP98-25_OL10	39.790	44.700	0.046	0.322	0.024	15.540	0.212	0.026	0.203	100.862	0.742	83.676
SP98-25_OL10	39.718	44.545	0.047	0.339	0.023	15.708	0.214	0.026	0.196	100.816	0.739	83.480

SP98-25_OL10	39.629	44.181	0.047	0.359	0.024	16.189	0.223	0.028	0.180	100.859	0.732	82.945
SP98-25_OL10	39.269	42.972	0.046	0.379	0.028	17.455	0.241	0.018	0.167	100.574	0.711	81.437
SP98-25_OL10	38.863	40.919	0.041	0.403	0.031	19.951	0.286	0.021	0.152	100.666	0.672	78.517
SP98-25_OL10	38.262	37.609	0.039	0.461	0.041	23.829	0.363	0.020	0.130	100.753	0.612	73.770
SP98-25_OL10-R	37.039	33.510	0.046	0.521	0.056	28.326	0.457	0.005	0.101	100.061	0.542	67.826
SP98-23_OL1-C	38.601	40.250	0.051	0.224	0.027	20.738	0.257	0.004	0.086	100.238	0.660	77.571
SP98-23_OL1	36.638	38.076	0.079	0.223	0.029	20.578	0.255	0.004	0.087	95.968	0.649	76.730
SP98-23_OL1	38.596	40.174	0.044	0.230	0.026	20.915	0.267	0.001	0.095	100.347	0.658	77.390
SP98-23_OL1	38.487	40.022	0.043	0.243	0.027	21.024	0.271	0.007	0.091	100.213	0.656	77.233
SP98-23_OL1-R	37.983	37.362	0.044	0.382	0.065	24.063	0.400	0.005	0.084	100.388	0.608	73.453
SP98-23_OL2-C	39.927	46.014	0.075	0.211	0.014	13.841	0.153	0.033	0.278	100.546	0.769	85.558
SP98-23_OL2	39.905	45.859	0.073	0.213	0.017	14.160	0.160	0.023	0.267	100.677	0.764	85.231
SP98-23_OL2	39.607	44.641	0.066	0.237	0.018	15.488	0.177	0.020	0.222	100.475	0.742	83.703
SP98-23_OL2	39.397	44.071	0.067	0.240	0.024	16.213	0.200	0.028	0.219	100.459	0.731	82.888
SP98-23_OL2-R	38.017	38.110	0.044	0.356	0.063	22.953	0.372	0.009	0.100	100.024	0.624	74.740
SP98-23_OL3-C	39.466	44.341	0.077	0.192	0.018	15.777	0.168	0.019	0.241	100.300	0.738	83.356
SP98-23_OL3	39.387	44.292	0.070	0.194	0.017	15.790	0.168	0.018	0.240	100.176	0.737	83.329
SP98-23_OL3	39.373	44.270	0.072	0.190	0.019	15.837	0.171	0.018	0.237	100.186	0.737	83.281
SP98-23_OL3	39.356	44.243	0.071	0.190	0.017	15.808	0.162	0.012	0.239	100.096	0.737	83.298
SP98-23_OL3	39.546	44.652	0.066	0.190	0.018	16.043	0.169	0.016	0.234	100.935	0.736	83.221
SP98-23_OL3	39.621	44.754	0.066	0.193	0.019	16.054	0.166	0.019	0.234	101.126	0.736	83.243
SP98-23_OL3	39.494	44.712	0.065	0.191	0.017	16.007	0.168	0.013	0.235	100.901	0.736	83.271
SP98-23_OL3	39.484	44.672	0.095	0.194	0.018	15.979	0.164	0.019	0.226	100.851	0.737	83.283
SP98-23_OL3	39.442	44.513	0.182	0.194	0.023	15.746	0.166	0.028	0.227	100.520	0.739	83.438
SP98-23_OL3	39.313	44.623	0.065	0.190	0.017	15.518	0.165	0.016	0.219	100.126	0.742	83.671
SP98-23_OL3	39.128	44.471	0.074	0.187	0.017	15.097	0.160	0.021	0.220	99.373	0.747	83.998
SP98-23_OL3	39.040	44.261	0.100	0.183	0.015	14.703	0.155	0.013	0.210	98.680	0.751	84.288
SP98-23_OL3	38.585	44.127	0.068	0.179	0.019	14.155	0.151	0.016	0.211	97.511	0.757	84.745
SP98-23_OL3	38.510	43.953	0.067	0.173	0.018	13.671	0.146	0.015	0.203	96.756	0.763	85.139

SP98-23_OL3	39.130	44.639	0.069	0.189	0.018	14.824	0.155	0.026	0.222	99.273	0.751	84.292
SP98-23_OL3	39.193	44.680	0.155	0.187	0.021	14.333	0.159	0.026	0.231	98.985	0.757	84.744
SP98-23_OL3	39.042	44.749	0.073	0.189	0.019	14.038	0.157	0.023	0.226	98.515	0.761	85.031
SP98-23_OL3	39.375	44.980	0.168	0.251	0.023	14.443	0.167	0.019	0.251	99.677	0.757	84.732
SP98-23_OL3	39.495	45.310	0.099	0.228	0.021	14.340	0.166	0.027	0.258	99.944	0.760	84.918
SP98-23_OL3	39.587	45.568	0.103	0.250	0.020	13.956	0.165	0.031	0.259	99.941	0.766	85.334
SP98-23_OL3	39.554	45.832	0.072	0.259	0.020	13.702	0.161	0.030	0.265	99.896	0.770	85.633
SP98-23_OL3	39.552	45.821	0.074	0.260	0.022	13.566	0.165	0.037	0.265	99.761	0.772	85.753
SP98-23_OL3	39.549	45.903	0.069	0.261	0.019	13.565	0.165	0.034	0.258	99.824	0.772	85.776
SP98-23_OL3	39.754	45.932	0.073	0.264	0.019	13.747	0.167	0.036	0.260	100.252	0.770	85.620
SP98-23_OL3	39.545	45.492	0.065	0.262	0.023	13.946	0.172	0.030	0.256	99.790	0.765	85.322
SP98-23_OL3	39.713	45.724	0.062	0.256	0.022	14.562	0.183	0.031	0.250	100.801	0.758	84.838
SP98-23_OL3	39.320	44.870	0.056	0.252	0.022	15.118	0.191	0.028	0.249	100.106	0.748	84.099
SP98-23_OL3	39.280	44.252	0.057	0.257	0.025	16.064	0.205	0.024	0.226	100.389	0.734	83.076
SP98-23_OL3	38.875	42.941	0.066	0.256	0.027	17.086	0.214	0.022	0.196	99.682	0.715	81.747
SP98-23_OL3	38.866	42.592	0.048	0.265	0.029	18.194	0.241	0.013	0.164	100.411	0.701	80.664
SP98-23_OL3	38.700	41.690	0.046	0.274	0.031	19.247	0.267	0.004	0.131	100.390	0.684	79.424
SP98-23_OL3	38.466	40.569	0.047	0.308	0.037	20.456	0.295	0.008	0.121	100.307	0.665	77.945
SP98-23_OL3	38.192	39.452	0.049	0.353	0.044	21.626	0.332	0.006	0.099	100.153	0.646	76.475
SP98-23_OL3	37.703	37.993	0.040	0.375	0.048	23.148	0.373	0.000	0.080	99.760	0.621	74.521
SP98-23_OL3	37.481	36.100	0.042	0.449	0.055	25.318	0.444	0.001	0.067	99.957	0.588	71.759
SP98-23_OL3	37.057	33.979	0.042	0.490	0.053	27.245	0.503	0.002	0.050	99.420	0.555	68.968
SP98-23_OL3-R	36.263	30.904	0.048	0.538	0.060	30.727	0.621	0.001	0.032	99.194	0.501	64.187
SP98-23_OL4-C	37.869	39.630	0.044	0.232	0.026	20.772	0.266	0.003	0.093	98.935	0.656	77.271
SP98-23_OL4	38.155	39.730	0.043	0.236	0.028	20.789	0.267	0.001	0.090	99.337	0.656	77.302
SP98-23_OL4	38.064	39.695	0.044	0.261	0.025	20.737	0.267	0.002	0.088	99.183	0.657	77.330
SP98-23_OL4	37.711	39.733	0.043	0.237	0.024	20.816	0.265	0.001	0.089	98.918	0.656	77.280
SP98-23_OL4	37.928	39.826	0.045	0.236	0.029	20.834	0.267	0.000	0.085	99.250	0.657	77.306
SP98-23_OL4	38.170	39.820	0.048	0.238	0.027	20.849	0.271	0.003	0.093	99.519	0.656	77.291

SP98-23_OL4	38.056	39.689	0.045	0.237	0.027	20.838	0.269	0.000	0.085	99.245	0.656	77.242
SP98-23_OL4	37.996	39.628	0.045	0.237	0.029	20.822	0.272	0.002	0.090	99.121	0.656	77.229
SP98-23_OL4	38.190	39.712	0.044	0.239	0.024	20.892	0.270	0.005	0.085	99.461	0.655	77.207
SP98-23_OL4	38.195	39.778	0.045	0.240	0.026	20.872	0.270	0.003	0.089	99.518	0.656	77.253
SP98-23_OL4	38.107	39.689	0.044	0.239	0.026	20.894	0.270	0.003	0.093	99.365	0.655	77.195
SP98-23_OL4	38.161	39.681	0.044	0.243	0.028	20.886	0.274	0.001	0.083	99.402	0.655	77.198
SP98-23_OL4	38.136	39.672	0.043	0.243	0.027	20.887	0.275	0.003	0.091	99.376	0.655	77.193
SP98-23_OL4	38.144	39.672	0.042	0.248	0.030	20.890	0.273	0.004	0.092	99.396	0.655	77.190
SP98-23_OL4	38.161	39.646	0.043	0.249	0.029	20.855	0.271	0.004	0.096	99.353	0.655	77.209
SP98-23_OL4	38.119	39.729	0.042	0.250	0.032	20.830	0.275	0.000	0.089	99.367	0.656	77.266
SP98-23_OL4	38.124	39.736	0.042	0.254	0.029	20.751	0.266	0.003	0.093	99.297	0.657	77.337
SP98-23_OL4	38.174	39.863	0.042	0.258	0.031	20.640	0.273	0.007	0.095	99.383	0.659	77.486
SP98-23_OL4	38.230	39.927	0.044	0.266	0.032	20.422	0.275	0.002	0.103	99.302	0.662	77.699
SP98-23_OL4	38.146	39.916	0.044	0.283	0.034	20.347	0.279	0.006	0.109	99.163	0.662	77.757
SP98-23_OL4	38.032	39.431	0.043	0.293	0.038	20.666	0.300	0.004	0.116	98.922	0.656	77.273
SP98-23_OL4	37.701	38.247	0.041	0.328	0.041	22.016	0.341	0.011	0.110	98.834	0.635	75.585
SP98-23_OL4-R	37.019	35.291	0.041	0.404	0.052	25.415	0.453	0.000	0.074	98.748	0.581	71.219
SP98-23_OL5-C	38.523	42.615	0.062	0.240	0.044	16.917	0.200	0.006	0.149	98.756	0.716	81.782
SP98-23_OL5	38.811	43.419	0.055	0.229	0.022	16.098	0.190	0.013	0.208	99.045	0.730	82.778
SP98-23_OL5	38.441	41.520	0.044	0.240	0.028	18.658	0.229	0.010	0.154	99.324	0.690	79.861
SP98-23_OL5	38.226	40.249	0.043	0.261	0.030	20.268	0.270	0.005	0.102	99.454	0.665	77.968
SP98-23_OL5-R	37.277	33.337	0.044	0.475	0.066	28.838	0.534	0.004	0.043	100.618	0.536	67.320
SP98-23_OL6-C	39.258	44.534	0.065	0.259	0.026	15.057	0.187	0.030	0.240	99.657	0.747	84.053
SP98-23_OL6	39.219	44.382	0.063	0.260	0.027	15.383	0.194	0.030	0.239	99.797	0.743	83.716
SP98-23_OL6	39.124	43.969	0.067	0.256	0.024	15.724	0.193	0.026	0.233	99.615	0.737	83.286
SP98-23_OL6	39.008	43.564	0.063	0.254	0.028	16.243	0.206	0.025	0.223	99.614	0.728	82.697
SP98-23_OL6	38.870	43.112	0.062	0.258	0.026	16.848	0.215	0.020	0.209	99.620	0.719	82.014
SP98-23_OL6	38.766	42.400	0.099	0.261	0.031	17.659	0.229	0.022	0.194	99.661	0.706	81.056
SP98-23_OL6	38.533	41.385	0.057	0.256	0.026	18.826	0.252	0.017	0.172	99.524	0.687	79.664

SP98-23_OL6	38.241	40.190	0.058	0.269	0.027	20.092	0.280	0.015	0.141	99.312	0.667	78.092
SP98-23_OL6	37.987	39.084	0.050	0.281	0.027	21.487	0.321	0.010	0.119	99.365	0.645	76.423
SP98-23_OL6	37.694	37.728	0.050	0.324	0.030	23.029	0.365	0.005	0.098	99.321	0.621	74.486
SP98-23_OL6	36.866	35.239	0.260	0.402	0.047	25.558	0.426	0.001	0.076	98.874	0.580	71.073
SP98-23_OL6	36.702	33.735	0.031	0.455	0.053	27.655	0.526	0.000	0.051	99.207	0.550	68.492
SP98-23_OL6	36.135	31.312	0.051	0.559	0.066	30.261	0.603	0.000	0.036	99.024	0.509	64.836
SP98-23_OL6-R	35.664	22.355	2.637	0.644	0.103	36.278	0.786	0.001	0.025	98.493	0.381	52.337
SP98-23_OL7-C	38.253	40.032	0.050	0.225	0.034	20.966	0.254	0.001	0.074	99.889	0.656	77.286
SP98-23_OL7	38.207	39.871	0.047	0.226	0.030	20.983	0.262	0.001	0.075	99.703	0.655	77.200
SP98-23_OL7	38.144	39.710	0.040	0.233	0.023	21.048	0.272	0.006	0.089	99.566	0.654	77.075
SP98-23_OL7	38.036	39.693	0.042	0.246	0.025	21.007	0.270	0.006	0.088	99.412	0.654	77.102
SP98-23_OL7-R	37.630	36.746	0.042	0.378	0.033	24.240	0.395	0.001	0.063	99.527	0.603	72.982
SP98-23_OL8-C	38.660	42.280	0.052	0.218	0.024	17.821	0.221	0.000	0.132	99.409	0.703	80.871
SP98-23_OL8	38.673	42.358	0.052	0.216	0.027	17.744	0.223	0.000	0.133	99.425	0.705	80.967
SP98-23_OL8	38.702	42.404	0.043	0.223	0.018	17.715	0.216	0.001	0.126	99.446	0.705	81.009
SP98-23_OL8	38.231	41.062	0.046	0.245	0.030	19.299	0.245	0.007	0.115	99.279	0.680	79.129
SP98-23_OL8-R	37.221	35.692	0.036	0.407	0.055	25.489	0.438	0.009	0.066	99.412	0.583	71.390
SP98-23_OL9-C	37.816	38.803	0.043	0.251	0.025	22.213	0.312	0.004	0.106	99.572	0.636	75.686
SP98-23_OL9	38.677	42.062	0.048	0.233	0.021	18.407	0.228	0.014	0.173	99.862	0.696	80.284
SP98-23_OL9	38.470	41.099	0.044	0.241	0.022	19.489	0.244	0.004	0.146	99.759	0.678	78.982
SP98-23_OL9	38.317	40.434	0.037	0.251	0.027	20.258	0.268	0.005	0.123	99.719	0.666	78.055
SP98-23_OL9-R	37.856	36.955	0.041	0.498	0.066	24.550	0.427	0.004	0.046	100.442	0.601	72.844
SP98-23_OL10-C	37.544	36.514	0.041	0.379	0.061	24.965	0.419	0.004	0.073	99.998	0.594	72.271
SP98-23_OL10	37.446	36.244	0.040	0.384	0.064	25.153	0.423	0.000	0.070	99.824	0.590	71.971
SP98-23_OL10	37.344	35.879	0.041	0.382	0.071	25.681	0.437	0.002	0.063	99.899	0.583	71.344
SP98-23_OL10	37.247	35.632	0.038	0.396	0.075	25.977	0.443	0.000	0.059	99.866	0.578	70.967
SP98-23_OL10	37.226	35.557	0.044	0.414	0.078	26.125	0.455	0.001	0.057	99.956	0.576	70.806
SP98-23_OL10	37.097	35.199	0.046	0.442	0.093	26.332	0.464	0.000	0.054	99.725	0.572	70.432
SP98-23_OL10	36.984	34.677	0.048	0.479	0.102	26.807	0.482	0.000	0.045	99.622	0.564	69.744

SP98-23_OL10	36.674	33.024	0.040	0.521	0.101	28.669	0.552	0.001	0.041	99.622	0.535	67.241
SP98-23_OL10-R	35.762	22.976	2.746	0.487	0.216	33.253	0.696	0.006	0.026	96.167	0.409	55.183
FXH-1 OL3.1-C	39.462	42.760	0.036	0.368	0.044	17.905	0.273	0.012	0.115	101.100	0.705	80.973
FXH-1 OL3.1	39.289	42.632	0.038	0.337	0.072	17.810	0.217	0.034	0.103	100.592	0.705	81.009
FXH-1 OL3.1	39.475	42.139	0.034	0.308	0.058	18.315	0.225	0.010	0.110	100.747	0.697	80.392
FXH-1 OL3.1	39.387	42.203	0.042	0.310	0.035	18.849	0.282	0.025	0.054	101.312	0.691	79.959
FXH-1 OL3.1	39.009	41.265	0.057	0.297	0.041	18.987	0.272	0.006	0.063	100.081	0.685	79.478
FXH-1 OL3.1-R	37.947	35.999	0.052	0.456	0.070	25.199	0.411	0.000	0.043	100.245	0.588	71.797
FXH-1 OL4.1-C	39.534	43.182	0.057	0.275	0.022	17.560	0.268	0.075	0.142	101.356	0.711	81.420
FXH-1 OL4.1	39.330	43.089	0.043	0.265	0.022	17.630	0.252	0.016	0.129	100.903	0.710	81.327
FXH-1 OL4.1	37.559	40.024	0.098	0.280	0.060	17.730	0.247	0.027	0.088	96.203	0.693	80.090
FXH-1 OL4.1	38.819	40.810	0.029	0.360	0.038	19.911	0.276	0.000	0.072	100.351	0.672	78.506
FXH-1 OL4.1-R	38.909	39.505	0.032	0.380	0.034	21.650	0.368	0.021	0.075	101.017	0.646	76.480
FXH-1 OL6.1-C	38.533	33.368	1.917	3.576	1.026	21.628	0.394	0.019	0.037	100.562	0.607	73.328
FXH-1 OL6.1	38.627	41.411	0.040	0.378	0.048	19.569	0.279	0.041	0.116	100.552	0.679	79.040
FXH-1 OL6.1	38.894	41.354	0.031	0.353	0.053	19.416	0.306	0.000	0.086	100.519	0.681	79.147
FXH-1 OL6.1	38.656	41.337	0.028	0.345	0.040	19.403	0.269	0.000	0.096	100.249	0.681	79.151
FXH-1 OL6.1	38.519	40.836	0.024	0.349	0.036	19.370	0.271	0.030	0.115	99.619	0.678	78.978
FXH-1 OL6.1	38.994	40.739	0.040	0.358	0.067	19.549	0.277	0.012	0.071	100.165	0.676	78.785
FXH-1 OL6.1	38.905	40.908	0.037	0.312	0.037	19.899	0.210	0.058	0.083	100.520	0.673	78.556
FXH-1 OL6.1	38.677	40.488	0.017	0.332	0.057	20.093	0.283	0.006	0.068	100.021	0.668	78.217
FXH-1 OL6.1	38.694	40.669	0.029	0.344	0.044	20.050	0.305	0.021	0.108	100.356	0.670	78.329
FXH-1 OL6.1	38.853	40.770	0.025	0.348	0.071	19.809	0.245	0.016	0.046	100.258	0.673	78.576
FXH-1 OL6.1	38.646	40.583	0.044	0.367	0.055	19.894	0.274	0.037	0.080	100.046	0.671	78.426
FXH-1 OL6.1-R	37.481	36.902	0.025	0.427	0.045	24.443	0.371	0.000	0.045	99.794	0.602	72.902
FXH-1 OL6.2-C	37.589	36.712	0.043	0.342	0.048	24.074	0.341	0.000	0.085	99.262	0.604	73.100
FXH-1 OL6.2	38.336	41.361	0.052	0.317	0.056	19.211	0.276	0.000	0.102	99.865	0.683	79.324
FXH-1 OL6.2	38.749	41.596	0.033	0.297	0.062	19.143	0.268	0.041	0.096	100.373	0.685	79.475
FXH-1 OL6.2	38.364	41.565	0.043	0.324	0.027	19.158	0.235	0.004	0.093	99.904	0.685	79.450

FXH-1 OL6.2	38.827	41.481	0.037	0.313	0.048	19.032	0.289	0.036	0.104	100.309	0.685	79.525
FXH-1 OL6.2	38.319	41.402	0.036	0.313	0.055	19.295	0.260	0.000	0.083	99.897	0.682	79.269
FXH-1 OL6.2	38.232	41.134	0.036	0.329	0.034	19.562	0.282	0.027	0.071	99.787	0.678	78.934
FXH-1 OL6.2	38.289	40.885	0.043	0.327	0.036	19.931	0.308	0.031	0.105	100.007	0.672	78.520
FXH-1 OL6.2	38.565	40.570	0.031	0.344	0.042	20.036	0.236	0.059	0.069	100.066	0.669	78.300
FXH-1 OL6.2	38.519	41.064	0.018	0.333	0.040	19.722	0.275	0.000	0.059	100.082	0.676	78.770
FXH-1 OL6.2	38.961	41.131	0.031	0.347	0.062	19.618	0.273	0.012	0.072	100.595	0.677	78.886
FXH-1 OL6.2	38.207	40.471	0.039	0.373	0.061	20.363	0.324	0.000	0.081	99.997	0.665	77.982
FXH-1 OL6.2-R	37.419	35.351	0.033	0.401	0.116	25.487	0.382	0.038	0.051	99.321	0.581	71.195
FXH-1 OL8.1-C	39.753	43.241	0.045	0.252	0.027	17.476	0.207	0.000	0.151	101.171	0.712	81.513
FXH-1 OL8.1	39.785	43.482	0.046	0.205	0.000	17.220	0.205	0.035	0.172	101.189	0.716	81.817
FXH-1 OL8.1	39.615	43.309	0.052	0.212	0.025	17.289	0.241	0.059	0.124	100.952	0.715	81.698
FXH-1 OL8.1	39.235	43.497	0.060	0.221	0.019	17.124	0.220	0.038	0.169	100.620	0.718	81.905
FXH-1 OL8.1	39.605	43.521	0.047	0.230	0.013	17.499	0.223	0.026	0.123	101.335	0.713	81.590
FXH-1 OL8.1	39.723	43.274	0.040	0.196	0.012	17.177	0.222	0.015	0.149	100.825	0.716	81.783
FXH-1 OL8.1	39.048	43.728	0.057	0.214	0.015	17.186	0.193	0.035	0.148	100.683	0.718	81.930
FXH-1 OL8.1	39.378	43.534	0.052	0.230	0.025	16.848	0.270	0.047	0.120	100.521	0.721	82.157
FXH-1 OL8.1	39.351	43.301	0.057	0.213	0.039	17.209	0.195	0.029	0.129	100.579	0.716	81.765
FXH-1 OL8.1	39.174	43.018	0.055	0.232	0.025	17.292	0.158	0.000	0.154	100.138	0.713	81.594
FXH-1 OL8.1	39.571	43.481	0.050	0.236	0.027	17.295	0.209	0.000	0.141	101.049	0.715	81.752
FXH-1 OL8.1	39.400	43.285	0.045	0.255	0.010	17.528	0.265	0.075	0.191	101.095	0.712	81.484
FXH-1 OL8.1	38.015	41.528	0.065	0.273	0.062	17.217	0.237	0.009	0.119	97.658	0.707	81.126
FXH-1 OL8.1	39.124	42.954	0.052	0.281	0.053	17.312	0.200	0.035	0.130	100.239	0.713	81.555
FXH-1 OL8.1	39.448	43.051	0.050	0.268	0.011	17.216	0.231	0.044	0.141	100.525	0.714	81.672
FXH-1 OL8.1	39.006	43.019	0.041	0.296	0.038	17.902	0.255	0.035	0.123	100.756	0.706	81.068
FXH-1 OL8.1	39.027	41.807	0.036	0.274	0.013	19.284	0.273	0.000	0.084	100.876	0.684	79.438
FXH-1 OL8.1	38.990	41.291	0.032	0.297	0.023	19.759	0.239	0.002	0.087	100.748	0.676	78.831
FXH-1 OL8.1	38.960	42.189	0.037	0.319	0.040	18.378	0.251	0.027	0.105	100.356	0.697	80.357
FXH-1 OL8.1	38.855	41.059	0.034	0.309	0.056	20.024	0.326	0.017	0.085	100.782	0.672	78.513

FXH-1 OL8.1-R	38.618	40.521	0.042	0.349	0.065	20.230	0.307	0.000	0.061	100.230	0.667	78.115
FXH-1 OL9.1-C	38.979	41.622	0.057	0.322	0.025	19.365	0.197	0.006	0.111	100.756	0.682	79.297
FXH-1 OL9.1	42.597	34.198	5.171	0.876	0.174	16.632	0.203	0.000	0.077	100.108	0.673	78.559
FXH-1 OL9.1	39.053	42.426	0.050	0.294	0.054	18.347	0.298	0.027	0.131	100.706	0.698	80.472
FXH-1 OL9.1	39.146	42.830	0.040	0.297	0.032	17.906	0.258	0.027	0.114	100.735	0.705	80.997
FXH-1 OL9.1	39.376	42.410	0.045	0.294	0.022	18.040	0.230	0.000	0.151	100.655	0.702	80.729
FXH-1 OL9.1	39.312	42.570	0.046	0.314	0.035	18.366	0.251	0.018	0.119	101.101	0.699	80.508
FXH-1 OL9.1	39.456	42.386	0.038	0.315	0.051	18.302	0.246	0.036	0.122	100.978	0.698	80.495
FXH-1 OL9.1	39.271	41.789	0.041	0.307	0.022	19.004	0.293	0.011	0.114	100.893	0.687	79.669
FXH-1 OL9.1	39.181	41.584	0.028	0.349	0.058	19.299	0.267	0.000	0.085	100.892	0.683	79.338
FXH-1 OL9.1	39.266	40.831	0.044	0.371	0.092	20.327	0.316	0.006	0.074	101.394	0.668	78.164
FXH-1 OL9.1	38.987	39.867	0.037	0.394	0.054	21.021	0.283	0.015	0.076	100.764	0.655	77.167
FXH-1 OL9.1-R	37.334	34.435	0.033	0.444	0.113	26.826	0.446	0.054	0.107	99.874	0.562	69.581
FXH-1 OL9.2-C	39.147	36.545	1.685	0.414	0.088	21.892	0.278	0.000	0.082	100.315	0.625	74.841
FXH-1 OL9.2	38.688	40.722	0.057	0.268	0.045	19.869	0.267	0.027	0.103	100.153	0.672	78.505
FXH-1 OL9.2	39.489	42.491	0.037	0.276	0.041	18.496	0.258	0.039	0.127	101.263	0.697	80.368
FXH-1 OL9.2	39.486	42.725	0.046	0.270	0.019	18.059	0.206	0.026	0.148	101.016	0.703	80.828
FXH-1 OL9.2	39.453	42.789	0.040	0.291	0.031	18.062	0.279	0.009	0.120	101.118	0.703	80.849
FXH-1 OL9.2	39.344	42.490	0.037	0.344	0.059	18.073	0.258	0.012	0.113	100.798	0.702	80.730
FXH-1 OL9.2	39.562	42.345	0.039	0.290	0.047	18.307	0.271	0.000	0.137	101.112	0.698	80.476
FXH-1 OL9.2	39.068	42.110	0.032	0.335	0.042	18.523	0.230	0.006	0.101	100.541	0.695	80.203
FXH-1 OL9.2	39.008	41.320	0.033	0.353	0.041	18.981	0.331	0.041	0.103	100.246	0.685	79.505
FXH-1 OL9.2	38.683	40.265	0.031	0.401	0.043	20.591	0.284	0.000	0.052	100.448	0.662	77.702
FXH-1 OL9.2	38.501	37.977	0.033	0.416	0.096	23.461	0.376	0.022	0.061	101.001	0.618	74.257
FXH-1 OL9.2-R	35.369	29.077	0.218	0.576	0.127	30.754	0.585	0.026	0.006	96.892	0.486	62.754
FXH-1 OL10.1-C	39.369	43.244	0.057	0.234	0.029	17.409	0.241	0.035	0.159	100.928	0.713	81.572
FXH-1 OL10.1	39.312	43.196	0.048	0.252	0.030	17.393	0.258	0.000	0.170	100.766	0.713	81.569
FXH-1 OL10.1	39.426	42.984	0.046	0.259	0.025	17.476	0.225	0.050	0.117	100.743	0.711	81.423
FXH-1 OL10.1	39.386	42.952	0.054	0.252	0.041	17.400	0.173	0.042	0.133	100.523	0.712	81.478

FXH-1 OL10.1	39.115	43.230	0.050	0.256	0.038	17.416	0.213	0.053	0.135	100.659	0.713	81.561
FXH-1 OL10.1	39.306	43.091	0.051	0.264	0.042	17.509	0.196	0.002	0.151	100.778	0.711	81.432
FXH-1 OL10.1	39.314	42.935	0.041	0.237	0.025	17.359	0.176	0.026	0.113	100.359	0.712	81.507
FXH-1 OL10.1	39.450	43.262	0.048	0.246	0.015	17.661	0.245	0.020	0.146	101.220	0.710	81.361
FXH-1 OL10.1	39.530	42.850	0.045	0.269	0.013	17.593	0.254	0.014	0.114	100.796	0.709	81.274
FXH-1 OL10.1	39.591	43.038	0.045	0.284	0.011	17.863	0.203	0.000	0.119	101.196	0.707	81.109
FXH-1 OL10.1	39.255	42.332	0.051	0.323	0.066	18.471	0.258	0.030	0.097	100.940	0.696	80.330
FXH-1 OL10.1-R	39.038	41.375	0.026	0.343	0.057	19.319	0.291	0.012	0.069	100.595	0.682	79.238

Mg# = Mg/(Mg+Fe)